

Aus der Kinderklinik und Kinderpoliklinik im Dr. von Haunerschen
Kinderspital der Ludwig-Maximilians-Universität München
Direktor: Prof. Dr. med. Dr. sci. nat. Christoph Klein



**Peptide-based platform enabling amphiphilic
block copolymers to acquire *in vitro*
transfection ability and more potent *in vivo*
lung gene transfer for cystic fibrosis**

Dissertation zur Erlangung des Doktorgrades der
Naturwissenschaften an der Medizinischen Fakultät
der Ludwig-Maximilians-Universität München

vorgelegt von

Shan Guan

aus Huopu, China

2017

Gedruckt mit Genehmigung der Medizinischen Fakultät der Ludwig-Maximilians-Universität München

Betreuer: PD. Dr. Carsten Rudolph

Zweitgutachter: Prof. Dr. Alexander Dietrich

Dekan: Prof. Dr. med. dent. Reinhard Hickel

Tag der mündlichen Prüfung: 06. 03. 2018

“We will hew out of the mountain of despair a stone of hope.”
Martin Luther King Jr., 1963

TABLE OF CONTENTS

1 INTRODUCTION	1
1.1 Gene therapy for cystic fibrosis	1
1.2 Clinical trials of CF gene therapy	5
1.2.1 Clinical trials of CF gene therapy using viral vectors	6
1.2.2 Clinical trials of CF gene therapy using nonviral vectors	9
1.3 Potential next generation nonviral delivery systems for CF gene therapy	12
1.4 Aims of the thesis	15
2 MATERIALS AND METHODS	19
2.1 Materials	19
2.1.1 Reagents	19
2.1.2 Nucleic acids	20
2.2 Methods	20
2.2.1 Synthesis of peptides	20
2.2.2 Cell culture	21
2.2.3 Preparation of mRNA/pDNA based binary and ternary complexes	21
2.2.4 Size and zeta potential measurements	22
2.2.5 Transmission electron microscopy	23
2.2.6 Agarose gel retardation assay	23
2.2.7 <i>In vitro</i> transfection	24
2.2.8 Nebulization study	25
2.2.9 Flow cytometry	25
2.2.10 Confocal microscopy	27

Table of Contents

2.2.11 Cytotoxicity assay	28
2.2.12 Animal studies.....	28
2.2.13 Histology	30
2.2.14 Immunohistochemical analysis	30
2.2.15 Statistics	31
3 RESULTS	32
3.1 Establishing poloxamine 704 (T704)-peptide ternary complexes.....	32
3.1.1 T704 based binary complexes were invalid for <i>in vitro</i> transfection	32
3.1.2 Investigations on parameters influencing <i>in vitro</i> transfection efficiency of ternary complex.....	34
3.2 Characterization of ternary complexes and binary counterparts	39
3.2.1 Agarose gel retardation assay.....	39
3.2.2 Dynamic light scattering (DLS) measurements	42
3.2.3 Transmission electron microscopy (TEM).....	43
3.2.4 Stability of ternary complexes.....	44
3.3 Investigations on the underlying mechanism of the superior transfection efficiency of ternary complex compared with the binary counterpart.....	47
3.3.1 Cellular internalization of binary and ternary complexes	47
3.3.2 Cellular internalization pathways of ternary complex	48
3.3.3 Subcellular localization of binary and ternary complexes	52
3.4 Optimizing peptide structure with different candidate modules	53
3.4.1 Each moiety that constitutes the peptide is imperative for the activity of peptide in ternary complex	53
3.4.2 Optimizing the peptide structure with different candidate modules	55
3.5 Comparisons between the ternary complexes and other nonviral transfection reagents	62

3.5.1 <i>In vitro</i> luciferase expression mediated by different carrier systems	62
3.5.2 <i>In vitro</i> enhanced green fluorescent protein (EGFP) expression mediated by different carrier systems	64
3.6 Cytotoxicity	68
3.6.1 Cytotoxicity of formulations based on ternary complexes, Lipofectamine2000 lipoplex and brPEI polyplex in the optimum composition.....	68
3.6.2 Cytotoxicity of T704, peptide 9, Lipofectamine2000 and brPEI	69
3.7 <i>In vivo</i> evaluation of ternary complexes	70
3.7.1 <i>In vivo</i> mRNA expression mediated by ternary complex	70
3.7.2 <i>In vivo</i> evaluation of pDNA transfection efficiency mediated by ternary complex	72
3.7.3 <i>In vivo</i> toxicity of ternary complex	74
3.8 <i>In vivo</i> long-term transgene expression mediated by ternary complexes containing SleepingBeauty (SB) transposon system.....	77
3.8.1 <i>In vivo</i> long-term luciferase expression	77
3.8.2 <i>In vivo</i> long-term CFTR expression	78
3.9 Preliminary evaluation of ternary complexes comprising other poloxamines or poloxamers	80
3.9.1 <i>In vitro</i> evaluation of ternary complexes consisting of T304.....	80
3.9.2 <i>In vitro</i> evaluation of T904 based ternary complexes	83
3.9.3 <i>In vitro</i> evaluation of ternary complexes consisting of T90R4	86
3.9.4 <i>In vitro</i> evaluation of ternary complexes consisting of L64.....	90
4 DISCUSSION	94
4.1 Establishing and characterization of ternary complexes	95
4.2 Investigations of the underlying mechanism of the superior transfection efficiency of ternary complex compared with the binary counterpart.....	96

Table of Contents

4.3 Optimizing peptide structure with different candidate modules	97
4.4 Comparison of the transfection efficiency of ternary complexes with other nonviral transfection reagents.....	99
4.5 Cytotoxicity	100
4.6 In vivo long-term restoration of CFTR deficiency.....	101
4.7 Distinct behaviors of ternary complexes comprising different poloxamines.....	105
5 SUMMARY	107
5 ZUSAMMENFASSUNG.....	109
6 APPENDIX	111
6.1 Abbreviations	111
6.2 Supporting figures and tables	115
7 REFERENCE	121
8 PUBLICATION	132
9 ACKNOWLEDGEMENTS	133
AFFIDAVIT.....	135

1 INTRODUCTION

1.1 Gene therapy for cystic fibrosis

Gene therapy is a potent therapeutic approach for many hereditary disorders in the lung which are intractable to current treatments. Among these genetic diseases, cystic fibrosis (CF) is the subject at the front line of numerous preclinical studies and human clinical trials. CF is a hereditary disease mainly occurred within Caucasian populations. Although CF is a rare disease with an incidence of one per 2,700-3,600 newborns¹, there are still more than 80,000 people in the European Union and the United States suffering from this disease. CF influences many organs of the CF patient, including the lung, the liver, the gastrointestinal tract and so on, with the airways most severely influenced². Different organs also display different clinical symptoms from non-typical one to classical presentations³. The most common clinical symptom of CF patients is that their airways are severely influenced by bacterial infection as well as neutrophilic inflammation resulted from the thickened mucus covered on the airway epithelia⁴. The majority of CF patients die from the deteriorated lung diseases. The lifespan of CF patients could currently reach to around 40 years because of the developed medical care conditions and some small molecular drugs. Nevertheless, there are still no remedies which target to correct the origin of the disease, and the CF patients still suffer from a heavy burden of medication⁵.

CF was first recorded as a disease entity in 1938, whereas the underlying mechanism of this disease at the genetic level was revealed until 1989 when scientists found that CF is caused by the mutations in the *cystic fibrosis transmembrane conductance regulator* (CFTR) gene⁶⁻⁸. The CFTR gene is composed of 27 exons and contains a region of 190 kb⁷. CFTR gene encodes for a protein (CFTR protein) which consists of ~1500 amino acids with many functional domains within⁹. The CFTR protein should be localized to the apical membrane of

the epithelium of many organs (e.g., the airway, the sweat gland and the gastrointestinal tract) to exert their functions¹⁰.

The CFTR protein plays a pivotal role in the regulation of cyclic adenosine monophosphate (cAMP) activated bicarbonate/chloride (Cl^-) transport and sodium channels within the epithelium (**Figure 1.1-1a**)¹¹. When the CFTR protein is dysfunctional, decreased mucociliary clearance and increased transepithelial water absorption would happen due to the abnormal transepithelial sodium absorption and decreased transepithelial Cl^- secretion (**Figure 1.1-1b**)¹²⁻¹⁴. At the same time, the reduced bicarbonate secretion due to the dysfunctional CFTR may down-regulate the airway surface pH, which subsequently abolishes the innate bacterial defense mechanism and destroys the antibacterial activity of the airways (**Figure 1.1-1b**)^{15,16}. The decreased antibacterial activity may initiate the deteriorated clinical symptoms in which a sterile newborn finally becomes a bacteria colonized condition⁵. Apart from that, many studies suggest that the CFTR protein is also expressed in some inflammatory cells including T cells, neutrophils and macrophages, indicating that the CFTR protein may have essential functions in the process of adaptive immune responses¹⁷⁻²¹. Though it is still in controversy, this hypothesis would be helpful in explaining the deteriorated inflammatory responses in the airway of CF patients²².

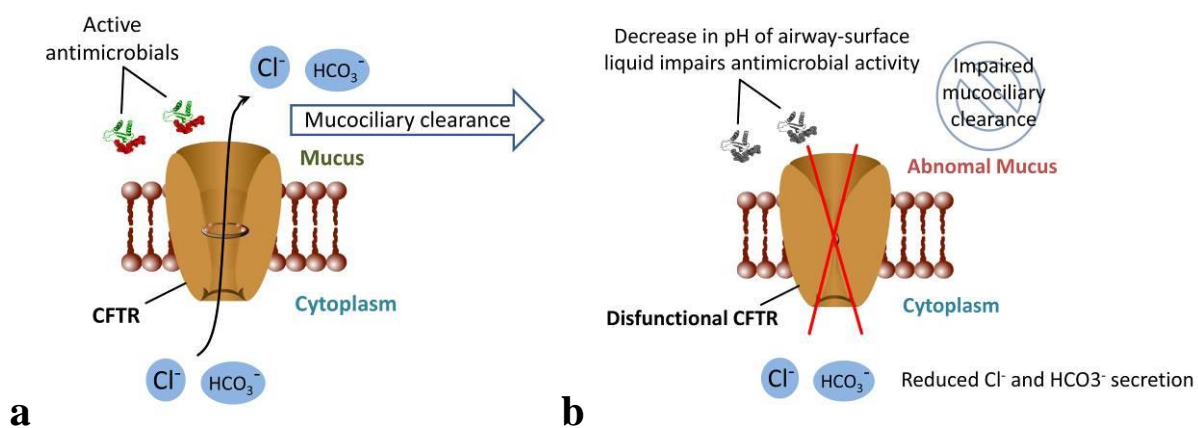


Figure 1.1-1 Schematic illustration of the CFTR functions in the case of the normal airway (a) and the case of CF airway induced by dysfunctional CFTR (b). CFTR regulates the transport of chloride (Cl^-) and bicarbonate (HCO_3^-) across the epithelial cells. The normal airway is protected from exogenous bacteria and substances via endogenous antimicrobial mechanism and mucociliary transport that removes the foreign materials (a). The dysfunctional CFTR induces a decreased pH of airway surface liquid and the subsequent inhibition of bacterial killing abilities (b). The malfunction of CFTR protein within submucosal glands also influences the properties of mucus which is incapable of fulfilling the mucociliary clearance ability (b).

The accurate presence of functional CFTR involves a set of cellular processes which should be occurred in a coordinated way. These processes include 1) the translation of primary CFTR transcript and its subsequent splicing; 2) the secretory process of CFTR protein; 3) localization of CFTR protein in the apical membrane of certain cells¹⁰. There are over 2000 kinds of mutations within the CFTR gene being revealed up to date, but not all of them are disease causing¹. Based on the resulting cellular phenotype, these mutations have been classified into six classes². CFTR expression is completely abolished within class I to III mutations while residual CFTR function could be found within classes IV to VI mutations. As a result, class I to III mutations are severe mutations and classes IV to VI mutations belong to mild mutations (**Table 1.1**)². In class I mutations, transcribed messenger RNA is degraded by premature stop codons, thus the transcription process of CFTR gene is interrupted. Regarding class II mutations, CFTR protein is excluded from reaching the apical membrane due to premature degradation induced by endoplasmic reticulum (ER) retention²³. The most frequently occurred CF phenotype causing mutation termed Phe508del, which can be detected in above 90% of CF patients worldwide and is associated with severe clinical symptoms, belongs to class II mutations²⁴. Phe508del is caused by the deletion of 3 nucleotides encoding phenylalanine within the CFTR protein^{6,25}. Such abnormal CFTR protein is misfolded and subsequently degraded due to the ER retention. For class III mutations, translated CFTR protein could reach the apical membrane but displays impaired channel function. The decreased flow rate of Cl^- and channel conductance could always be observed in class IV mutants due to the wrong location of CFTR protein within the channel conducting pore. Class V mutations could result in partial abnormal transcripts, and the amount of CFTR proteins

within this class of mutations could be varied from patient to patient^{26,27}. Class VI mutations always result in the production of CFTR protein with reduced surface retention ability. One reasonable approach for CF treatment is to correct the abnormal CFTR proteins that produced in a specific class of mutations. For example, some aminoglycoside antibiotics and synthetic small molecular drugs could camouflage the premature termination codons within class I mutations and subsequently suppress the translational fidelity to produce full-length CFTR transcript^{28,29,30}. For the treatment of class II mutations, some potent pharmacological chaperones are employed to bind with dysfunctional CFTR proteins in order to increase their stability³¹. The resulting complex is able to escape from ER retention and correctly localizes to the apical membrane³². Some CFTR activators (also termed as CF potentiators) have shown their promising in the correction of the channel defects within class III mutations³³. The most successful CFTR activator is ivacaftor (developed by Vertex Pharmaceuticals with the trademark of Kalydeco[®]) which has been approved by FDA³⁴. In clinical studies, the administration of ivacaftor led to improvement in pulmonary function and to lower levels of sweat chloride concentrations. Ivacaftor showed efficiency in clinical studies lasting from 24 to 96 weeks in subjects with the forced expiratory volume in the first second greater than 40% of the expected value³⁵. Fewer hospital stays, pulmonary exacerbations and antibiotic use were also observed. However, this revolutionary drug faces one serious drawback, since ivacaftor is only effective in a small group of CF patients carrying G551D mutation in the class III CF mutations, which affects less than 5% of patients with CF^{35,36}. Another FDA-approved CFTR “potentiators” is Lumacaftor/ivacaftor (Orkambi[®]). Lumacaftor is a CFTR corrector which is able to aid in the maturation of CFTR protein and its trafficking to the cell surface within patients who hold the Phe508del mutation³⁷. However, the efficacy of Orkambi[®] appears much lower than the one of the Kalydeco[®], which significantly limits the wide applications of Orkambi[®]³⁸. The treatment of class IV to class VI mutations is normally

fulfilled by the utilization of “class II pharmacological chaperones” and “class III CFTR activators” to increase the total amount of CFTR protein localized to the apical membrane¹⁰.

Table 1.1 Classifications of mutant CFTR gene

Mutation class	Underlying reason	example
I	Abnormal protein translation	G542X
II	Abnormal protein processing	Phe508del
III	Abnormal channel regulation	G551D
IV	Abnormal protein conductance	R117H
V	Decreased protein production	A455E
VI	Decreased protein surface retention	c.120del23

Nevertheless, there are still many CF mutations that could not be classified because the mechanism of these mutations is not revealed yet². Moreover, CF patients who share the identical class of mutations may show different responses after receiving the same type of therapeutic compound. Bisaminomethylbithiazole would be a prominent example for such case in which this remedy is valid for the treatment of Phe508del in class II mutants but is invalid for another class II mutation named P574H³¹. Therefore, therapeutic approaches aiming to target specific mutations are not ideal in the practical applications where more complicated CFTR genotypes occur. Different from the established small molecule drugs that are only valid for one specific mutation, there are no limitations in the approaches of utilizing gene therapy which aims to correct the dysfunctional CFTR at the genetic level. All types of classified and unclassified CF mutations could be beneficial from the same kind of gene therapy, without the need to determine what types of mutations the patients hold. Moreover, gene therapy could prevent pulmonary diseases at the very early stage.

1.2 CF gene therapy in clinical trials

Gene therapy for CF was enabled by the discovery of the CFTR gene in 1989⁶⁻⁸. The successful utilization of gene therapy in the case of other monogenic disorders significantly inspired the application of gene therapy for CF. The most common strategy of CF gene

therapy is to deliver therapeutic payloads containing genetic information to the airways of CF patients as their life expectancy and quality of life are mainly determined by the severity of lung diseases. Gene therapy is well-suited to the treatment of CF because the major target organ could be easily accessible via noninvasive topical application routes. The restoration of CFTR function in the airways could only be achieved when the wild-type CFTR gene is successfully delivered into the differentiated airway epithelial cells. Despite urgent needs for potent therapeutics, gene therapy for CF has been extensively investigated for decades and is still on the march through the windy road.

Up to date, twenty-six clinical trials of CF gene therapy have been performed³⁹. The majority of them were designed for “proof of concept” and to test the safety profiles. By the application of nonviral or viral-based approaches, two clinical trials of CF gene therapy were powered to evaluate the improvements of the lung conditions of CF patients^{40,41}. The inefficient delivery of the exogenous therapeutic gene due to the limited understanding of numerous barriers existed within the pulmonary gene delivery, the transient gene expression and difficulties with repeat-dosing contribute to the limited success of CF gene therapy in clinical trials⁴².

1.2.1 CF clinical trials with the utilization of viral vectors

Adenovirus The first clinical trial for CF gene therapy was performed in 1993, just 4 years after the cloning of CFTR gene, when Zabner and colleagues adopted adenoviral vectors expressing functional CFTR to transfect the airway epithelial cells of CF patients. Although this study was not placebo controlled and the number of patients enrolled was low, this initial work proved that gene therapy is feasible regarding the correction of the Cl⁻ transport defect

among CF patients⁴³. Based on this study, 9 clinical trials for CF gene therapy using adenoviral vectors have been performed in the following years^{44–52}. Even though the adenoviral vectors hold the advantage of large packaging capacity, all the clinical trials based on this vector were failed due to the transient and low levels of gene expression. Apart from that, patients who receive adenoviral vectors tend to develop severe immune responses which in turn make the repeated-dosing impossible. All these disadvantages of adenoviral vectors suggest that they are unqualified candidates in the CF gene therapy field. However, many investigations aiming to address these disadvantages of adenoviral vectors have been performed. In order to enhance the cellular uptake of adenoviral vectors via increased interactions between adenoviral vectors and their receptors which are expressed in airway epithelium, sodium caprate which acts as a tight junction opener was applied^{53,54}. In the effort to decrease the immune stimulating properties of adenoviral vectors, scientists optimized the viral coding sequences of adenoviral vectors based on immune suppressive strategies^{55–57}. Nevertheless, all these improvements were just validated in pre-clinical studies. More investigations performed in the bacteria infected lungs of or CF patients are required to prove their efficiency.

Adeno-associated viruses adeno-associated virus (AAV) belongs to a type of non-enveloped and nonpathogenic viral vector which contains a single-stranded DNA. AAV vectors are attractive candidates for CF gene therapy because they have a tropism to the lung and provide long-term gene expression. Clinical trial for CF gene therapy using AAV vectors initiated in 1998 and followed with 5 other trials^{40,58–62}. The results from all these clinical trials revealed that using AAV vectors for the transfecting the airways of CF patients is relatively safe, but their expression efficiency is still not enough to reach an obvious therapeutic effect^{40,62}. The reason for their low transfection efficiency is the size limitation of packaging. A full-length functional promoter could not be integrated to drive the expression of the CFTR gene loaded

within the vectors because the packaging capacity of AAV vectors is limited to five kb⁶³. Apart from the deficient transfection profile, AAV vectors also make the CF patients develop severe immune responses which significantly exclude the chances for repeated-dosing^{59,60,62}. Although improvements towards overcoming the inherent limitations of AAV vectors (such as immunogenicity and low transfection efficiency) have been done^{64,65}, there is a report showing that AAV vectors may potentially integrate into the genome and the mitochondrial genome of recipient⁶⁶. Even though such integration was found to be random, the safety issues related to the applications of AAV vectors in human studies still need to be carefully considered.

Lentiviruses Up to date, there are no results of the clinical trial for CF gene therapy using lentiviral vectors yet, but the United Kingdom Cystic Fibrosis Gene Therapy Consortium is now preparing for a lentiviral vectors based phase I clinical trial for CF patients¹, because the lentiviral vectors have shown promising results in many pre-clinical studies. The lentiviral vectors are ideal for transfecting the well-differentiated airway epithelial cells within CF patients as they contain RNA based genetic information which is suitable for the transfection of both dividing and nondividing cells⁶⁷. Study using lentiviral vectors to transfect the airways of CF pigs indicated that *in vivo* gene transfection mediated by lentiviral vectors was very efficient⁶⁸. Besides, lentiviral vectors are advantageous over the above-mentioned AAV and adenoviral counterparts because they do not result in significant inflammatory responses. Previous studies also revealed that lentiviral vectors are suitable for repeated-dosing^{69–71}. Lentiviral vectors have been successfully applied in the treatments of Wiskott Aldrich syndrome as well as metachromatic leukodystrophy^{72,73}, their long-term tolerability and safety profile have also been proved in Parkinson patients⁷⁴. Despite all these promising profiles of lentiviral vectors, knowledge on their long-term systematical toxicity as well as the potential

possibility of insertional mutagenesis is still limited, and more evaluation should be performed before lentiviral vectors are translated into clinical applications for CF patients.

1.2.2 CF Clinical trials with the utilization of nonviral-vectors

Nonviral vectors are emerging and promising candidates for gene therapy. Increasing numbers of studies have adopted nonviral vectors to deliver *in vitro* transcribed messenger RNA (mRNA) or plasmid DNA (pDNA) in the theme of gene therapy^{75,76}. Nonviral vectors could achieve the purpose of efficient *in vivo* delivery and controlled-release properties^{77–79}, because they were biocompatible and can be easily adjusted to possess different properties. Nonviral vectors are typically composed of a genetic payload such as pDNA or mRNA encoding CFTR protein and a carrier system that can interact with and condense the genetic payload. The carrier system is generally derived from nature-product or biocompatible materials. The function of the carrier system is to increase the amount of functional nucleic acids payloads that being delivered to the target destination. This process could be facilitated by enhanced cellular uptake, efficient endosome escape and decreased nuclease degradation of the nucleic acids payloads etc⁸⁰. The most commonly used carrier systems can be classified into cationic lipids and polymers. Cationic lipids have been used to deliver nucleic acids for decades. Nucleic acids payloads with negative charge could spontaneously interact with the positively charged lipids materials through the electrostatic force, the resulting complexes are named lipoplexes. Some previous studies revealed that cationic lipids are more advantageous in increasing the transfection efficiency of mRNA based genetic payloads compared with the cationic polymer-based delivery vehicles^{81,82}. At the same time, numerous kinds of cationic polymers with different structures and properties have been synthesized and extensively applied as the delivery systems for the gene transfection^{83,84}. Similar to the lipoplexes, the negatively charged nucleic acids payloads could readily complex with cationic polymers,

forming polyplexes that display improved stability compared with lipoplexes counterparts⁸⁰. Many cationic polymer-based delivery systems have been optimized to an equal status of those well-established cationic lipid-based delivery systems, but cationic polymers with different structures may display completely different profiles of toxicity and transfection efficiency⁸⁵.

The first nonviral vectors based CF clinical trial was performed in 1995 by Caplen et al. Gill and colleagues conducted another CF clinical trial using the same type of nonviral vector two years later. Both of these two trials used liposomes consisting of dioleoylphosphatidylethanolamine/[N-(N',N'-dimethylaminoethane)-carbomoyl]/cholesterol to deliver pDNA encoding CFTR via an intranasal route^{86,87}. Results from these trials indicated that CFTR-pDNA could be successfully delivered to the airways of CF patients and the ion channel function regulated by functional CFTR can be partially detected, without the observation of significant immune responses and clinical adverse effects^{86,87}. However, the scientists failed to observe a significant therapeutic benefit after the treatment due to the limited duration and extent of transgene expression⁸⁶. In the following CF clinical trials using nonviral vectors, optimized formulations prepared by pDNA carrying CFTR encoding gene with EDMPC/Cholesterol liposome or GL67A liposome were investigated^{41,88-92}. It turns out that GL67A-based formulation is the most promising candidate in terms of gene transfection for airway epithelia⁹³. GL67A lipids based formulations also do not cause clinically adverse events⁴¹. This is precisely the reason why GL67A-based formulation was selected as the delivery vehicle in the most recent clinical trial for CF gene therapy⁴¹. Even though most of the nonviral-based CF clinical trials utilized cationic lipids based formulations, Konstan and colleagues adopted a cationic polypeptide based formulation to deliver pDNA encoding CFTR via single intranasal dosing to CF patients, they found this polypeptide based delivery

system displayed a comparable transfection efficiency with that achieved by the cationic lipids based formulation⁹⁴.

When compared with viral vectors, a huge advantage of nonviral vectors in the field of CF gene therapy is that they are suitable to repeated-dosing. Hyde et al. first revealed that three-times repeated dosing of formulations consisted of pDNA encoding CFTR and cationic lipids via intranasal delivery did not compromise its transfection efficiency⁹⁵. The most recent clinical trial also suggested that twelve repeated-dosing of formulations prepared by GL67A lipids and pDNA containing CFTR encoding gene once per month induced a stabilized lung function for CF patients, while the lung function of CF patients receiving placebo deteriorated after the investigated periods⁴¹. However, it should be noted that the expected endpoint, namely an improved lung function in the treatment group, was failed to be observed in this clinical trial but end up with a stabilized lung function with heterogeneous response among the CF patients⁴¹. This result indicated that the transfection efficiency and the consistency of the GL67A based formulation still need to be optimized. Meanwhile, the discovery and evaluation of next-generation genetic transfecting vectors into clinical trials should be actively pursued⁴¹.

Except for the influence of delivery vehicles, the dosing route for administering nonviral vectors is also one of the critical parameters influencing the final results of CF gene therapy. Clinical trials for CF gene therapy being performed in the first decade utilized the nasal epithelium and maxillary sinus of CF patients as the surrogates which are similar to pulmonary epithelium in cell composition and are potentially safer for early-stage clinical trials⁸⁶⁻⁸⁹. However, the pulmonary epithelium lining the airway should be the primary target for a successful CF gene therapy. Alton and colleagues first conducted a pulmonary delivery of nonviral based formulations in 1999⁹⁰ and followed by Ruiz et al.⁹², both of them observed

the correction of Cl⁻ transport defect in the lower airways of CF patients. Afterward, the pulmonary delivery route becomes the priority route when evaluating novel formulations for CF gene therapy.

1.3 Potential next generation nonviral delivery systems for CF gene therapy

The further development of delivery systems will be a key to the successful application of CF gene therapy in routine clinical practice. In the past decades, substantial advances have been achieved in the development of nonviral-based delivery systems for gene transfection. However, the vector design and mechanism understanding in this field are still limited. Continuous works are necessary to find more potent delivery vehicles which can provide high transfection activity and biocompatibility with minimal toxicity, high selectivity and specificity.

As mentioned above, polyplexes and lipoplexes comprising therapeutic nucleic acids condensed within positively charged biomaterials have proved their gene transfecting efficacy in many *in vitro* investigations^{96,97}. But these formulations may be problematic for some *in vivo* applications as they nonspecifically interact with irrelevant components (e.g., proteins or blood opsonins) or unrelated cells in biological fluids and tend to form aggregates in the physiological environment, leading to poor biodistribution, low *in vivo* efficiency and immune responses^{98,99}. In contrast, some uncharged amphiphilic polymers were found to be useful substitutions in promoting *in vivo* gene delivery^{100,101}. Among the massive numbers of amphiphilic copolymers with diverse chemical structures, poloxamine-based copolymers, comprising four poly(propylene oxide)/poly(ethylene oxide)/ (PPO/PEO) branches conjugated with an ethylenediamine moiety, represent an emerging and promising nonviral-based gene

delivery system, due to the ability of simultaneously exhibiting the properties of hydrophobicity and hydrophilicity¹⁰². The hydrophilic part (PEO) is able to create a sufficient interface with the aqueous surrounding while the hydrophobic parts (PPO) self-associate¹⁰³.

Poloxamines are typically synthesized via two steps. The propylene oxide (PO) blocks are first conjugated to the central ethylenediamine, then followed by the adding of ethylene oxide (EO) blocks, yielding in the tetrafunctional poly(ethylene oxide) terminated X-shape structure¹⁰³. Poloxamines with a broad range of molecular weights (Mw) and EO/PO ratios are commercially available with the trademark of Tetronic[®]. The hydrophilic-lipophilic balance (HLB), The Mw and the EO/PO ratio of poloxamines strongly determine their capability to self-assemble and to undergo a solution-to-gel transition in physiological conditions, as well as their performance as drug/gene delivery vehicles^{104–106}. Furthermore, the properties of the medium, especially the ionic strength and pH, also significantly influence the degree of protonation of the central ethylenediamine molecule, affecting the interactions between hydrophobic groups which finally determine the self-assembly process¹⁰³. As a result, both stimuli responsiveness and structural parameters have huge impacts on their performance as drug or gene delivery systems. Poloxamines can be classified into three main categories according to the HLB values: i) highly hydrophobic; ii) medium hydrophilic and iii) highly hydrophilic¹⁰³.

Poloxamines were first produced by BASF GmbH in the 1950s and subsequently have found a broad range of applications within the pharmaceutical and biomedical fields. Commercial utilization of such tetrafunctional block copolymers covers the field of washing solution for contact lens in a way that poloxamines are incorporated for the purpose of removing attached impurity and as a result to improve the compliance of users^{107,108}, and the field of petroleum industry where poloxamines are applied as de-emulsifier and anti-foaming agents at high

concentrations^{109,110}. The increasing knowledge in underlying mechanism and the self-assembly properties under physiological conditions¹¹¹, as well as the improvement of simplified methods for the accurate detection of target molecules within complexed samples^{112,113}, have resulted in growing interest in poloxamines as drug delivery systems. As a result, poloxamines based block copolymers have been extensively applied in the biomedical fields as tissue scaffolds^{114–119}, as components of transdermal formulations¹²⁰, as adjuvants for DNA vaccination^{121–123}, as structural elements for the polycation based nonviral vectors and for low Mw drugs delivery^{111,124,125}. Although still few, the investigations performed in the gene delivery field have shown the potential of poloxamines as promising vehicles for *in vivo* applications. In the beginning, poloxamines were found to be the most potent vehicles by Prokop *et al.* in a screen of many synthetic and natural polymers for their ability to facilitate *in vivo* gene delivery into the subcutaneous tissue¹²⁶. In the following studies, Pitard *et al.* revealed that intramuscular injection of DNA-poloxamine formulations, in both healthy mice and mice in pathological conditions, enhanced several folds the amount of recombinant protein produced with safety profiles, including luciferase, β -galactosidase, green fluorescent protein and therapeutic protein^{102,127,128}. Besides, poloxamine based formulations were also suggested to be relevant as pulmonary gene transfer reagents¹²⁹.

A recent study revealed that intratracheal delivery of a formulation comprising poloxamine 704 (T704) and pDNA in mice induced a better level of reporting gene expression in epithelial cells compared with that achieved with the “gold standard” GL67A-based formulation which was utilized in the latest CF gene therapy clinical trial¹³⁰. Moreover, the level of immune response caused by the T704-mediated gene transfection was significantly lower compared with that associated with the GL67A-based formulation¹³⁰. The authors also indicated that repeated dosing of the T704 formulation is feasible¹³⁰. These results, together

with the fact that GMP-grade T704 is commercially available, highlight the application of the T704 copolymer as a promising non-viral gene transfer reagent for pulmonary gene delivery.

1.4 Aims of the thesis

While the *in vivo* gene transfection efficiency of poloxamine-based copolymers has been well proved^{121,122,126}, their *in vitro* gene delivery profile is still poorly understood. To the best of our knowledge, apart from a few studies showing that poloxamine 904 increased the *in vitro* transfection efficiency of branched- or jet-polyethyleneimine-based polyplex (poloxamine 904 acted as tissue engineering scaffolds) and the cellular uptake of poly (lactic-co-glycolic acid)-based polyplex^{131–133}, none of the *in vitro* gene transfection profile of poloxamine-based copolymers has been systematically investigated. In a set of initial investigations, we found that neither pDNA nor *in vitro* transcribed messenger RNA (mRNA) could be transfected into cultured airway epithelial cells mediated by T704. These unexpected results suggested that T704 alone is not able to overcome various barriers posed by *in vitro* transfection, including cellular uptake, intracellular transport, endosome escape and nucleus import¹³⁴. All these barriers significantly inhibit the exogenous genetic payloads from reaching its final destination where they take effect¹³⁵. As a result, there are still huge unexplored potentials on the utilization of these tetrafunctional copolymers both *in vitro* and *in vivo*. We postulated that a significant improvement on the *in vitro* transfection efficiency by means of T704-based copolymer also promotes its *in vivo* transfection efficiency. Based on this hypothesis, we designed and developed a small library of short peptides comprising three functional moieties (**Figure 1.4-1**), namely 1) Anchor moiety containing hydrophobic moiety used to interact with PPO blocks of T704; 2) Cationic moiety consisting of several basic amino acids which are positively charged at neutral pH. The effect of this moiety is not only to efficiently condense nucleic acids but also facilitates an efficient endosomal escape; 3) Targeting moiety

comprising an amino acid sequence that direct the nucleic acid payloads to target cells or a specific subcellular compartment.

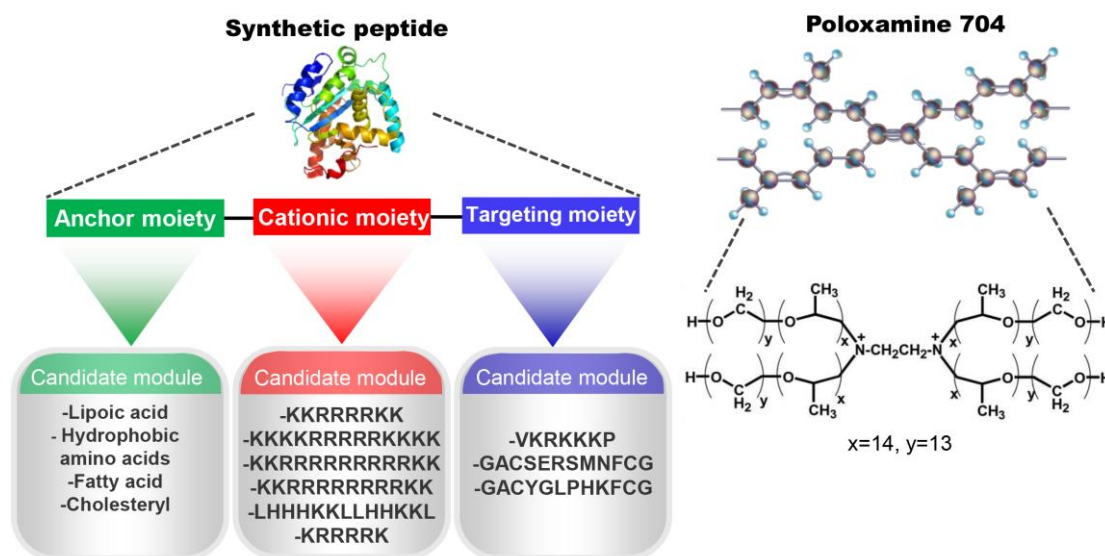


Figure 1.4-1 Structures of the synthetic peptides and T704 used in this study.

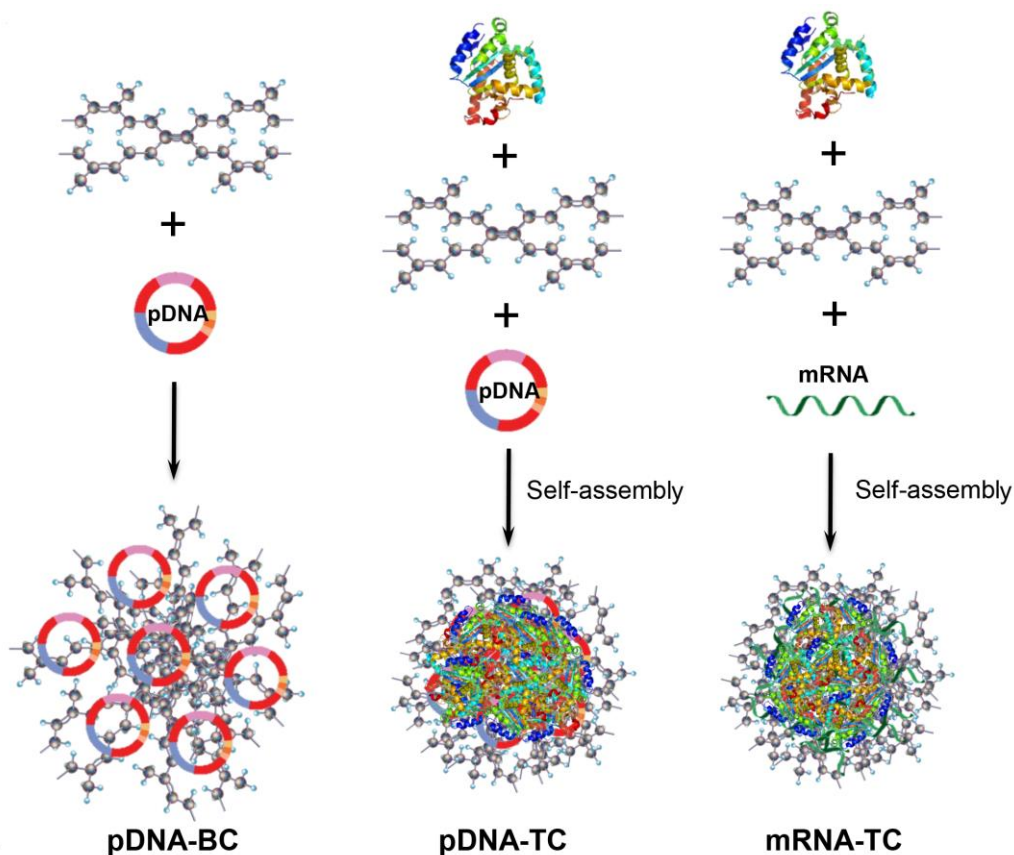


Figure 1.4-2 Schematic showing the complex formation. pDNA based binary complex (pDNA-BC) was formed by direct mixing of pDNA with T704; pDNA based ternary complex (pDNA-TC) was prepared via self-assembly of the synthetic peptide, T704 and pDNA; mRNA based ternary complex (mRNA-TC) can be obtained in the similar way of the pDNA-TC counterpart.

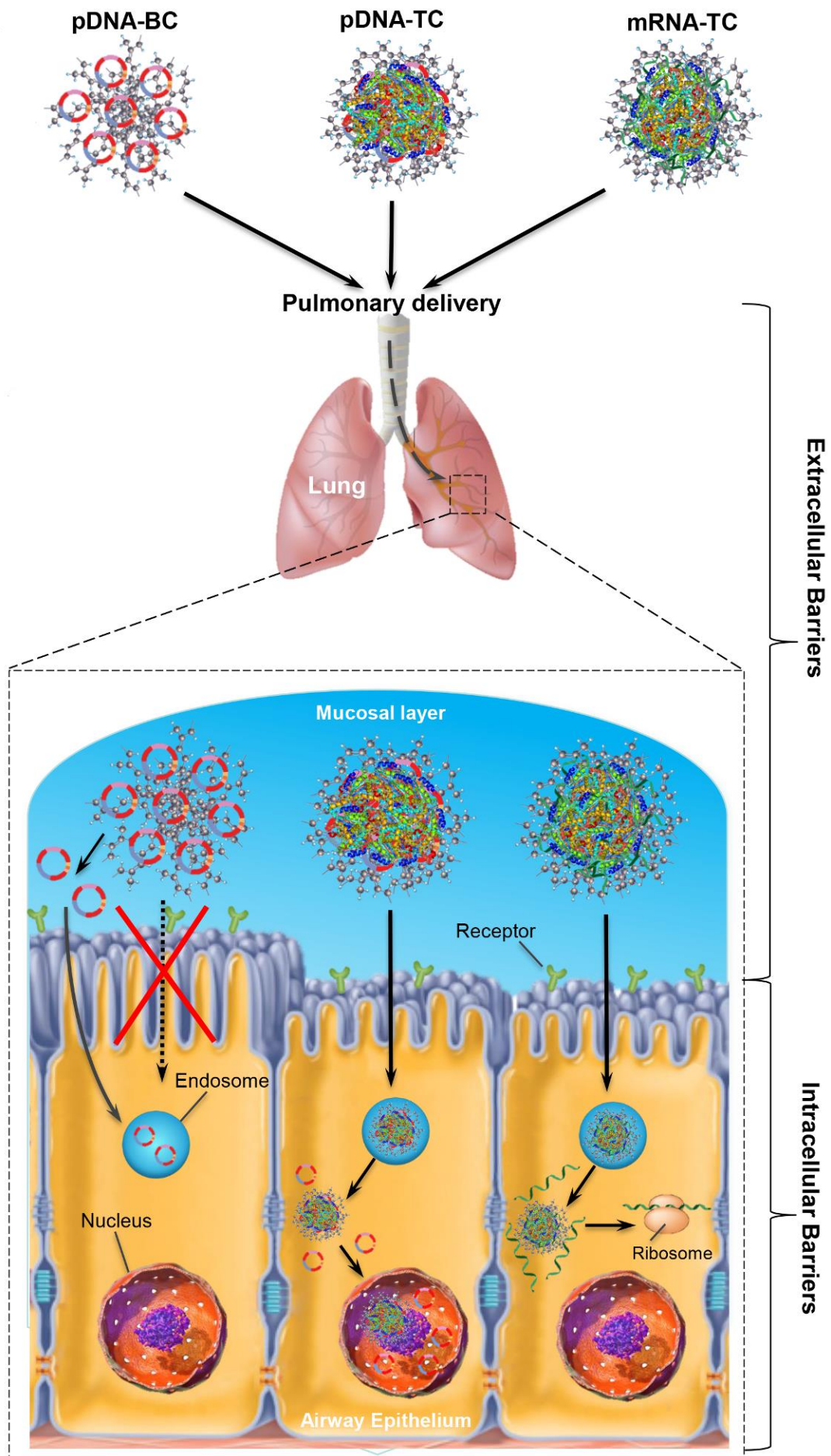


Figure 1.4-3 Hypothetical pulmonary delivery process of pDNA-BC, pDNA-TC and mRNA-TC. Although all these nanocomplexes could overcome extracellular barriers in lung tissue by virtue of T704, pDNA-BC were prevented from entering target cells by various intracellular barriers, its pDNA payloads presumably translocate into cells via passive diffusion. In contrast, the synthetic peptide in ternary complexes affords the ability of efficient delivery of genetic payloads into target cells and organelles by addressing intracellular barriers.

These peptides are expected to spontaneously form ternary complexes with the T704 copolymer and nucleic acids via a simple self-assembly process (**Figure 1.4-2**), thus to address above-mentioned subcellular barriers (**Figure 1.4-3**). In the present study, we first confirmed the formation of ternary complexes and characterized their physicochemical properties. After clarifying the critical role of each moiety within peptide structure, the cellular uptake and the subcellular fate of ternary complex as well as binary counterpart (complex formed by T704 and nucleic acids) were evaluated and compared in order to prove the advantage of the ternary complex in terms of overcoming intracellular barriers. Subsequently, we assessed and optimized the *in vitro* transfection efficiency of pDNA or mRNA based ternary complexes consisting of different peptide candidates, and compared the most potent one with other prominent nonviral gene transfer reagents regarding the transfection efficiency and toxicity. In a second phase, intratracheal application of ternary complex containing mRNA or pDNA into CF mice further demonstrated the superiority of ternary complex compared with either binary complex or cationic lipid-based formulations. Finally, we evaluated the capability of the ternary complex in the delivery of *Sleeping Beauty* (*SB*)-based transposon system consisting of *SB*-transposon (pDNA) and transposase-encoding *SB100X*-mRNA (As a transient source of transposase to avoid transposon re-integration) for *in vivo* long-term restoration of CFTR. Although previous studies established long-term gene expression within the lung of mice via intravenous delivery^{136,137}, gene transfer by this route is confined within pneumocytes and alveolar endothelial cells due to the vector entrapment¹³⁸. In terms of gene therapy for CF, genetic payloads have to be targeted to the pulmonary epithelia lining the airway which are the primary sites of CFTR expression¹³⁸.

2 MATERIALS AND METHODS

2.1 Materials

2.1.1 Reagents

Poloxamine 704 (T704) was kindly provided by InCellArt (Nantes, France). Poloxamine 304 (T304) and poloxamine 904 (T904) were generous gifts from BASF GmbH (Ludwigshafen, Germany). Poloxamine 90R4 (T90R4), poloxamer 184 (L64) and were obtained from Sigma-Aldrich Chemie GmbH (Munich, Germany). Lipofectamine2000 was obtained from Invitrogen (Schwerte, Germany). A mixture (at the molar ratio of 1:1) of 1,2-dioleoyl-sn-glycero-3-phosphoethanolamine (DOPE) and 1,2-dioleoyl-3-trimethylammoniumpropane (DOTAP) in chloroform was obtained from Avanti Polar Lipids (Alabaster, Alabama, USA). 4,6-diamidino-2-phenylindole (DAPI) and LysoTracker[®] Red DND-99 were purchased from Life technologies GmbH (Karlsruhe, Germany). Branched polyethyleneimine (brPEI, average $M_w = 25\text{kDa}$), lipoic acid, myristic acid, cholesteryl chloroformate, heparan sulfate and 3-(4,5-Dimethyl-2-tetrazolyl)-2,5-diphenyl-2H-tetrazolium bromide (MTT) were all obtained from Sigma-Aldrich (Munich, Germany). CFTR antibodies were provided by Dr. John Riordan (the University of North Carolina at Chapel Hill). D-Luciferin was purchased from Synchem (Felsberg/Altenburg, Germany). Fmoc and Boc protected amino acids, piperidine, 2-Chlorotrityl chloride resin, trifluoroacetic acid (TFA) and N,N-diisopropylethylamine (DIPEA) were obtained from Iris Biotech (Marktredwitz, Germany). All other solvents and small molecular reagents were obtained in high quality (analytical or HPLC grade) from Sigma-Aldrich (Munich, Germany).

2.1.2 Nucleic acids

Stabilized, non-immunogenic messenger RNA (SNIM mRNA) encoding metridia luciferase (MetLuc-mRNA), SNIM mRNA encoding enhanced green fluorescent protein (EGFP), SNIM mRNA encoding firefly luciferase (fLUC-mRNA) and SNIM mRNA encoding *Sleeping Beauty* (SB) transposase (SB100X-mRNA) were kindly provided by ethris GmbH (Planegg, Germany). Plasmid DNA encoding metridia luciferase (MetLuc-pDNA) was provided by Prof. Dr. Christian Plank (Technical University of Munich, Germany). SB-based plasmids, pGM206-fLUC-CFTR/T2 which contains a T2 SB transposon encoding both firefly luciferase and *Cystic Fibrosis Transmembrane Conductance Regulator*, were constructed by the group of Dr. Zoltan Ivics (Paul-Ehrlich-Institute, Langen, Germany). EGFP-pDNA was purchased from Plasmid Factory (Bielefeld, Germany). Fluorescein labelled plasmid DNA (Fluo-pDNA) was obtained from Mirus (Goettingen, Germany).

2.2 Methods

2.2.1 Synthesis of peptides

All peptides were produced by Fmoc solid phase peptide synthesis. Briefly, the solid phase was 2-Chlorotrityl chloride resin. 2-(6-chloro-1H-benzotriazole-1-yl)-1,1,3,3-tetramethylaminium hexafluorophosphate (HCTU) was used as the coupling reagent and N,N-diisopropylethylamine (DIPEA) served as the base. Lipoic acid, myristic acid or cholesterol was coupled to the peptides before deprotection and cleaving. The peptides were subsequently cleaved from the resin by incubation in dichloromethane methylene chloride/trifluoroethanol/acetic acid (70/20/10, v/v/v) at RT for 2 h. The resin was filtrated, and the solvent was removed by evaporation. After deprotection with trifluoroacetic acid/water/phenol/triisopropylethylamine (88:5:5:2) at RT for 2 h, the yield solution was

added into diethyl ether on ice for precipitation. The final peptides were purified using reverse-phase HPLC. The molecular weight (Mw) of peptides was confirmed by liquid chromatography-mass spectroscopy (LC/MS).

2.2.2 Cell culture

BEAS-2B (human bronchial epithelial cell line) cells were obtained from the ATCC (American Type Culture Collection, Wesel, Germany) and were cultured in RPMI 1640 medium (Gibco, Germany) supplemented with 10% heat-inactivated fetal bovine serum (FBS, Gibco, Germany) and 1% (v/v) penicillin/streptomycin (Gibco, Germany). 16HBE (human bronchial epithelial cell line) cells were generously provided by Prof. Dr. Dieter C. Gruenert (University of California at San Francisco, CA, USA) and were cultured in Eagle's Minimal Essential Medium (Gibco, Germany) with 10% heat-inactivated FBS (Gibco, Germany) and 1% (v/v) penicillin/streptomycin (Gibco, Germany) at 37 °C and 5% CO₂. CFBE-WT cells expressing wild-type CFTR and CFBE-delF cells which contain the most common CF phenotype causing mutation (Phe508del) were obtained from Gregory Fleming James Cystic Fibrosis Research Center (University of Alabama at Birmingham) and were cultured in the same Eagle's Minimal Essential Medium as described above. All experiments were performed on cells in the logarithmic growth phase.

2.2.3 Preparation of mRNA/pDNA based binary and ternary complexes

Stock solution of T704 (5 mg/ml) and peptide (1 mg/ml) were prepared in nuclease-free water (NF-water) and stored at 4 °C. Binary complex (T704/mRNA or T704/pDNA) was prepared

by mixing equal volumes of diluted T704 stock solution with mRNA or pDNA solution at the desired concentration in 2X Tyrode's solution¹⁰². Peptide-based binary complex was prepared in the same way in NF-water. Ternary complex was formulated via two-steps incubation. Briefly, T704 solution at a particular concentration (always be defined as weight/weight ratio of T704 to nucleic acids) in NF-water were mixed with equal volume of peptide solution at a specific concentration (defined as N/P ratio, namely the ratio between nitrogen residues in peptide and nucleic acids phosphate groups). After 20 min incubation at room temperature (RT), the same volume of nucleic acid (mRNA or pDNA) solution in NF-water was added to the above T704/peptide solution and mixed gently by pipetting up and down several times. Subsequently, the complex was incubated for another 20 min at RT prior to further use. mRNA or pDNA solution in NF-water was complexed with brPEI (25kDa) at an optimum N/P ratio, the resulting complex served as a control polyplex. As for control lipoplex, Lipofectamine2000 complex was prepared according to the manufacturer's instructions using the optimum concentration. In order to prepare DOTAP/DOPE liposomes, a lipid film was formed by removing the chloroform solvent in DOTAP/DOPE mixture solution under nitrogen atmosphere. The lipid film is hydrated with NF-water to make the final concentration of 10 mM DOTAP/DOPE. The DOTAP/DOPE liposome formulation was formed by mixing 250 μ l of pGM206-fLUC-CFTR/T2 (150 μ g) solution and 250 μ l diluted DOTAP/DOPE solution (190 μ l of 10 mM DOTAP/DOPE liposome and 60 μ l NF-water). The mix solution was incubated at RT for 20 min before further use.

2.2.4 Size and zeta potential measurements

Particle size and zeta potential measurements of binary and ternary complexes were performed using a Zetasizer Nano ZS (Malvern Instruments Ltd.) at 25 °C. The binary complex was prepared at a weight/weight ratio (T704/mRNA or pDNA) of 63:1. Ternary

complex was prepared with T704 at a weight/weight ratio of 63:1 and peptide at optimum N/P ratio using methods described above. The mRNA and pDNA concentration in both binary and ternary complexes was fixed at 10 µg/ml.

2.2.5 Transmission electron microscopy

Transmission electron microscopy (FEI Tecnai G2 F20 STWIN) was used to observe the morphology of both binary and ternary complexes. The complexes were freshly prepared using methods described above and dropped onto Quantifoil holey carbon foil (Micro Tools GmbH, Germany) to obtain the images. The concentration of T704 and nucleic acids (mRNA or pDNA) were fixed at 0.25% (w/v) and 0.2 µg/µl in both binary and ternary complexes. Peptide 9 at N/P ratio of 5 was applied in ternary complexes.

2.2.6 Agarose gel retardation assay

The extent of mRNA and pDNA condensation in binary and ternary complexes was investigated by electrophoresis on a 1% agarose gel containing 1 µg/ml ethidium bromide. Briefly, T704 at the concentration of 63 (w/w, relative to nucleic acids) and mRNA or pDNA were used to prepare binary complexes. Peptides at varying N/P ratios (1 to 6) were used to form ternary complexes with T704 at the concentration of 63 (w/w) and mRNA or pDNA. 200 ng mRNA or pDNA were added per well. To all samples, 3 µl of 6 X loading buffer (0.25% w/v bromophenol blue, 0.25% xylene cyanol FF, 30% glycerol in water) was added before loading the samples onto the gel in Tris-acetate-EDTA (TAE) buffer at 120 V for 60 min. The stability of binary and ternary complexes was examined by DNase I (ThermoFisher Scientific, Karlsruhe, Germany) digestion followed by agarose gel electrophoresis. 3 µg pDNA was complexed with T704 at the concentration of 63 (w/w) to prepare pDNA/T704

binary complex, pDNA/T704/peptide 9 ternary complex was prepared with additional peptide 9 at N/P ratio of 5. The complexes were incubated with 2.5, 5, and 10 U DNase I for 1 h at 37 °C. After phenol/chloroform extraction the pDNA was precipitated with ethanol overnight and air-dried, and the pellet was re-dissolved in NF-water. The DNA was transferred on a 1% agarose gel containing 1 µg/ml ethidium bromide. The binding strength of nucleic acids within the ternary complex was evaluated by heparan sulfate (HS) competition assay. Briefly, pDNA/T704/peptide 9 or mRNA/T704/peptide 9 ternary complex (with the same composition) was incubated with different amounts of HS at RT for 45 min, the resultant samples were resolved by agarose gel electrophoresis as above described.

2.2.7 *In vitro* transfection

For the luciferase assay, cells were seeded at a density of 1.8×10^4 /well (BEAS-2B) or 3.5×10^4 /well (16HBE) in 96-well plates 24 h before transfection to reach 60-80% confluence. Following removal of growth medium, cells were rinsed with DPBS (Gibco, Germany). 170 µl of fresh serum-free OptiMEM (Gibco, Germany) were added per well, subsequently 30 µl of complexes containing mRNA or pDNA, prepared as described above (corresponding to 400 ng mRNA or pDNA per well), was added in replicates of five. After 4 h of incubation at 37 °C in a humidified atmosphere containing 5% CO₂, the transfection medium was replaced with culture medium supplemented with 10% FBS and 1% (v/v) penicillin/streptomycin. Luciferase activity in 50 µl supernatants from transfected cells was assayed with 30 µl Metridia luciferase substrate (coelenterazine, Invivogen, France) at predetermined time point using a FLUOstar microplate reader (BMG Labtech, Germany) and relative light units (RLU) was used to express its activity. The cell culture medium was replaced with fresh one every day after sampling.

For enhanced green fluorescent protein (EGFP) expression, cells were seeded at a density of 6.8×10^4 /well (BEAS-2B) or 7.0×10^4 /well (16HBE) in 8-well slides (ibidi GmbH, Munich, Germany) 48 h before transfection to reach a monolayer (90-100% confluence). EGFP-mRNA at the dose of 600 ng/well was used to prepare complexes for transfection. The transfection procedure was the same as described above. 24 h after transfection, cells were evaluated by means of a fluorescence microscopy (Zeiss Axiovert 200 M, Carl Zeiss Microscopy GmbH, Germany).

2.2.8 Nebulization study

Nebulization experiments were conducted using a PARI Boy[®] Nebulizer (PARI GmbH, Germany)¹³⁹. Briefly, a fraction of complexes was kept apart and used as a “non-nebulized” control. The remaining solution was aerosolized for 5 minutes by employing PARI Boy[®] Nebulizer. The nebulized aerosol was collected in a separate tube. “Non-nebulized” control, collected solution (nebulized) and those remain in the nebulizer (reservoir) was incubated with pre-seeded BEAS-2B cells and 16HBE cells in 96-well plates for 4 h at 37 °C in a humidified atmosphere. Luciferase activity in 50 µl of supernatants was assayed 24 h, 48 h, and 72 h after transfection and its activity is expressed in RLU. The cell culture media was replaced each day after sampling.

2.2.9 Flow cytometry

To quantitatively determine the percentage of transfected cells expressing EGFP, EGFP-mRNA or EGFP-pDNA was complexed with T704 at the concentration of 63 (w/w) and peptide 9 at the N/P ratio of 5 to form ternary complexes. Lipofectamin2000 at a concentration of 6.7 µl/well and brPEI at N/P ratio of 20 were used as lipoplex and polyplex

control. The amount of EGFP-mRNA or EGFP-pDNA in each sample was 4 µg/well. Then the complexes were incubated for 4 h with BEAS-2B cells (6×10^5 /well) or 16HBE cells (7.5×10^5 /well) which were pre-seeded in 6-well plate 24 h before transfection. Cells were harvest 24 h (EGFP-mRNA transfection) or 48 h (EGFP-pDNA transfection) after transfection and suspended in a flow buffer (Sigma-Aldrich, Munich, Germany). 7-AAD (eBioscience, Germany) staining was used to exclude dead cells. 10 000 live cells per sample were analyzed by flow cytometry (FACS LSRFortessa, BD Bioscience, Germany). Data were analyzed with FLOWJO (Version 9.8.3, FlowJo LLC, USA).

In order to study the cellular uptake of T704-based binary and ternary complexes, 16HBE cells (7×10^5 /well) were seeded in 6-well plate 24 h before investigation. Binary complex and ternary complex containing Fluo-pDNA were prepared as described above. The amount of Fluo-pDNA in each sample was 4 µg/well. Naked Fluo-pDNA served as a negative control formulation. After 4 h incubation, the medium was removed. The cells were harvested and rinsed with cold PBS for three times followed immediately by flow cytometry analysis. The amount of 10 000 live cells were collected for each sample.

With the purpose of identifying possible internalization mechanism of the ternary complex, 16HBE cells were pre-incubated at different temperatures or treated with specific reagents at 37 °C for 1 h, then incubated with the ternary complex under the same conditions for another 4 h. (I, II) To study the effects of clathrin- and caveolae-mediated endocytosis, 10 µg/ml chlorpromazine or 1 µg/ml filipin in OptiMEM was used. (III) To examine the effect of macropinocytosis mediated endocytosis, 0.5 mM amiloride was added. (IV) To study the adsorptive mediated endocytosis, 1 mM protamine sulfate was applied. (V) Cells were pre-incubated with 35 mM sodium chlorate in cell culture medium for 24 h to investigate the effect of desulfurization, (VI) To examine the effect of an active transport inhibitor, sodium

azide dissolved in OptiMEM at the concentration of 0.5 mg/ml was incubated with cells. (VII) To study the influence of temperature on endocytosis, the experiment was carried out at 4 °C. (VIII) Excess amount of free peptide 0 (0.01 µg/µl), K4R4 peptide (cationic fragment of peptide 0, 0.005 µg/µl), lipoic acid (0.0008 µg/µl) or nuclear localization signal (NLS, 0.0035 µg/µl), were used as potential receptor-mediated endocytosis competitor for peptide 0 based ternary complex. In addition, peptide 0 based ternary complex transfected cells without any other treatments were used as the positive controls. (IX) To study the receptor-mediated endocytosis of peptide 9 based ternary complex, excess amount of free peptide 9 (0.02 µg/µl), “KWET” peptide (hydrophobic moiety of peptide 9, sequence: KETWWETWWTEWWTEW, 0.009 µg/µl), or “ligand” (targeting moiety of peptide 9, sequence: GACSERSMNFCG, 0.005 µg/µl), were used as receptor-mediated endocytosis competitors. The cellular uptake of non-treated peptide 9 based ternary complex was used as the control. The results are shown as relative uptake rate of different groups which normalized according to the positive control group.

2.2.10 Confocal microscopy

16HBE cells at the density of 4×10^5 /well were seeded in 6-well plate 24 h before investigation. Binary complex and ternary complex containing Fluo-pDNA (T704/peptide 0/Fluo-pDNA) were prepared as described above. The amount of Fluo-pDNA in each sample was 3 µg/well. LysoTracker[®] Red DND-99 was applied as endocytic vesicles marker according to the manufacturer’s instructions. After 4 h incubation, cells were rinsed with cold PBS three times. DAPI was added to visualize the nuclei 10 min before imaging. The cells were mounted with anti-fade medium and imaged on a confocal laser scanning microscope (CLSM, Carl Zeiss LSM 510, Jena, Germany).

2.2.11 Cytotoxicity assay

The effect of T704, peptide 9, Lipofectamine2000 and brPEI (25 kDa) at different concentrations on the cell viability of BEAS-2B and 16HBE cells was evaluated using a MTT assay as described in¹³⁹. Meanwhile, the cytotoxicity of T704/peptide 9/pDNA ternary complex (prepared under the condition showing highest transgene expression) against BEAS-2B and 16HBE cells were investigated and compared with Lipofectamine2000-based and brPEI-based counterparts using the same assay, 24 h after the transfection. Cell viability was calculated as a relative value (in %) compared to the control, untransfected cells.

2.2.12 Animal studies

All *in vivo* studies were performed according to the guidelines of German animal welfare law and were authorized by the local ethics committee and animal welfare authorities. B6cf mice (between 20-30 weeks of age) were obtained from the laboratory of Hans J Hedrich (Hannover, Germany) and kept under specific pathogen-free conditions undergoing a 12 h/12 h light/dark cycle with free access to food and water. Animals were conceded an adaption time of at least 7 days prior to the beginning of experiments. For all experiments, the animals were anesthetized with a mixture of medetomidine (0.5 mg/kg), midazolam (5 mg/kg) and fentanyl (0.05 mg/kg), injected intraperitoneally. For intratracheal dosing, mice received the formulations via a high-pressure MicroSprayer device as described before⁷⁷. For bioluminescence imaging, mice were anesthetized and followed by injection of the substrate D-luciferin (1.5 mg/50 ml PBS per mouse) intraperitoneally. Bioluminescence was measured 10 min later using a Xenogen IVIS In Vivo Imaging System 100 (Caliper Life Sciences, California, USA).

Transfection of mRNA-based formulations. After anesthesia, 10 µg fLUC-mRNA formulated with 0.25% T704 (Binary complex) or 0.25% T704/Peptide 9 (N/P = 5) (Ternary complex) in a final volume of 50 µl, was intratracheally administered to one mouse. NF-water (50 µl/mouse) treated mice were used as negative controls. Lungs were excised 24 h post dosing and the bioluminescence intensity was measured.

Transfection of pDNA-based formulations. pGM206-fLUC-CFTR/T2 formulated with 0.25% T704 (Binary complex) or 0.25% T704/Peptide 9 at N/P ratio of 5 (Ternary complex) or DOTAP-based cationic lipids (Lipoplex), was intratracheally administered (50 µl/mouse) to anesthetized mice. All formulations contained 15 µg pDNA/mouse. Mice which received NF-water (50 µl/mouse) were studied as negative controls. Luciferase activity was determined 48 h post dosing.

Transfection of SB transposon system-based formulations for long-term gene expression. Ternary complex comprising pGM206-fLUC-CFTR/T2 (15 µg/mouse), 0.25% T704 and peptide 9 (N/P = 5) was administered to anesthetized mice intratracheally (50 µl/mouse). After 15 min, mice received another formulation (25 µl/mouse) consisting of SB100X-mRNA (10 µg/mouse), 0.25% T704 and peptide 9 (N/P = 5). Mice treated with single dose of pGM206-fLUC-CFTR/T2-based or SB100X-mRNA-based formulations were applied as controls. All mice received repeated-dosing in an interval of 5 days (three times in total). Luciferase activity was measured at predetermined time points.

2.2.13 Histology

To detect pathohistological signs of inflammation, lung (or trachea) tissues were obtained from mice 48 h after intratracheal dosing of pDNA-based binary complex or ternary complex or DOTAP-based lipoplex as described above. Lung tissues were filled with Tissue-Tek® O.C.T.™/PBS (1:10), fixed in 4% formalin and embedded in paraffin. Tissue sections (5 µm) were stained by Haematoxylin-Eosin and evaluated using light microscopy.

2.2.14 Immunohistochemical analysis

Lung tissue cryosections were fixed in acetone at -20°C for 10 minutes and air dried. After incubation in 10% donkey serum 100 µl primary antibody mixture was applied to the section. Antibodies detecting CFTR (“570”, University of North Carolina at Chapel Hill) and ZO1 (Abcam, ab99462) were used at dilutions of 1:100 and 1:200 respectively. After incubation at RT for 1h, excess primary antibody was removed in washing buffer. A mixture of 100µl secondary antibodies labelled with Cy3 (donkey anti mouse, 1:500) and Alexa488 (donkey anti goat, 1:200), incubated for 1h, were used for detection. Stained slides were washed in washing buffer and demineralized water and mounted with medium containing Prolong/DAPI. All images were obtained on an automated digital fluorescence microscope (Keyence BZ-9000) at 40x magnification using filters appropriate for the chosen indicators. Image post-processing (linear intensity adjustment, merging) was performed with Affinity Photo (version 1.5.1.54) and Affinity Designer (version 1.5.2.58).

2.2.15 Statistics

Unless otherwise specified, all the experiments were repeated at least two other occasions with 5 or more replicates to ensure the reproducibility of the data. Data for all bar charts were plotted using means and error bars that correspond to standard deviations. Statistical analysis was performed using Prism 7 (GraphPad Software Inc, USA). Dual comparisons were made using the Student's t-test and comparisons between multiple conditions were analyzed using ANOVA. All the tests were two-tailed. Significant differences were defined as *: $p < 0.05$; **: $p < 0.01$; ***: $p < 0.005$; ****: $p < 0.001$; *****: $p < 0.0001$; N.S. meant not significant.

3 RESULTS

3.1 Establishing poloxamine 704 (T704)-peptide ternary complexes

3.1.1 T704 based binary complexes were invalid for *in vitro* transfection

Although poloxamine copolymers have shown their efficiency as non-viral gene delivery vectors in many *in vivo* applications^{102,121,122,126,127,130}, we surprisingly recognized that these promising block copolymers are rather poor transfection reagents in delivering nucleic acids into cultured cells. Data obtained from *in vitro* transfection on human bronchial epithelial cells (BEAS-2B and 16HBE) revealed that transfection efficiency of T704-based binary complexes (unless otherwise mentioned, always refers to nanocomplexes formed by T704 and nucleic acids in following paragraphs) formed by *in vitro* transcribed messenger RNA encoding Metridia Luciferase (MetLuc-mRNA) and a broad range of T704 was all lower than 600 relative light units (RLU), which was similar to the intensity of background signal (**Figure 3.1-1a**). Binary complexes containing plasmid DNA encoding Metridia Luciferase (MetLuc-pDNA) also showed similar transfection efficiency under the same conditions (**Figure 3.1-1b**).

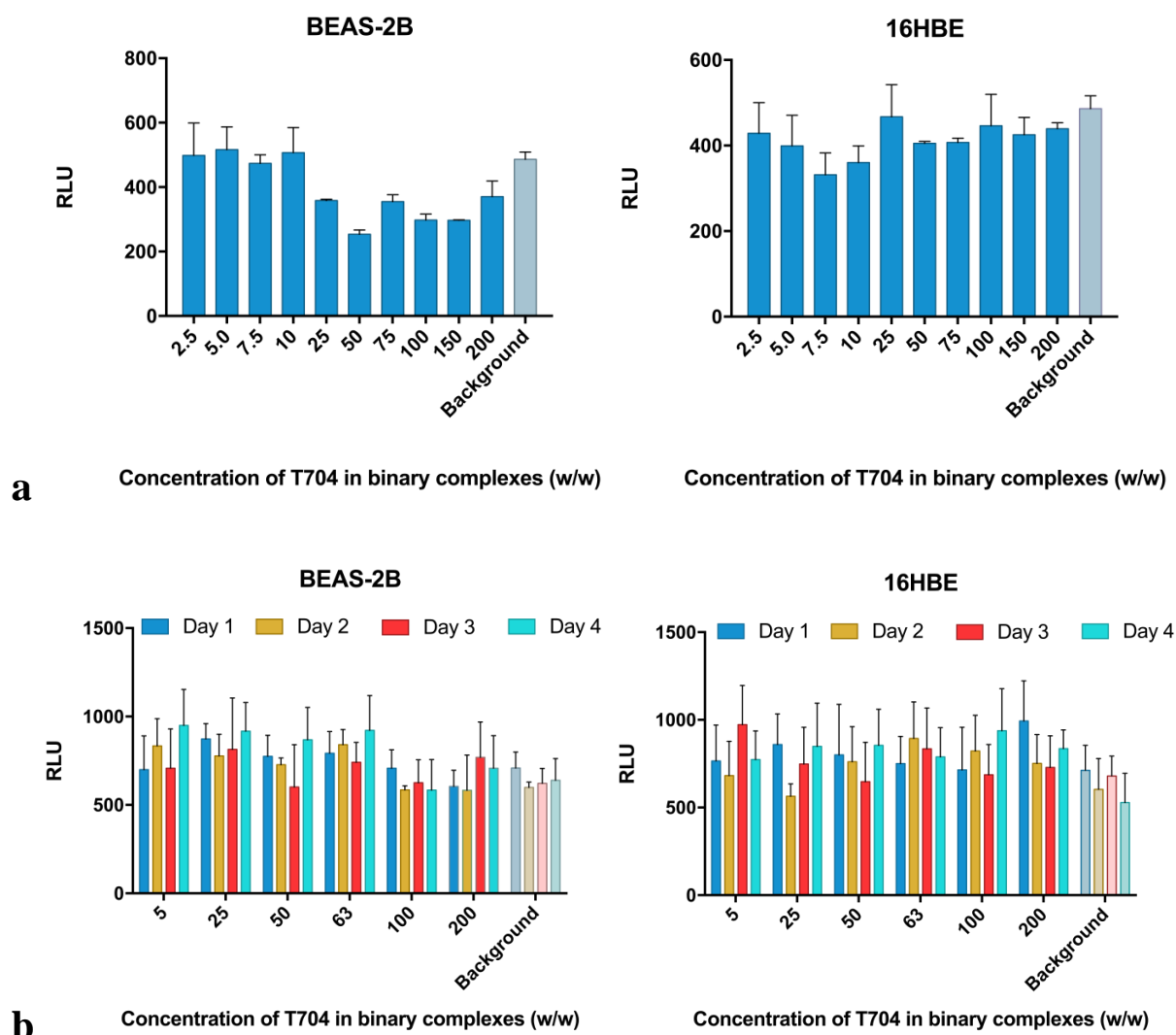


Figure 3.1-1 *In vitro* transfection profile of T704 based binary complexes in cultured human bronchial epithelial cells (BEAS-2B and 16HBE). (a) 400 ng/well MetLuc-mRNA was complexed with T704 at different concentrations from 2.5 to 200 (w/w, the concentration of T704 is always defined as the weight to weight ratio of T704 to nucleic acids in the following text) in Tyrode's solution. After 30 min incubation at room temperature (RT), samples were added into 96-well plate containing pre-seeded cells and incubated with cells in OptiMEM (without serum and antibiotics) for 4 h at 37 °C in a humidified atmosphere (95% air, 5% CO₂). Luciferase activity in 50 µl supernatants from transfected cells was assayed after 24 h and its activity was expressed in relative light units (RLU). (b) MetLuc-pDNA/T704 binary complexes were prepared in the same way of mRNA counterpart. Luciferase activity in 50 µl supernatants from transfected cells was measured at 24 h, 48 h, 72 h and 96 h after transfection and its activity was expressed in RLU. Supernatants from non-treated cells were used as the background samples. All experiments were performed at least three times. Data represent the mean ± standard deviation (SD) (n>5).

3.1.2 Investigations on parameters influencing *in vitro* transfection efficiency of ternary complex

In order to enable *in vitro* transfection of T704-based copolymers, a small library (**Table 3.1**) of synthetic peptides comprising three different functional moieties was developed to form ternary complexes (unless otherwise mentioned, always refers to nanoparticles formed by T704/peptide/nucleic acid in following paragraphs) with T704 and nucleic acids. Apart from the extensively studied pDNA molecules, the attractive and rapidly emerged mRNA therapeutics were also evaluated in current study^{140,141}.

Table 3.1. The structure of all synthetic peptides used in current study.

Name	Sequence
Peptide 0	<i>Lipoic acid-WKKRRRRKKVKRKKKP</i>
Peptide 1	KKKRRRRKKVKRKKKP
Peptide 2	<i>Lipoic acid</i>
Peptide 3	<i>Lipoic acid-WKKRRRRKKVKRKTTP</i>
Peptide 4	<i>Lipoic acid-WKKKKRRRRRKKKKGACSERSMNFCG</i>
Peptide 5	<i>Lipoic acid-WKKKKRRRRRKKKKGACYGLPHKFCG</i>
Peptide 6	<i>Lipoic acid-WKKRRRRRRRRRKKGACSERSMNFCG</i>
Peptide 7	<i>Lipoic acid-WKKRRRRRRRRRKKGACYGLPHKFCG</i>
Peptide 8	<i>Lipoic acid-WLHHHKKLLHHHKKLGACSERSMNFCG</i>
Peptide 9	<i>KETWWETWWTEWWTEWKKKKRRRRRKKKKGACSERSMNFCG</i>
Peptide 10	<i>VVVVVVKRRRRKGACSERSMNFCG</i>
Peptide 11	<i>C₁₃H₂₇CONH-KKKRRRRRKKKKGACSERSMNFCG</i>
Peptide 12	<i>Cholesteryl-KKKRRRRRKKKKGACSERSMNFCG</i>

Sequences given in italics are targeting moieties. Underlined sequences represent anchor moieties. Sequences given in bold represent cationic moieties.

We started from a prototype (peptide 0), comprising lipoic acid (LA, produced naturally in the human body and represents a well-accepted medical materials¹⁴²) which acts as anchor moiety, cationic moiety containing lysine/arginine and nuclear localization signal (NLS) at the position of targeting moiety, to investigate parameters influencing *in vitro* transfection efficiency of ternary complex in bronchial epithelial cells. As shown in **Figure 3.1-2**, the mRNA expression increased with an enhanced concentration of T704 or an enhanced N/P

ratio (the ratio between nitrogen residues in peptide and nucleic acids phosphate groups) of peptide 0, reaching maximum when T704 concentration = 63 (w/w, relative to mRNA) and peptide 0 N/P = 10. Then the mRNA expression progressively declined at higher T704 concentrations and higher N/P ratios of peptide 0. In terms of pDNA based ternary complex, a similar tendency of transfection efficiency could be observed (**Figure 3.1-3**). However, the optimum concentration of T704 and peptide 0 within ternary complex showing highest pDNA expression was cell line dependent. Ternary complex consisted of T704 at concentration of 50 (w/w) and peptide 0 at N/P = 30 showed highest transfection rate in BEAS-2B cells (**Figure 3.1-3**), whereas counterparts comprising T704 at concentration of 63 (w/w) and peptide 0 at N/P = 20 showed the highest transfection efficiency in 16HBE cells (**Figure 3.1-3**). Besides, we also found that the peptide 0 alone is not capable of mediating efficient nucleic acids transfection (**Figure 3.1-4**), emphasizing the superiority of ternary complex.

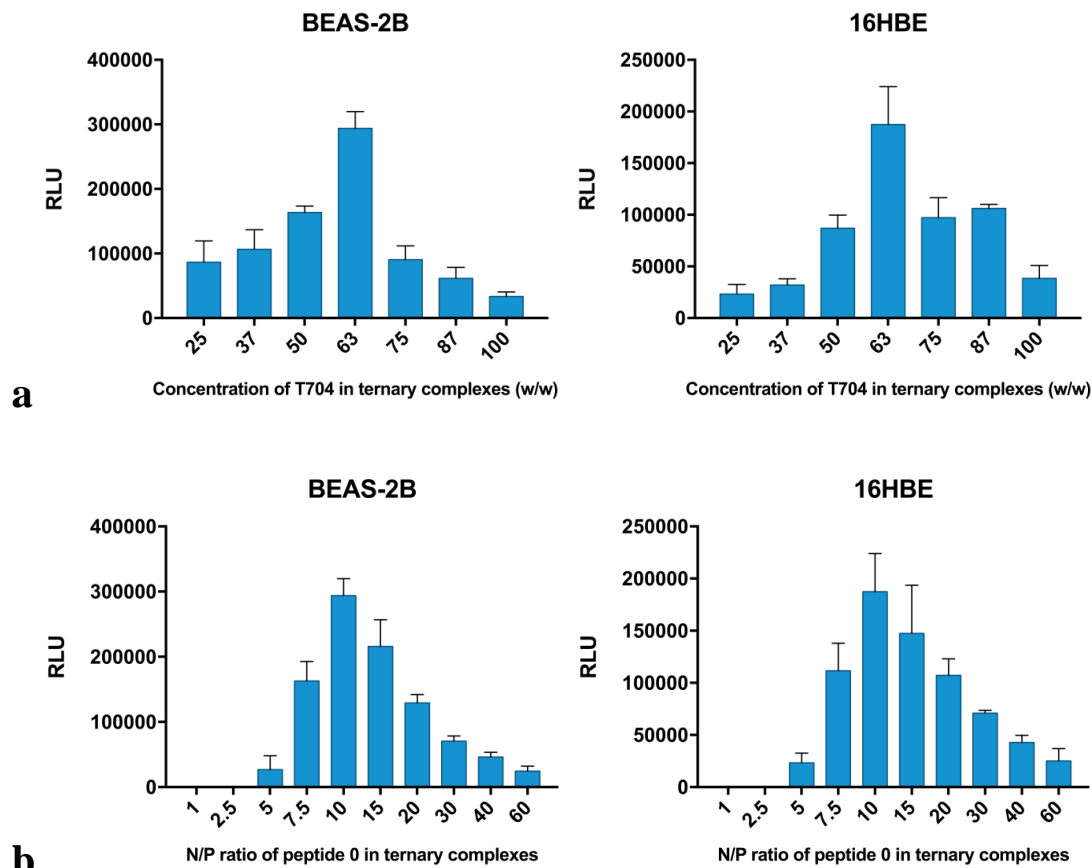


Figure 3.1-2 Investigations on parameters influencing *in vitro* transfection efficiency of the ternary complex. (a) The influence of T704 concentration (w/w, relative to nucleic acids) on the transfection of MetLuc-mRNA based ternary complex in BEAS-2B and 16HBE cells. The N/P ratio of peptide component within ternary complex was fixed at 10; **(b)** The effect of peptide 0 concentration on the transfection efficiency of MetLuc-mRNA based ternary complex in BEAS-2B and 16HBE cells. The concentration of T704 component within ternary complex was fixed at 63 (w/w, relative to nucleic acids); Luciferase activity in 50 μ l supernatants from transfected cells was assayed after 24 h and its activity was expressed in RLU. All experiments were performed at least three times. The data are given as the mean \pm SD (n>5).

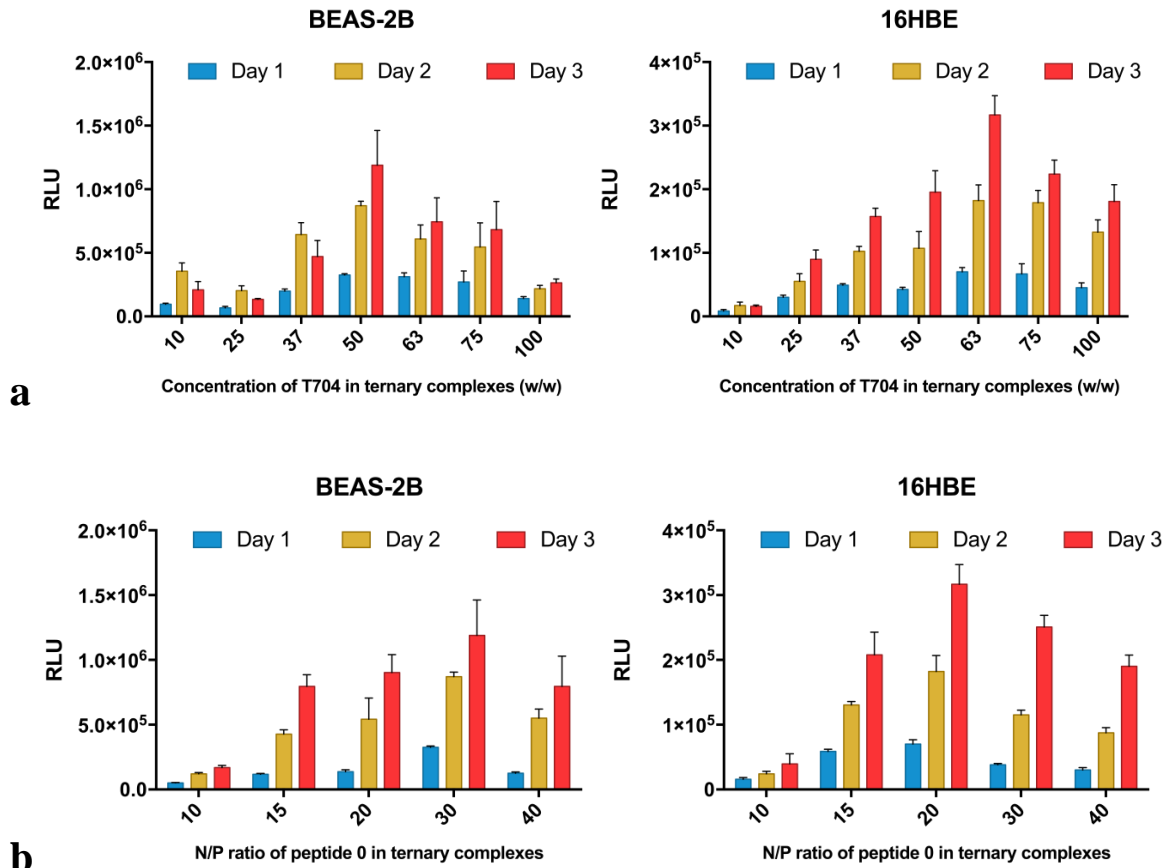


Figure 3.1-3 Investigations on parameters influencing *in vitro* transfection efficiency of the ternary complex. (a) Transfection efficiency of MetLuc-pDNA based ternary complexes consisting of different concentrations of T704 in BEAS-2B and 16HBE cells. The N/P ratio of peptide component in the case of BEAS-2B cells transfection was 30 and in the case of 16HBE cells transfection was 20; **(b)** Evaluation of MetLuc-pDNA expression mediated by ternary complexes comprising different concentrations of peptide 0 in BEAS-2B and 16HBE cells. The concentration of T704 component in the case of BEAS-2B cells transfection was 50 (w/w) and in the case of 16HBE cells transfection was 63 (w/w); Luciferase activity in 50 μ l supernatants was measured 24 h, 48 h and 72 h after transfection and its activity was expressed in RLU. All experiments were performed at least three times. The data are given as the mean \pm SD (n>5).

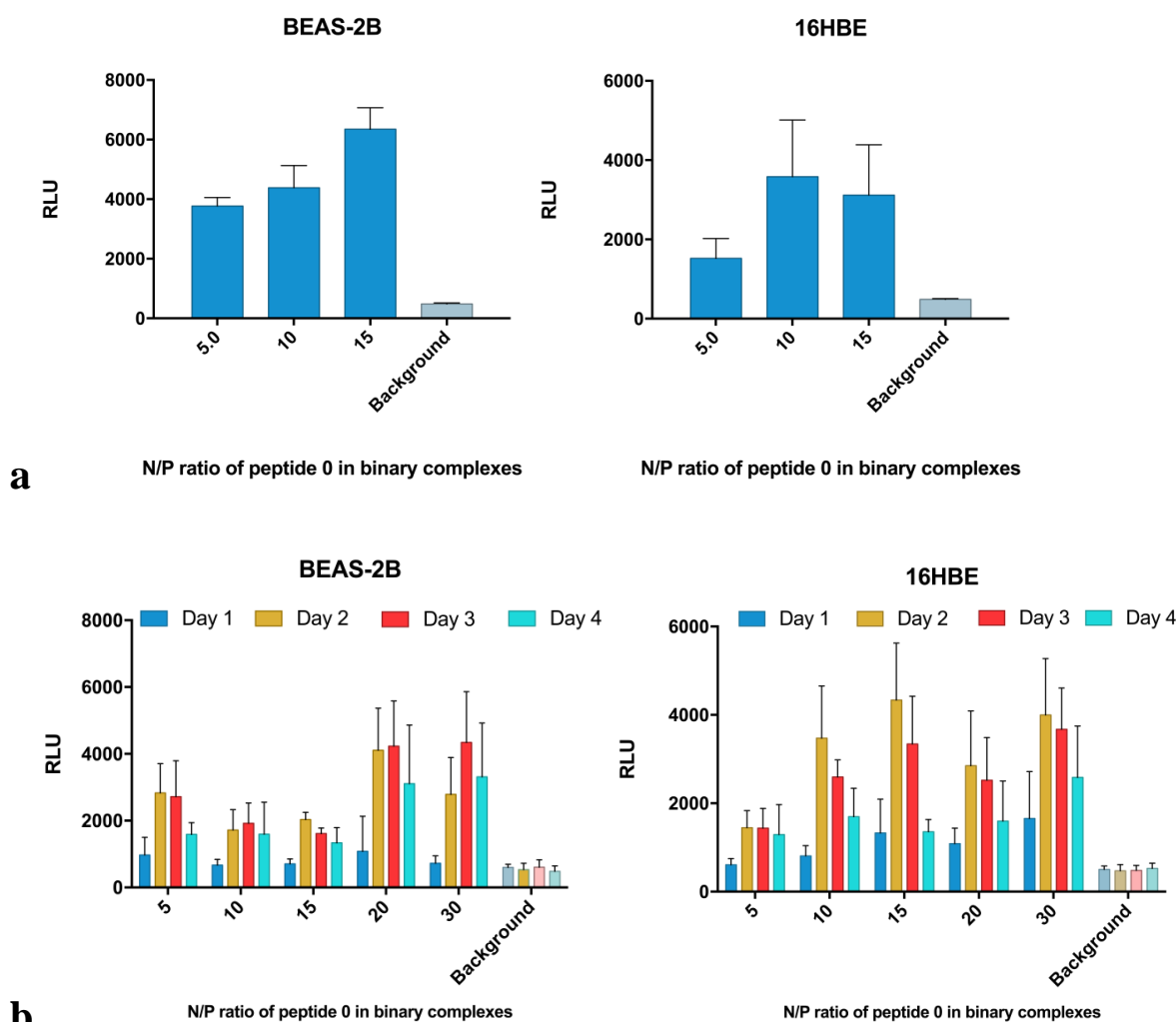


Figure 3.1-4 *In vitro* transfection profile of peptide 0 based binary complexes in cultured human bronchial epithelial cells (BEAS-2B and 16HBE). (a) 400 ng/well MetLuc-mRNA was complexed with peptide 0 at different N/P ratios from 5 to 15 (relative to nucleic acids) in nuclease-free water (NF-water). After 30 min incubation at RT, samples were added into 96-well plate containing pre-seeded cells and incubated with cells in OptiMEM (without serum and antibiotics) for 4 h at 37 °C in a humidified atmosphere (95% air, 5% CO₂). Luciferase activity in 50 µl supernatants from transfected cells was assayed after 24 h and its activity was expressed in RLU. (b) MetLuc-pDNA/peptide 0 binary complexes were prepared in the same way of mRNA counterpart, luciferase activity in 50 µl supernatants from transfected cells was measured 24 h, 48 h, 72 h and 96 h after transfection and its activity was expressed in RLU. Supernatants from non-treated cells were used as the background samples. All experiments were performed at least three times. The data are given as the mean ± SD (n>5).

Based on these results, we further evaluated other parameters that affect the transfection efficiency of the ternary complex using MetLuc-mRNA as a reporter to transfect 16HBE cells. Transfection efficiency of ternary complex was significantly influenced by the mRNA concentration (**Figure 3.1-5a**), the method of preparation (**Figure 3.1-5b**), the complex forming medium (**Figure 3.1-5c**) and the incubation time (**Figure 3.1-5d**). Therefore, we fixed the following parameters for all *in vitro* transfections of ternary complex: i) the

concentration of mRNA or pDNA in ternary complex was fixed at 400 ng/well (relative to 96-well plate); ii) ternary complex was prepared by first mixing equal volume of T704 and peptide stock solution, followed by adding equal volume of mRNA or pDNA solution; iii) ternary complex was consistently prepared in nuclease-free water (NF-water); iv) ternary complex was incubated with cultured cells for 4 h in consideration of transfection efficiency and cytotoxic side-effect.

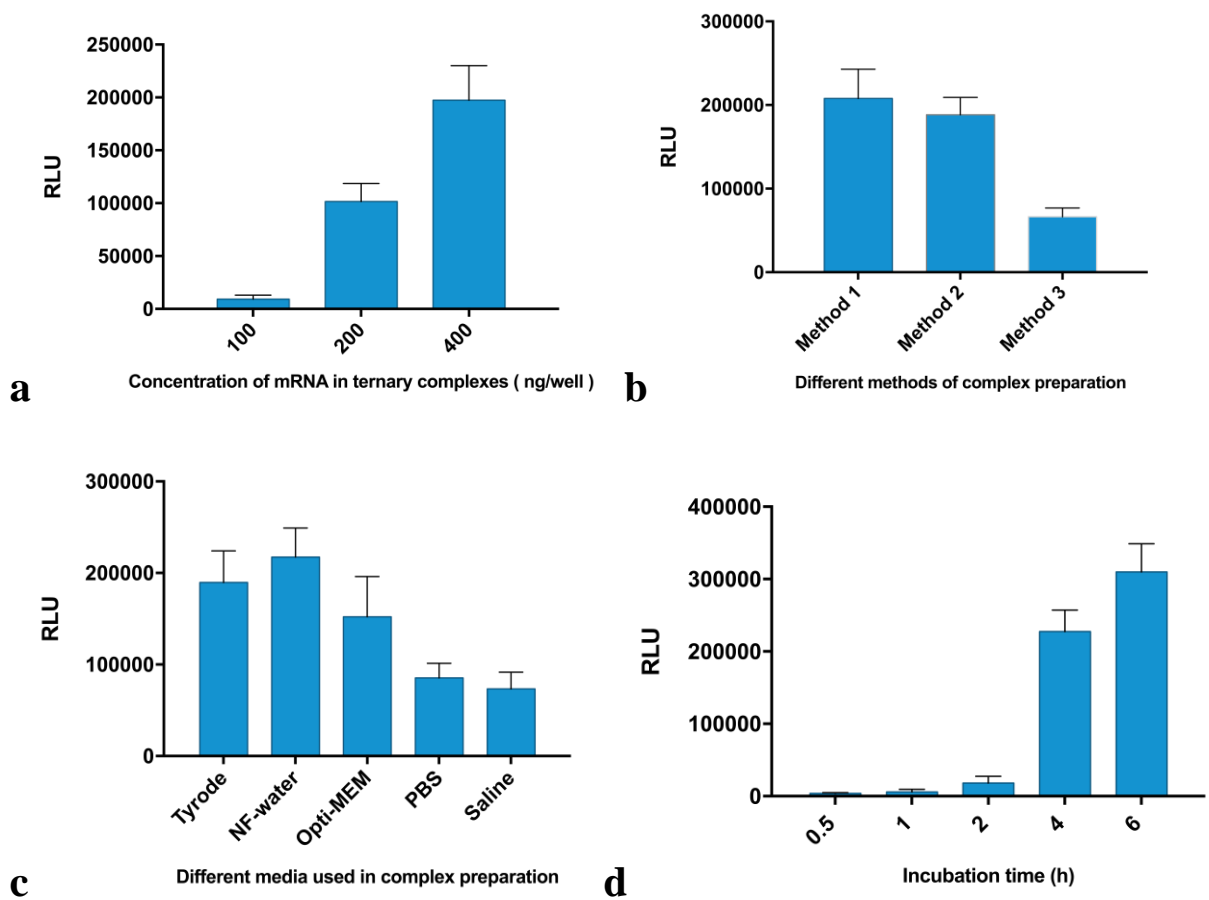


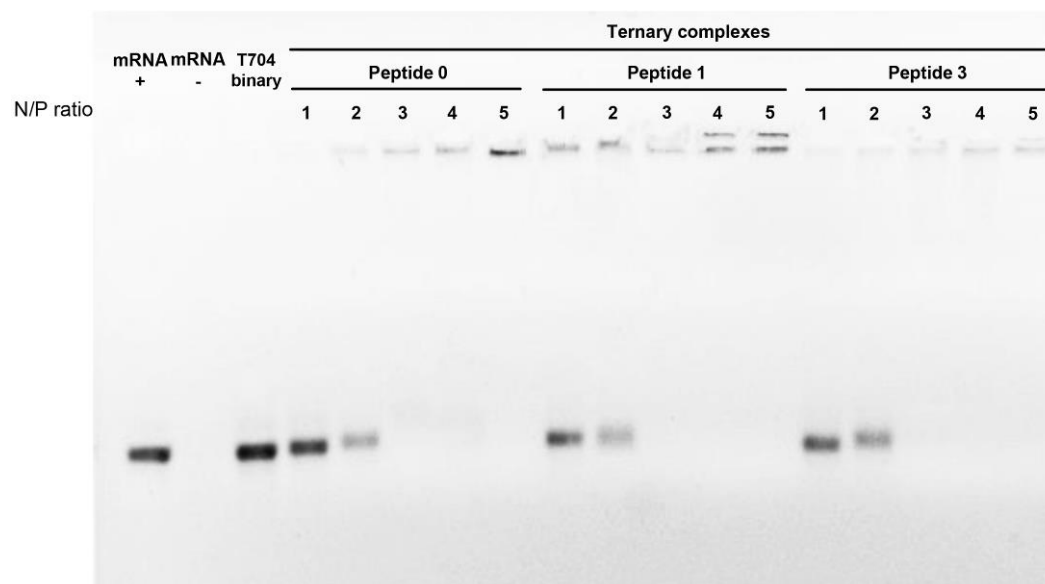
Figure 3.1-5 Investigations on parameters influencing *in vitro* transfection efficiency of the ternary complex. The transfection efficiency of mRNA based ternary complexes depending on (a) the concentration of mRNA in ternary complexes; on (b) different methods of complex preparation: Method 1: T704 and peptide 0 at optimum concentration were first mixed and incubated for 20 min, followed by adding of equal volume of mRNA solution with another 20 min incubation at RT. Method 2: in the first step, T704 and mRNA solution were mixed and incubated for 20 min incubation at RT, an equal volume of peptide 0 were added and incubated for another 20 min at RT in the second step. Method 3: peptide 0 was complexed with mRNA by 20 min incubation at RT, then an equal volume of T704 solution was introduced and incubated for another 20 min to form the ternary complex; on (c) different media used in the complex preparation; and on (d) incubation time with 16HBE cells. Luciferase activity in each assay was measured 24 h after transfection. The results represent the mean \pm SD of three independent experiments.

3.2 Characterization of ternary complexes and binary counterparts

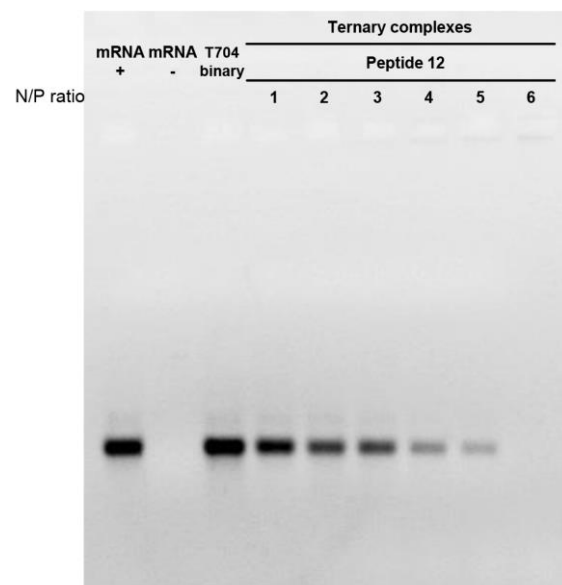
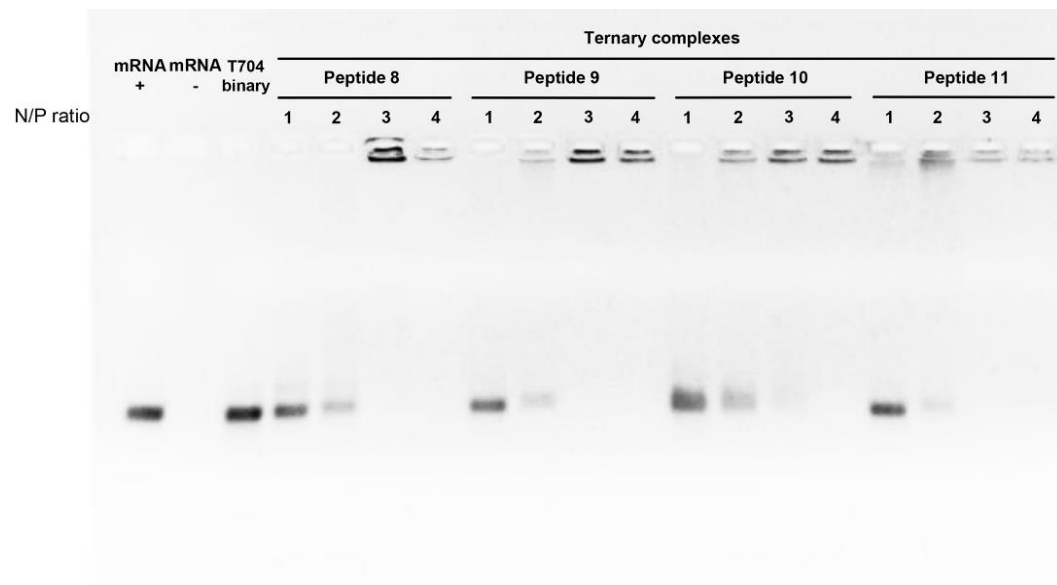
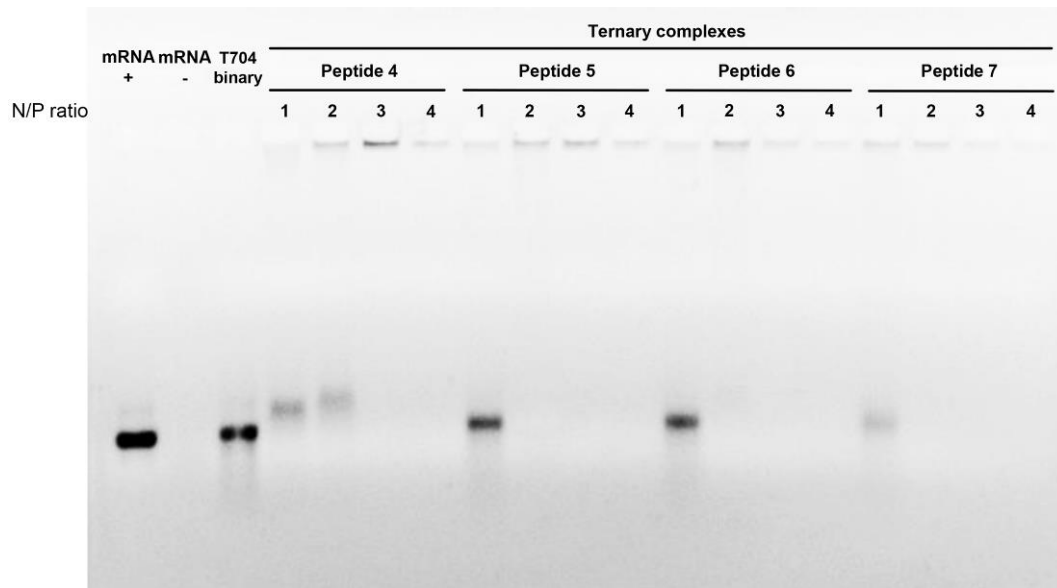
3.2.1 Agarose gel retardation assay

We analyzed the capacity of ternary complexes comprising different peptides to condense mRNA or pDNA by agarose gel retardation assay. As shown in **Figure 3.2-1**, all ternary complexes (except peptide 2-based ternary complexes because there is no positively charged amino acid within peptide 2, data not shown) can efficiently condense mRNA (**Figure 3.2-1a**) or pDNA (**Figure 3.2-1b**) when the N/P ratio of peptide component was above 3 (for peptide 12, the N/P ratio should be above 5). However, T704 at the same concentration alone was not able to retard mRNA or pDNA at all (lane “704 binary”).

a



Results



b

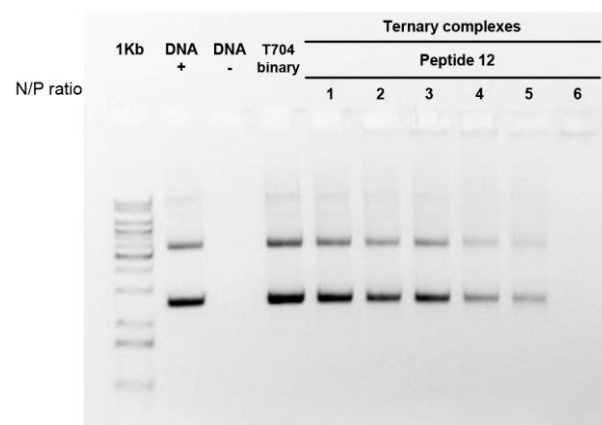
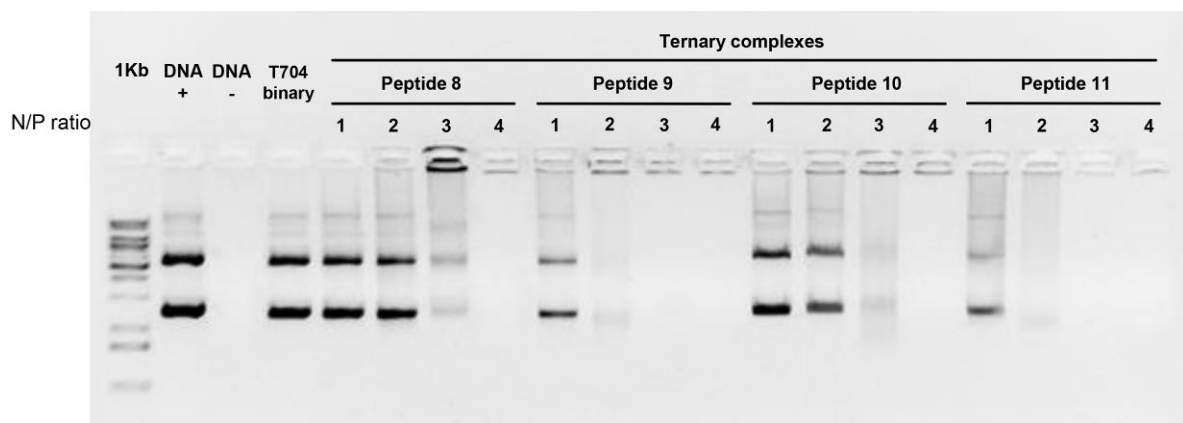
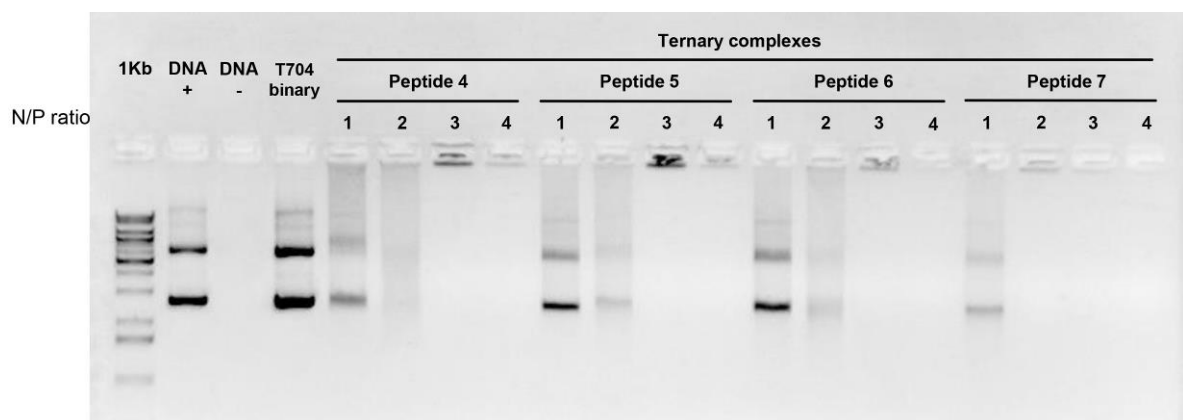
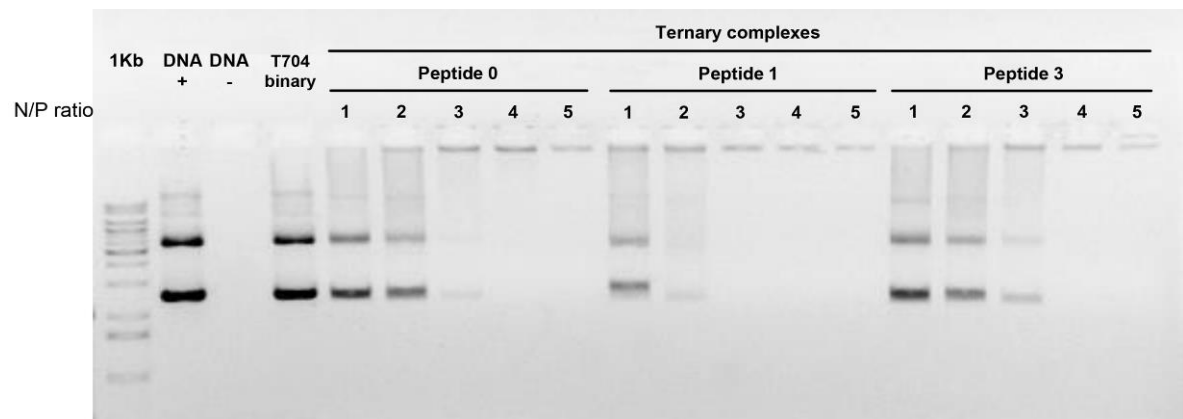


Figure 3.2-1 Agarose gel retardation assay of ternary complexes and binary counterparts. (a) mRNA condensation studies using ternary complexes comprising different peptides at various N/P ratios. Binary complex consisting of mRNA and T704 at the same concentration served as a binary control. Naked mRNA was used as a positive control (+), with NF-water as the negative control (-). (b) pDNA condensation studies using ternary complexes comprising different peptides at various N/P ratios. Binary complex consisting of pDNA and T704 at the same concentration served as binary control. 1kb DNA standard was used as a reference (1kb), naked pDNA was used as a positive control (+) with NF-water as the negative control (-).

3.2.2 Dynamic light scattering (DLS) measurements

We further evaluated and compared the physiochemical properties of binary complexes and ternary complexes via DLS measurements. pDNA formed nanoparticles with T704 in an average diameter of 206 ± 18 nm (**Table 3.2**), which was in agreement with previously published reports^{102,130}. Particles of mRNA/T704 binary complex showed, however, an average diameter of 65.2 ± 6.5 nm under the same condition, suggesting mRNA and pDNA behave distinctively with respect to polymer binding and complexation. Interestingly, the particle size of all T704/peptide/pDNA ternary complexes remarkably declined below 100 nm compared with the binary counterpart. Whereas mRNA based ternary complexes just showed a slight decrease in nanoparticle size compared with the binary counterpart. The addition of peptide component into both mRNA and pDNA based complexes on one hand increased the zeta potential of resultant complexes from negative to positive, on the other hand, ternary complexes tend to form monodisperse nanoparticles compared with binary counterparts as indicated by the polydispersity index (PDI) of each complex in **Table 3.2**.

Table 3.2 The size and zeta potential measurements of T704 based binary and ternary complexes containing mRNA or pDNA.

Complex	Particle size (nm)	Zeta-potential (mV)	PDI
mRNA + T704	65.2 ± 6.5	-23.0 ± 1.6	0.449
mRNA + T704 + Peptide 0 (N/P=10)	55.2 ± 6.3	19.3 ± 1.3	0.237
mRNA + T704 + Peptide 4 (N/P=5)	51.2 ± 5.4	15.8 ± 0.6	0.233
mRNA + T704 + Peptide 9 (N/P=5)	44.2 ± 4.2	12.8 ± 1.6	0.313
pDNA + T704	206 ± 18.0	-19.0 ± 2.3	0.518
pDNA + T704 + Peptide 0 (N/P=20)	69.8 ± 4.9	22.8 ± 0.7	0.324
pDNA + T704 + Peptide 4 (N/P=5)	68.7 ± 1.8	20.3 ± 0.5	0.238
pDNA + T704 + Peptide 9 (N/P=5)	59.6 ± 4.6	16.9 ± 2.2	0.276

All the complexes used in the assay were prepared with the T704 at the ratio of 63 (w/w, relative to nucleic acid) and the peptide at the respective N/P ratio indicated in the bracket using methods described in “METHODS”. The mRNA or pDNA concentration in all complexes was fixed at 10 µg/ml.

3.2.3 Transmission electron microscopy (TEM)

The morphology of binary and ternary complexes was investigated by TEM. As shown in **Figure 3.2-2a**, mRNA/T704 binary complex appeared as either individual or clustered suborbicular particles with uneven size, some uncomplexed mRNA molecules could also be observed (marked with arrows in **Figure 3.2-2a**). The pDNA/T704 binary complex appeared to be of large irregular shape with varying sizes (**Figure 3.2-2b**). In contrast, both mRNA (**Figure 3.2-2c**) and pDNA (**Figure 3.2-2d**) based ternary complexes spontaneously self-assembled into more compact and spherical nanoparticles with a smooth surface. Neither uncomplexed nucleic acids nor obvious aggregation could be observed within ternary complexes.

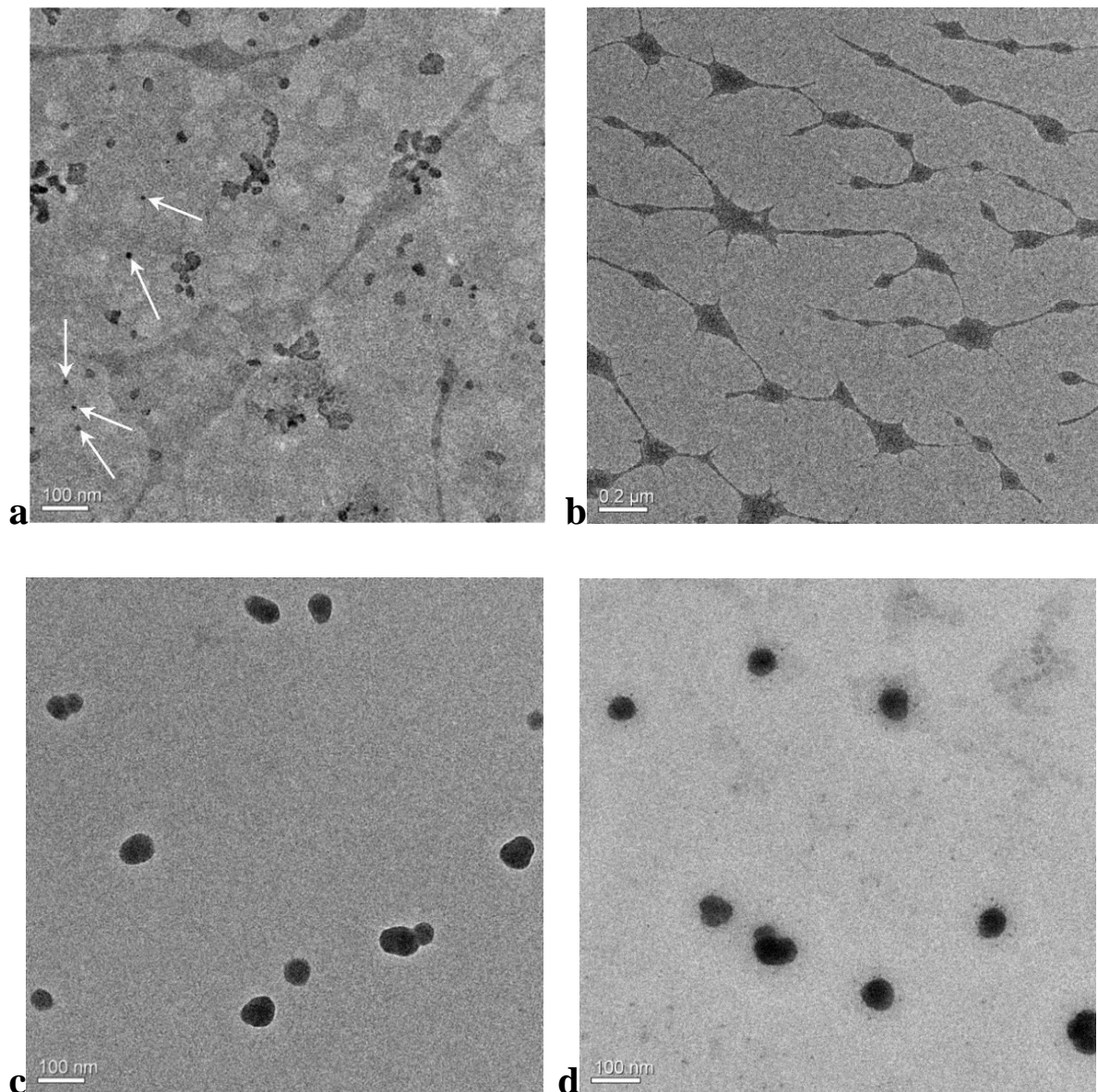


Figure 3.2-2 Transmission electron microscopy (TEM) of binary and ternary complexes. (a) TEM micrograph of mRNA/T704 binary complex, non-complexed mRNA was marked with arrows. (b) TEM micrograph of pDNA/T704 binary complex. (c) TEM micrograph of mRNA-based ternary complex. (d) TEM micrograph of pDNA-based ternary complex. The concentration of mRNA or pDNA and T704 in ternary complexes was the same with that in binary counterparts.

3.2.4 Stability of ternary complexes

To examine the vector complex stability, a DNase I protection assay was carried out. pDNA based binary and ternary complexes were incubated with 2.5-10 U DNase I for 1 h. Remaining pDNA was then extracted from each sample and examined by agarose gel electrophoresis (**Figure 3.2-3**). The gel showed that even the highest concentration of DNase I

did not completely degrade pDNA within the ternary complex. In contrast, pDNA within the binary complex was completely degraded in the presence of the lowest amount of DNase I (2.5 U), which was similar to that of naked pDNA (negative control).

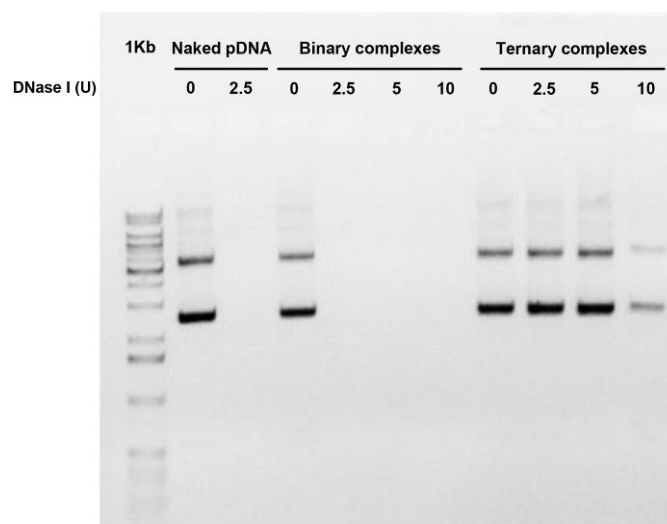


Figure 3.2-3 DNase I protection assay. Stability of pDNA-based binary and ternary complexes in the presence of increasing DNase I activity. 1kb DNA standard was used as a reference (1kb), naked-pDNA (without DNase I) was used as a positive control and (naked-pDNA + 2.5 U DNase I) was used as a negative control.

For the potential clinical application of peptide-poloxamine complexes, the aerosol inhalation would be a preferred approach when administering the formulation to the airway of patients, rather than the invasive intratracheal instillation with low patient compliance. As a result, it is important to see if ternary complexes could resist the shear force created during nebulization and whether they remain the activity after nebulization. We evaluated the transfection efficiency of non-nebulized and nebulized pDNA/T704/peptide 0 ternary complexes as well as pDNA/Lipofectamine2000 lipoplexes. Nebulized lipoplex showed significantly lower transfection efficiency compared with the non-nebulized one in both cell lines ($p < 0.001$), whereas the nebulization process did not severely affect the transfection efficiency of pDNA/T704/peptide 0 ternary complex (**Figure 3.2-4**), indicating that peptide-poloxamine complexes were more resistant to the shear-force created by jet-nebulizer compared with lipid-based formulations.

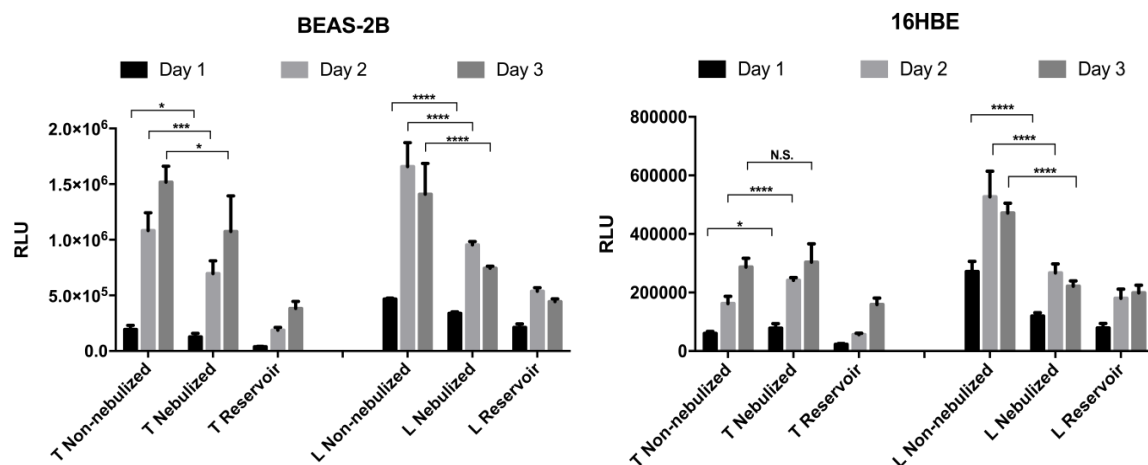


Figure 3.2-4 The influence of nebulization process on the transfection efficiency of pDNA/T704/peptide 0 ternary complex and Lipofectamine2000 based formulation. "T" means pDNA/T704/peptide 0 ternary complex and "L" represents pDNA/Lipofectamine2000 lipoplex. The data are given as the mean \pm standard deviation (SD) of the mean ($n > 5$). Significant differences are defined as *: $p < 0.05$; **: $p < 0.01$; ***: $p < 0.005$; ****: $p < 0.001$; N.S. meant not significant.

3.3 Investigations on the underlying mechanism of the superior transfection efficiency of ternary complex compared with the binary counterpart

To reveal the underlying mechanism of the dramatically enhanced transfection efficiency of ternary complex compared with the binary counterpart, the subcellular fate of binary and peptide 0 based ternary complex was systemically investigated.

3.3.1 Cellular internalization of binary and ternary complexes

Flow cytometry was employed to obtain detailed insights into cellular internalization of naked fluorescein-labelled pDNA (Fluo-pDNA), binary and ternary complexes containing Fluo-pDNA in 16HBE cells. The reason we choose 16HBE cells as the model cell line was that 16HBE cells are more static compared with fast-dividing BEAS-2B cells, thus providing huger subcellular barriers and better mimicking *in vivo* status. As illustrated in **Figure 3.3-1**, binary complex containing Fluo-pDNA was just internalized by less than 0.2 % 16HBE cells after 4 h incubation, which was similar to that of naked Fluo-pDNA. In contrast, the ternary complex containing Fluo-pDNA successfully entered around 60% of 16HBE cells with a six-time higher mean fluorescence intensity compared with the binary counterpart.

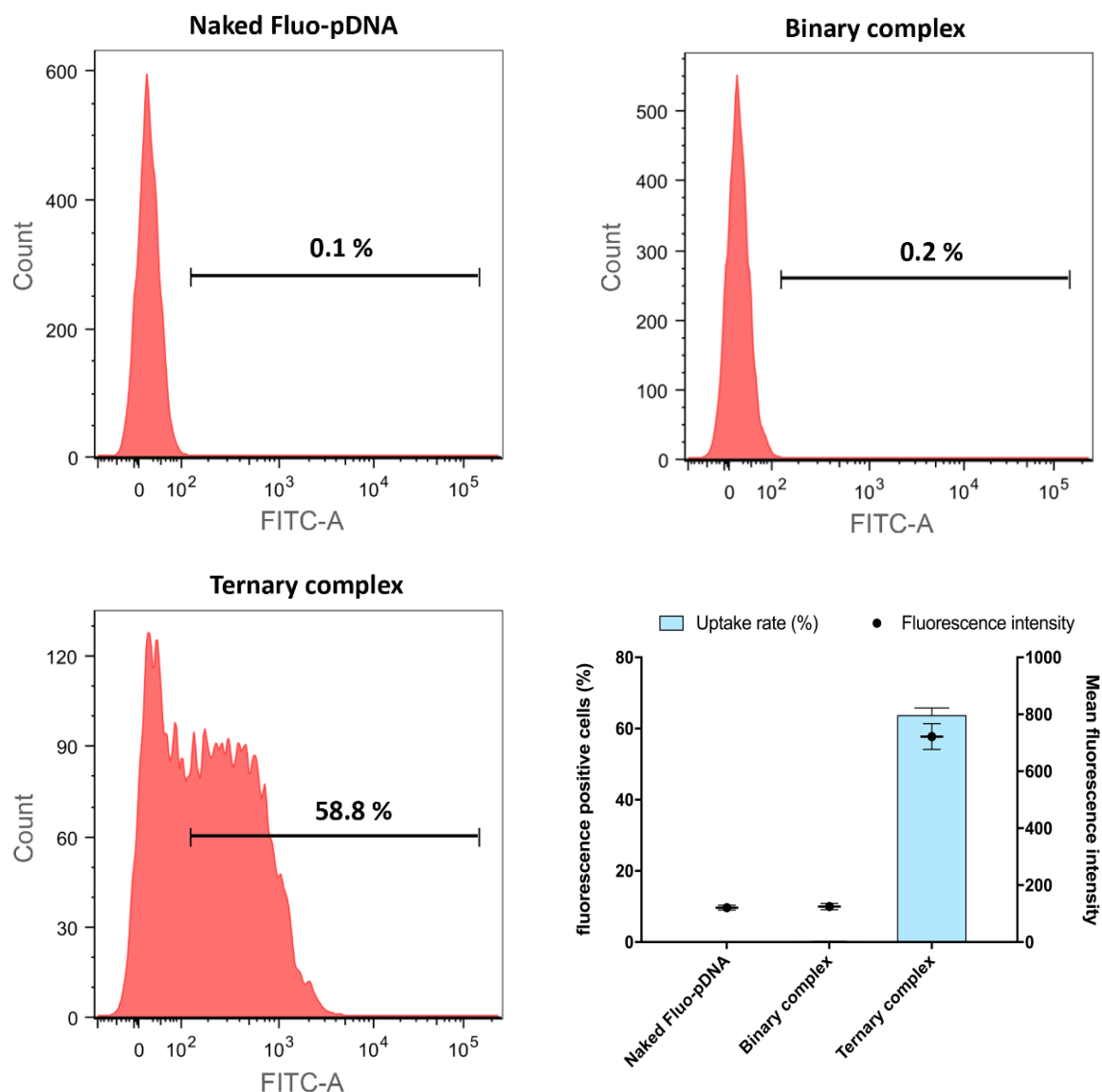
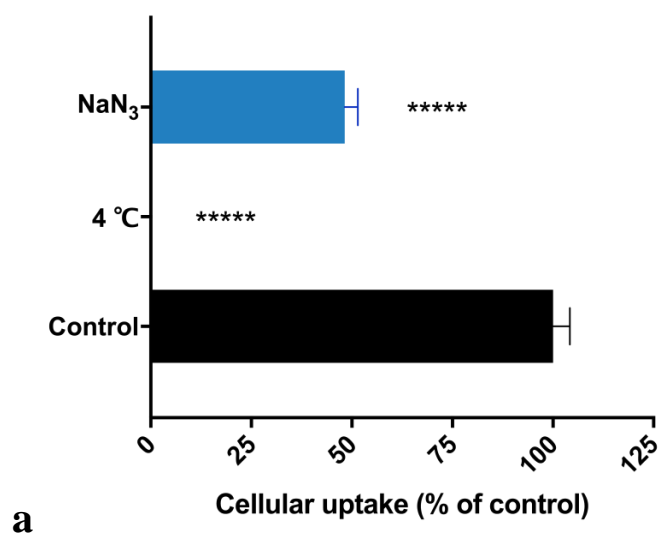


Figure 3.3-1 The cellular uptake of binary and ternary complexes. The uptake of naked fluorescein labelled pDNA (Fluo-pDNA), Fluo-pDNA/T704 binary complex, and Fluo-pDNA/T704/peptide 0 ternary complex after 4 h incubation with 16HBE cells measured by the flow cytometry.

3.3.2 Cellular internalization pathways of ternary complex

In order to understand the cell entry pathways of ternary complex, the cellular uptake of ternary complex was studied in the presence of different inhibitors or at different temperatures. As shown in **Figure 3.3-2a**, either the low temperature (4 °C) which constrains the energy metabolism of cells at a low level or the presence of sodium azide (a metabolic inhibitor to deplete ATP), drastically inhibited the cellular uptake of the ternary complex,

indicating that their uptake occurred through the energy-dependent endocytosis. To further reveal the endocytic pathways of the ternary complex, selective inhibitors of chlorpromazine, filipin, protamine, amiloride and sodium chlorate were applied. The cellular uptake of ternary complex was partially suppressed by chlorpromazine, a selective inhibitor of clathrin-mediated endocytosis, but not by filipin, an inhibitor of caveolae-mediated endocytosis (**Figure 3.3-2b**). Both protamine and amiloride significantly inhibited the cellular uptake of the ternary complex, indicating that absorptive endocytosis and macropinocytosis which play important roles in the uptake process of macromolecules were involved. However, sodium chlorate did not influence the internalization process of the ternary complex (**Figure 3.3-2b**). These results suggested that efficient energy-dependent cellular uptake mediated by macropinocytosis, electrostatic absorptive endocytosis and clathrin-mediated endocytosis could be utilized by the ternary complex.



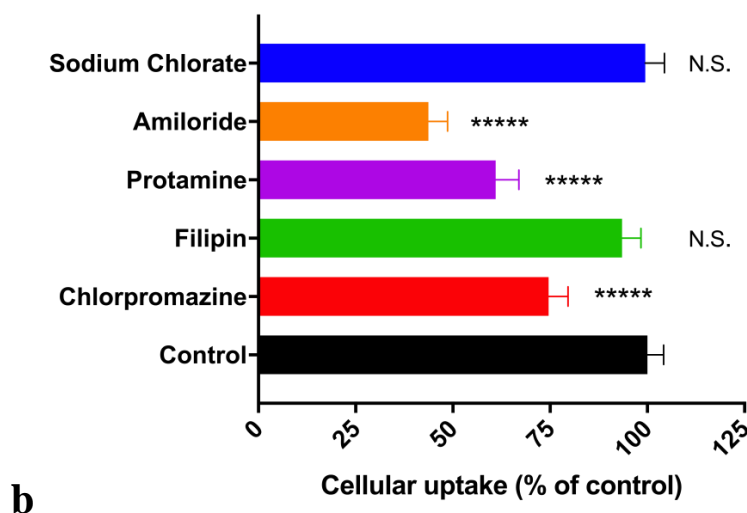


Figure 3.3-2 Investigations on the cellular uptake pathways that utilized by the ternary complex. (a) Energy-dependent cell uptake of peptide 0 based ternary complex at 4 °C and in the presence of NaN_3 . **(b)** Inhibitory effect of chlorpromazine, filipin, protamine, amiloride and sodium chlorate on the uptake of peptide 0 based ternary complex. The non-inhibited cellular uptake of peptide 0 based ternary complex was used as the control in each assay. Significant differences were defined as *****: $p < 0.0001$. N.S. meant not significant compared with the control.

Additionally, potential receptor-mediated endocytosis was directly examined by the competition of excess free peptides. **Figure 3.3-3a** indicated that free K4R4 peptide (KKRRRRKK, the cationic moiety of peptide 0) and free peptide 0 had no influence on the cellular uptake of the peptide 0 based ternary complex. This might be due to the fact that positively charged peptides did not have specific receptors in the cells and could utilize alternative pathways to enhance translocation through the plasma membrane¹⁴³. A similar situation could be observed in the case of free lipoic acid and free NLS (**Figure 3.3-3a**). However, the excess amount of free targeting ligand of peptide 9 (GACSERSMNFCG, more details in 3.4.2) and free peptide 9 significantly decreased the cellular uptake of the Fluo-pDNA/T704/peptide 9 ternary complex (**Figure 3.3-3b**), indicating that the targeting ligand played an essential role in mediating the cellular uptake of peptide 9 based ternary complex into bronchial epithelial cells.

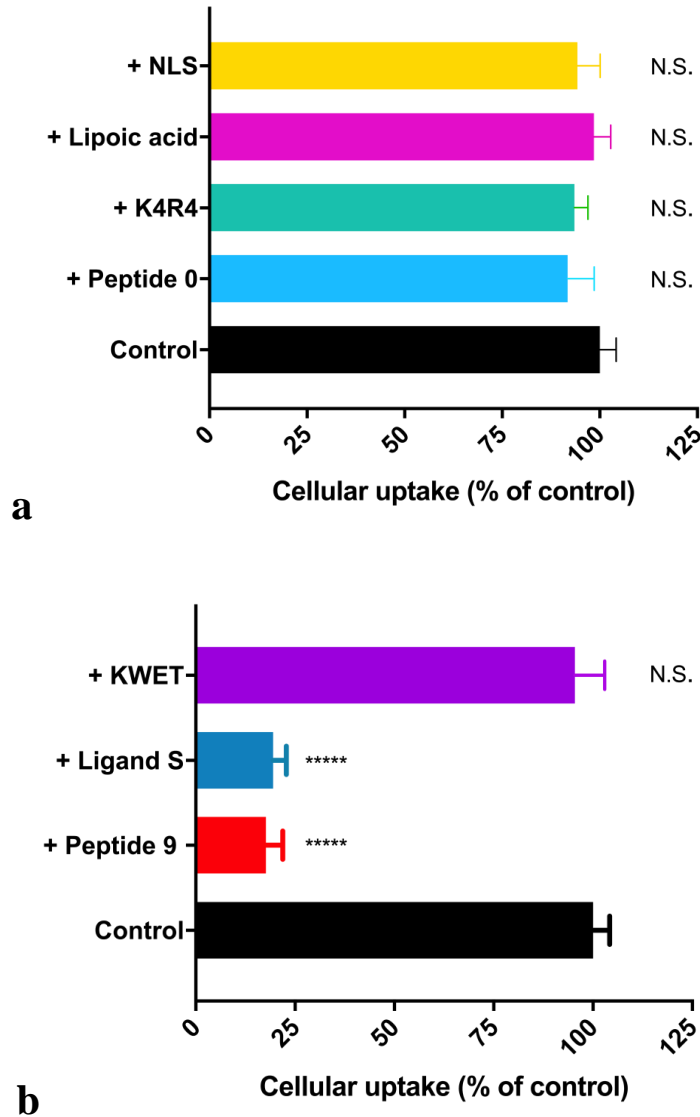


Figure 3.3-3 Investigations on receptor-mediated cellular uptake of the ternary complex. (a) Non-receptor mediated endocytosis of peptide 0 based ternary complex, which cannot be inhibited by the excess amount of free peptide 0 and its fragment sequence (i.e., NLS, Lipoic acid and K4R4). K4R4 represents the peptide KKRRRRKK. The non-inhibited cellular uptake of peptide 0 based ternary complex was used as a control. N.S. meant not significant compared with the control. (b) Receptor-mediated cellular uptake of peptide 9 based ternary complex, which was significantly inhibited by the excess amount of free peptide 9 and the free ligand S (GACSERSMNFCG) which is contained in peptide 9. KWET represents the peptide KETWWETWWTEWWTEW which is the hydrophobic moiety of peptide 9. The non-inhibited cellular uptake of peptide 9 based ternary complex was used as a control. Significant differences were defined as *****: $p < 0.0001$; N.S. meant not significant compared with the control.

3.3.3 Subcellular localization of binary and ternary complexes

Based on these results, the subcellular location of binary and ternary complexes was further investigated by confocal microscopy. The amount of Fluo-pDNA delivered into cells by binary complex was very limited and their subcellular location was in a punctate staining pattern, indicating that the binary complex was confined within endo/lysosomal compartments (**Figure 3.3-4**). In contrast, plenty of dispersed fluorescence could be observed in the cytosol and nucleus of ternary complex transfected cells with the majority of Fluo-pDNA localized within the nucleus (**Figure 3.3-4**). In particular, few of the Fluo-pDNA delivered by ternary complex was observed in the endocytic vesicles (**Figure 3.3-4**, merged), suggesting that ternary complex was capable of facilitating efficient endosomal escape which has been regarded as the key step “providing the major opportunity to improve gene transfer”¹⁴⁴. The efficient endosomal escape of ternary complex probably resulted from its distinct cellular uptake pathways and/or “proton sponge effect” induced by the cationic moiety within peptide component¹⁴⁵. Once the ternary complex localized in the cytoplasm, the targeting ligand (NLS) could exert its function to direct the Fluo-pDNA to the final destination.

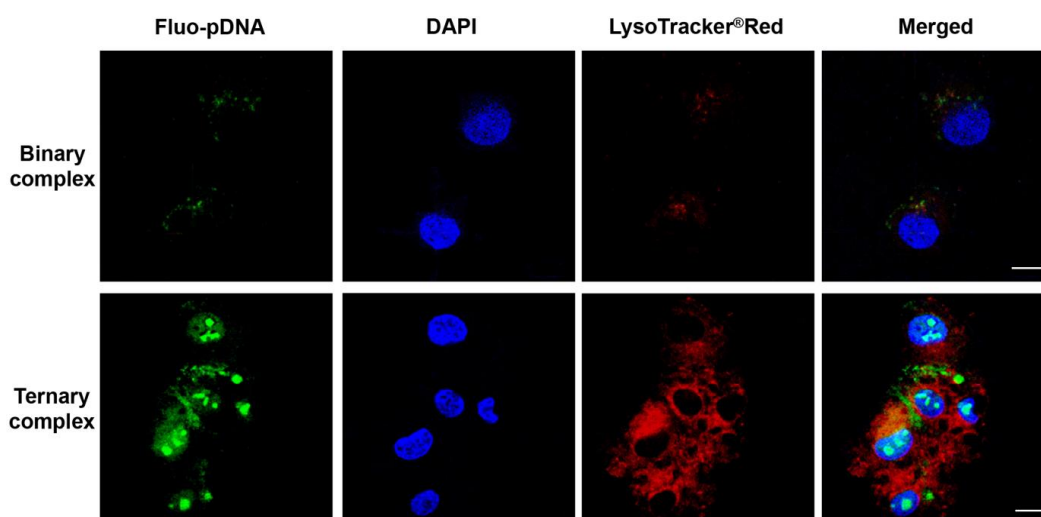


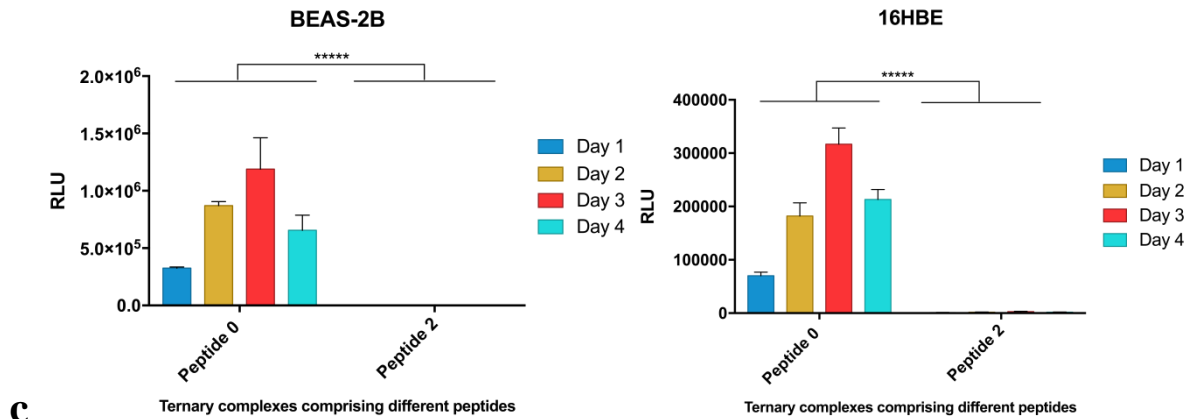
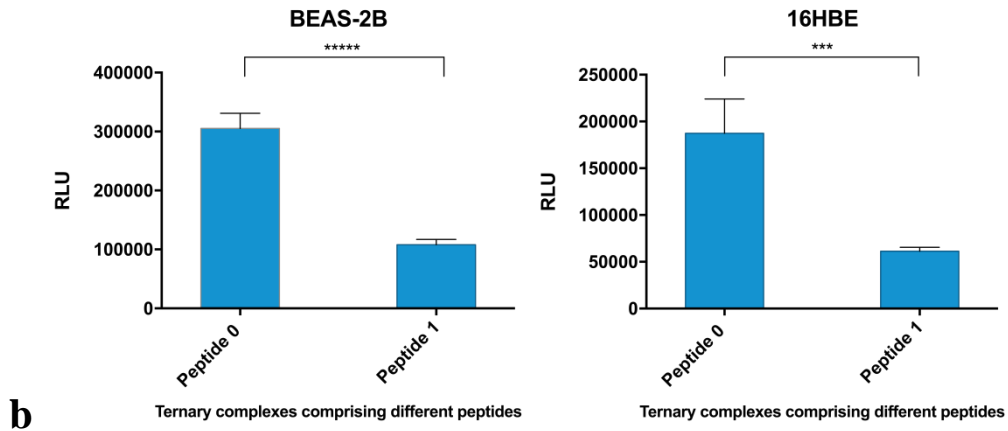
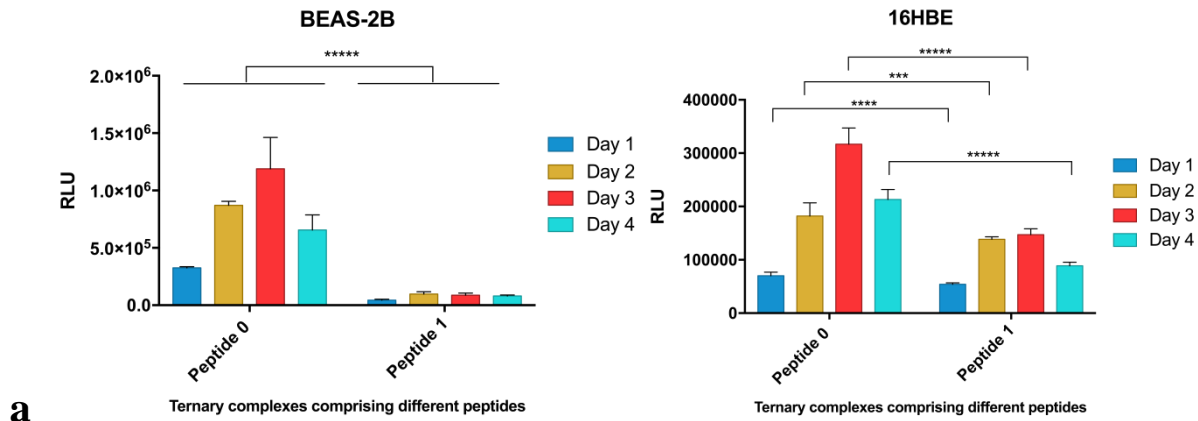
Figure 3.3-4 The subcellular location of Fluo-pDNA/T704 binary complex and Fluo-pDNA/T704/peptide 0 ternary complex after 4 h incubation with 16HBE cells measured by confocal laser scanning microscopy (CLSM). Green channel: Fluo-pDNA; Blue channel: nuclei stained by DAPI; Red channel: endocytic vesicles marked by LysoTracker® Red DND-99; Merged: the combination of above channels. Scale bar: 10 μ m.

3.4 Optimizing peptide structure with different candidate modules

3.4.1 Each moiety that constitutes the peptide is imperative for the activity of peptide in ternary complex

To prove that those functional moieties within the peptide play pivotal roles in boosting the transfection efficiency of ternary complex, we utilized three control peptides to prepare ternary complexes and compared their activities in transfecting airway epithelial cells with peptide 0 based ternary complexes. Peptide 1 shares the same cationic moiety and targeting moiety with peptide 0 but has no anchor moiety. Peptide 2 is a cationic moiety negative control of peptide 0 (NLS sequence was simultaneously eliminated from Peptide 2, as there are also many basic amino acids in NLS). Peptide 3 shares the same anchor moiety and cationic moiety with peptide 0 but contains a mutated NLS targeting sequence in which the lysine at position 5 has been replaced by threonine. This mutation is known to be nuclear transport deficient¹⁴⁶. The transfection efficiency of peptide 1, peptide 2 and peptide 3 based ternary complexes were optimized (**Figure 3.4-2 to 3.4-5**) and compared with that of the ternary complex containing peptide 0. In terms of pDNA transfection, peptide 1 based ternary complex could just reach 7% (in BEAS-2B cells) or half (in 16HBE cells) of the maximum signal intensity (on day 3) of peptide 0 counterpart as illustrated in **Figure 3.4-1a**. mRNA/T704/peptide 1 complex showed only one-third of the transfection efficiency of mRNA/T704/peptide 0 complex in both BEAS-2B and 16HBE cells (**Figure 3.4-1b**). Interestingly, both pDNA and mRNA based ternary complexes prepared with peptide 2 displayed a rather low transfection efficiency which was similar to binary counterparts in both cell lines (**Figure 3.4-1c and 3.4-1d**). In the evaluation of the NLS function, pDNA

expression from the ternary complex containing peptide 0 was almost 5 times better than the counterpart from peptide 3 based ternary complex in BEAS-2B cells (**Figure 3.4-1e**). Although the pDNA expression from peptide 0 based ternary complex and peptide 3 based ternary complex were similar on day 2 in 16HBE cells, the former was significantly higher than the latter on other days in this cell line (**Figure 3.4-1e**).



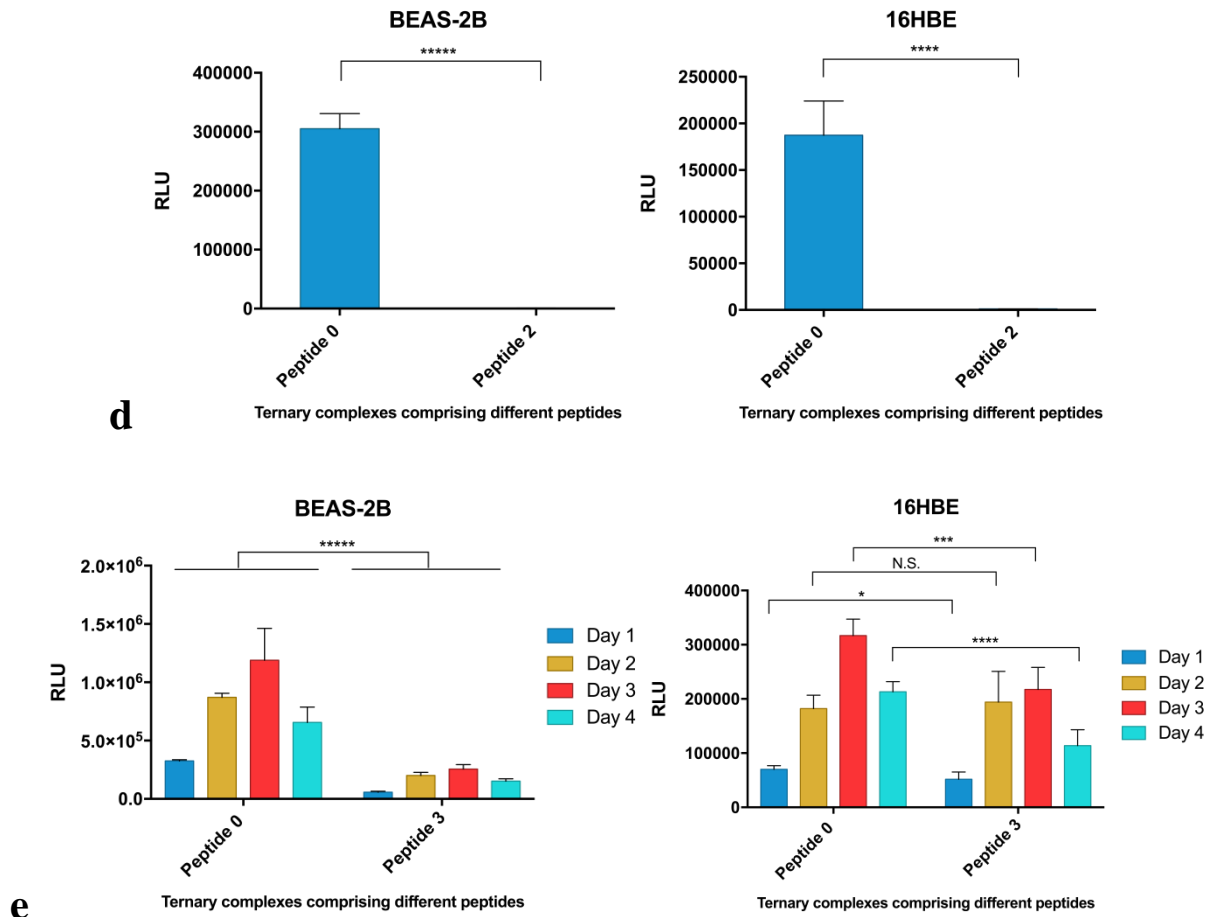
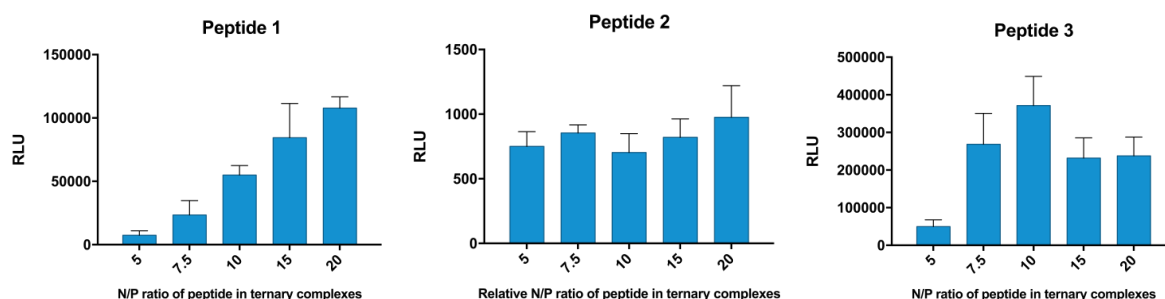


Figure 3.4-1 Evaluation of the important roles of functional moieties that constitute peptide 0. The function of “anchor moiety” in peptide 0 was proved by comparing the optimum (a) pDNA and (b) mRNA transfection efficiency of peptide 0 based ternary complexes with that of peptide 1 based ternary complexes in BEAS-2B and 16HBE cells. Peptide 1 which did not have hydrophobic “Anchor moiety” was a negative control of peptide 0. The function of “cationic moiety” in peptide 0 was studied by comparing the optimum (c) pDNA and (d) mRNA transfection efficiency of peptide 0 based ternary complexes with peptide 2 based counterparts in BEAS-2B and 16HBE cells. Peptide 2 which did not have positively charged amino acids at neutral pH served as a negative control of peptide 0. (e) The function of “targeting moiety” (nuclear localization signal, NLS) in peptide 0 was evaluated by comparing the optimum pDNA transfection efficiency of peptide 0 based ternary complex with that of peptide 3 based ternary complex in BEAS-2B and 16HBE cells. Peptide 3 containing a transport deficient NLS was a negative control of peptide 0. Luciferase activity mediated by mRNA transfection was assayed 24 h after transfection. Luciferase activity mediated by pDNA transfection was measured on day 1, day 2, day 3 and day 4 after transfection. The data are given as the mean \pm SD (n>5). Significant differences were defined as *: $p < 0.05$; **: $p < 0.01$; ***: $p < 0.005$; ****: $p < 0.001$; *****: $p < 0.0001$; N.S. meant not significant.

3.4.2 Optimizing the peptide structure with different candidate modules

Having clarified that how and why peptide 0 was able to mediate efficient transfection of the ternary complex, we further evaluated another set of peptides that were composed of different candidate modules. Peptide 4 and peptide 5 kept the same anchor moiety and cationic moiety

with peptide 0 (same numbers of lysine and arginine in the sequence) but contained different targeting moieties. Ligand SERSMNF (ligand S) in peptide 4 and ligand YGLPHKF (ligand Y) in peptide 5 were discovered by the phage display and showed high affinity to human airway epithelial cells¹⁴⁷. The receptor of Ligand S is the intercellular adhesion molecule-1, because Ligand S closely resembles part of the structure of the receptor binding proteins of rhinovirus¹⁴⁸. The receptor of Ligand Y is currently unknown but Ligand Y displays close similarity to a targeting protein within the pathogen *Legionella pneumophila*¹⁴⁹. The function of the amino acids sequence “GAC...CG” is to provide the ligand component with better conformational stability¹⁵⁰. Peptide 6 and peptide 7 shared a similar structure with peptide 4 and peptide 5 but differed in the cationic moiety. Unlike the cationic moiety of peptide 4 and peptide 5 wherein lysine outnumbered arginine, the cationic moiety of peptide 6 and peptide 7 contained more arginine than lysine. Peptide 8 had same anchor moiety and targeting moiety with peptide 4 but contained a cationic moiety dominated by histidine. Peptide 9, peptide 10, peptide 11 and peptide 12 were derived from peptide 4 by substitution of different anchor moieties, while peptide 10 comprised a shortened cationic moiety. The optimum composition of ternary complexes comprising peptide 4 to peptide 12 showing maximum transfection efficiencies was first identified (**Figure 3.4-2 to Figure 3.4-5**).



Results

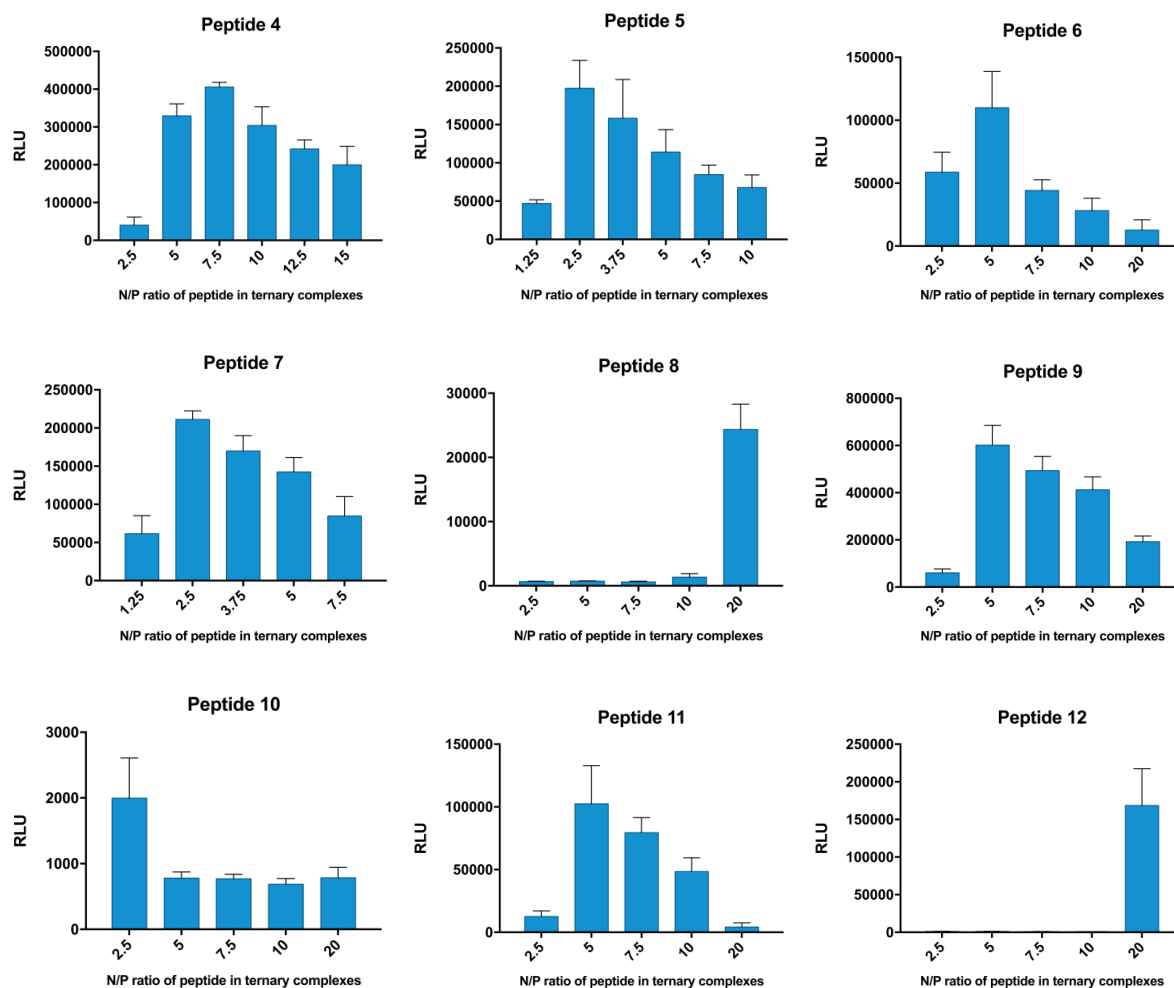
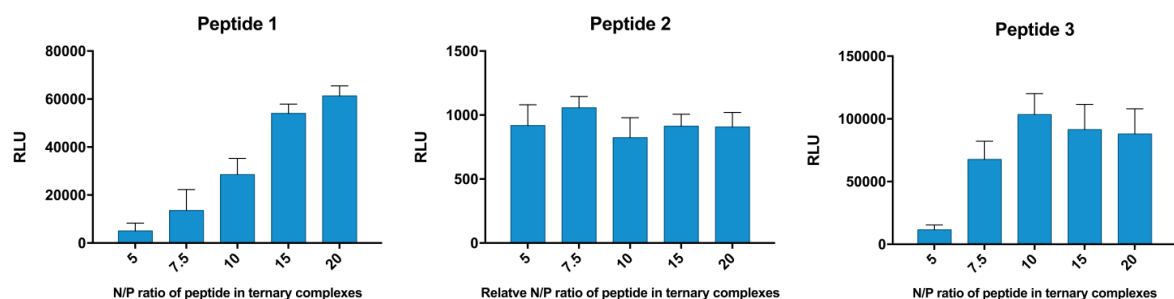


Figure 3.4-2 Transfection efficiency of mRNA based ternary complexes (comprising different peptides) in BEAS-2B cells. Peptide 1 to peptide 12 at different N/P ratios (as peptide 2 did not contain positively amino acids at neutral pH, peptide 2 was applied with the same molar concentration of peptide 0 accordingly) were complexed with T704 at the concentration of 63 (w/w) respectively, then followed by adding MetLuc-mRNA (400ng/well). Luciferase activity was measured 24 h after transfection and was expressed in RLU. Data represent the mean ± SD (n>5).



Results

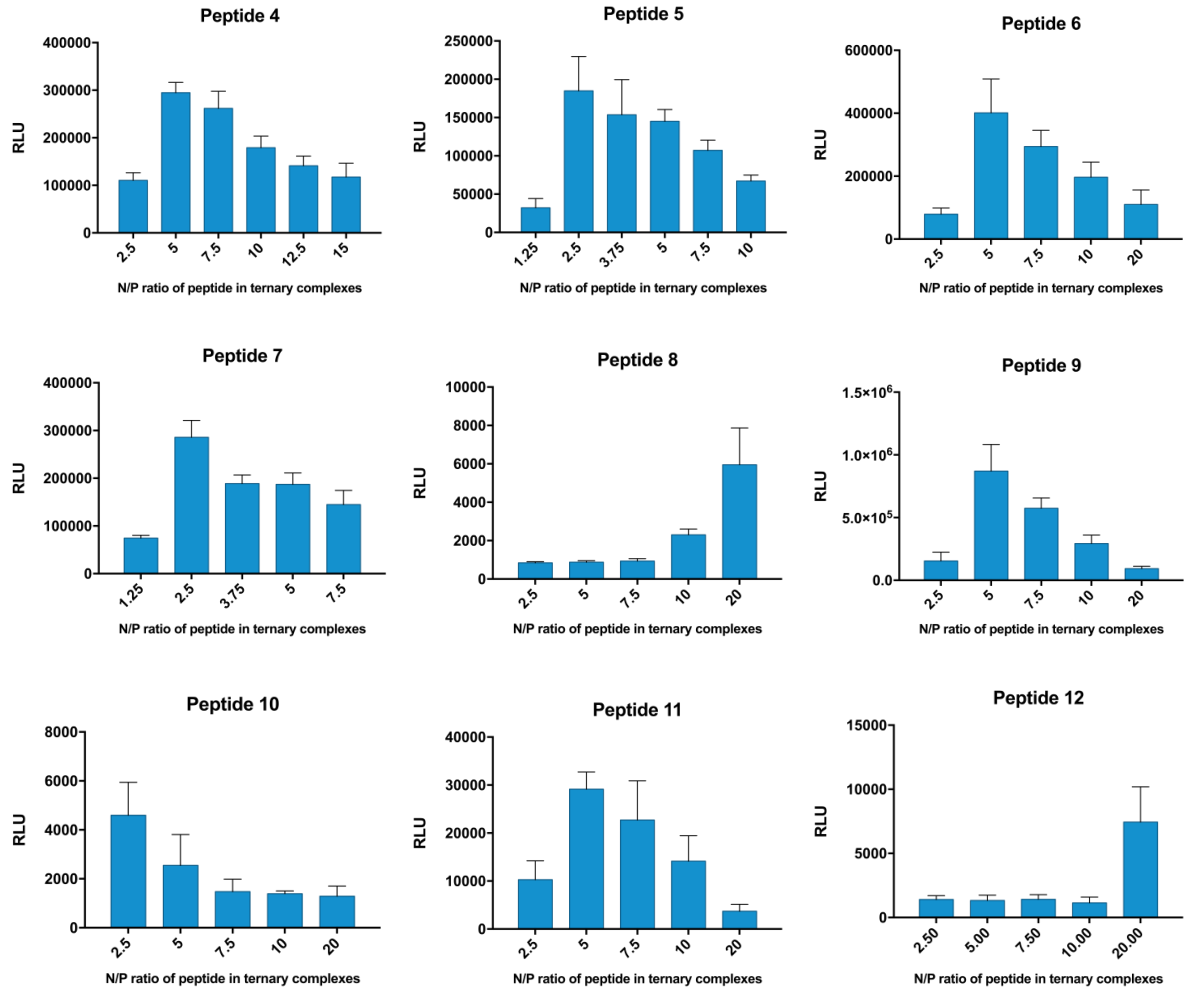
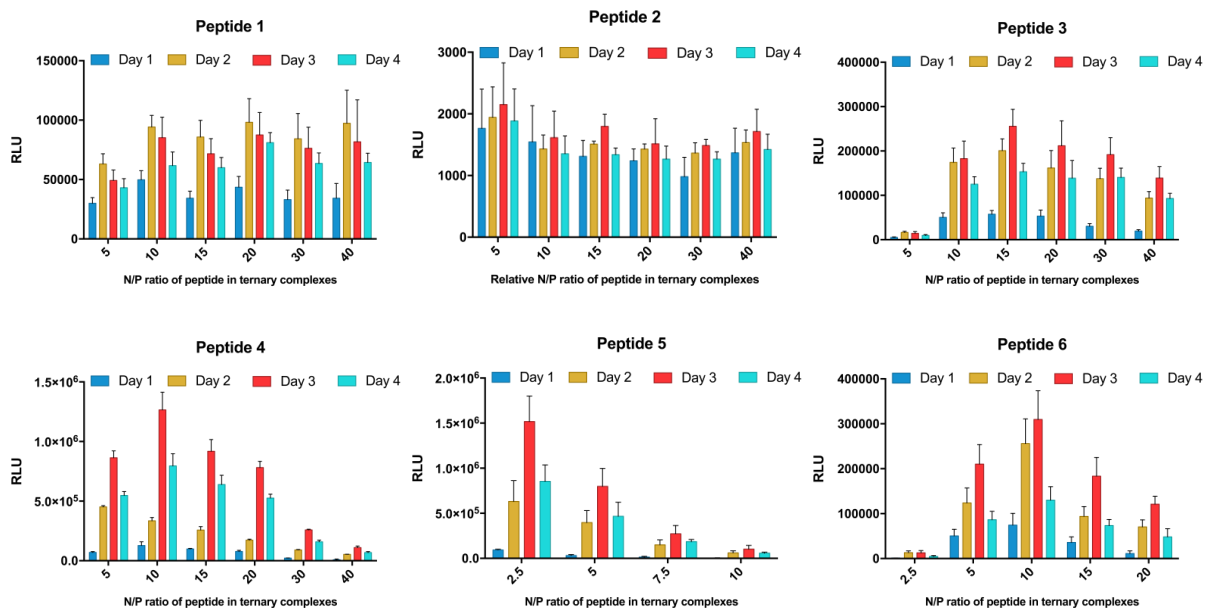


Figure 3.4-3 Transfection efficiency of mRNA based ternary complexes (comprising different peptides) in 16HBE cells. Peptide 1 to peptide 12 at different N/P ratios (peptide 2 was applied with the same molar concentration of peptide 0 accordingly) were complexed with T704 at the concentration of 63 (w/w) respectively, then followed by adding MetLuc-mRNA (400ng/well). Luciferase activity was measured 24 h after transfection and was expressed in RLU. The data are given as the mean \pm SD (n>5).



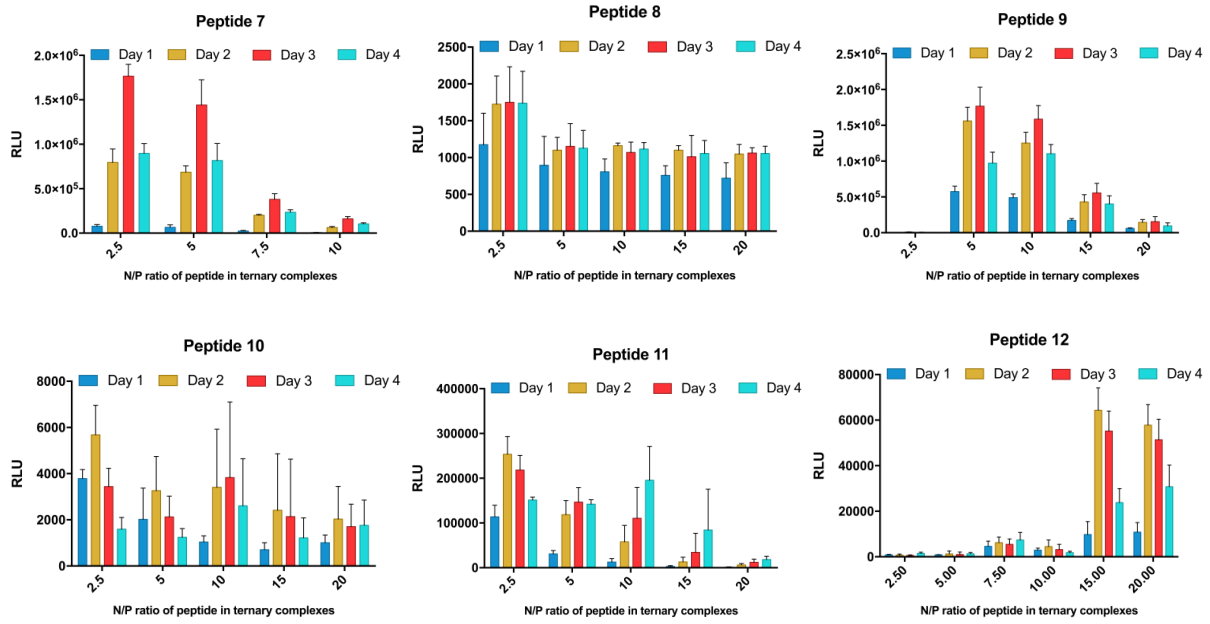
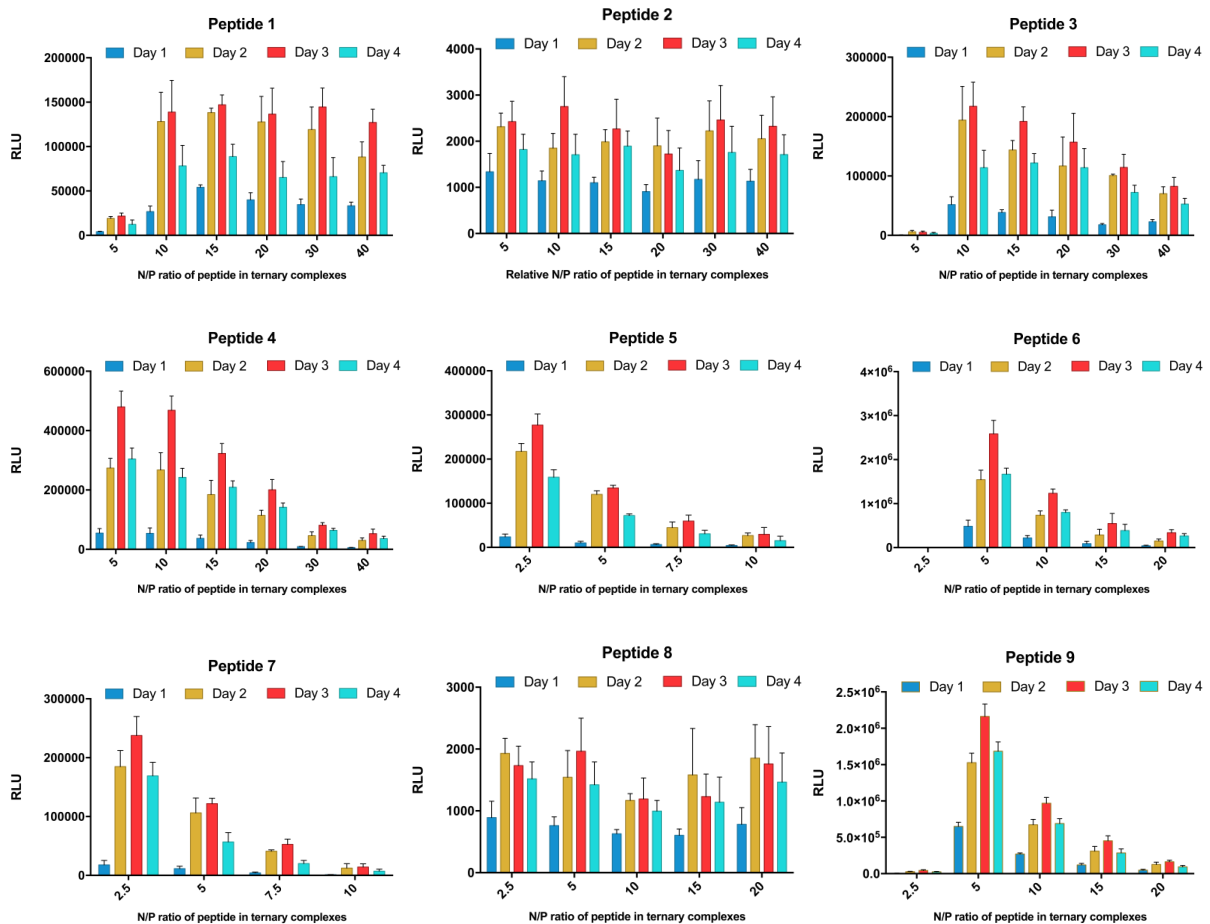


Figure 3.4-4 Transfection efficiency of pDNA based ternary complexes (comprising different peptides) in BEAS-2B cells. Peptide 1 to peptide 12 at different N/P ratios (as peptide 2 did not contain positively amino acids at neutral pH, peptide 2 was applied with the same molar concentration of peptide 0 accordingly) were complexed with T704 at concentration of 50 (w/w) respectively, then followed by adding MetLuc-pDNA (400ng/well). The same transfection procedure as described above was applied. Luciferase activity was measured 24 h, 48 h, 72 h and 96 h after transfection and was expressed in RLU. The data are given as the mean \pm SD (n>5).



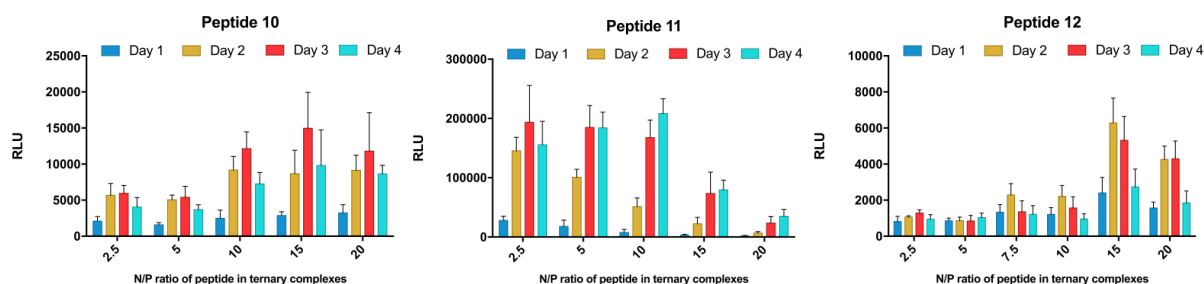


Figure 3.4-5 Transfection efficiency of pDNA based ternary complexes (comprising different peptides) in 16HBE cells. Peptide 1 to peptide 12 at different N/P ratios (as peptide 2 did not contain positively amino acids at neutral pH, peptide 2 was applied with the same molar concentration of peptide 0 accordingly) were complexed with T704 at the concentration of 63 (w/w) respectively, then followed by adding MetLuc-pDNA (400ng/well). The same transfection procedure as described above was applied. Luciferase activity was measured 24 h, 48 h, 72 h and 96 h after transfection and was expressed in RLU. The data are given as the mean \pm SD (n>5).

The comparison of pDNA or mRNA transfection efficiency mediated by ternary complexes comprising these peptides in optimum conditions was displayed in **Figure 3.4-6**. As illustrated in **Figure 3.4-6a**, pDNA expression from peptide 4, peptide 5 and peptide 7 based ternary complexes was similar (peptide 5 and peptide 7 were slightly better at day 3) to that from peptide 0 based ternary complexes in BEAS-2B cells. In contrast, peptide 9 based ternary complexes showed the highest transfection efficiency from day 1 to day 4 among all the tested groups in this cell line. For the transfection of 16HBE cells, both pDNA/T704/peptide 6 and pDNA/T704/peptide 9 ternary complexes showed overwhelming signals at each time point compared with other counterparts (**Figure 3.4-6a**). In terms of mRNA transfection, peptide 9 based ternary complex was more efficient than other counterparts in both BEAS-2B and 16HBE cells (**Figure 3.4-6b**). These results revealed that peptide 9 was the most promising peptide candidate in all aspects. Based on these results, peptide 9 based ternary complexes were selected as leading candidates for the following studies.

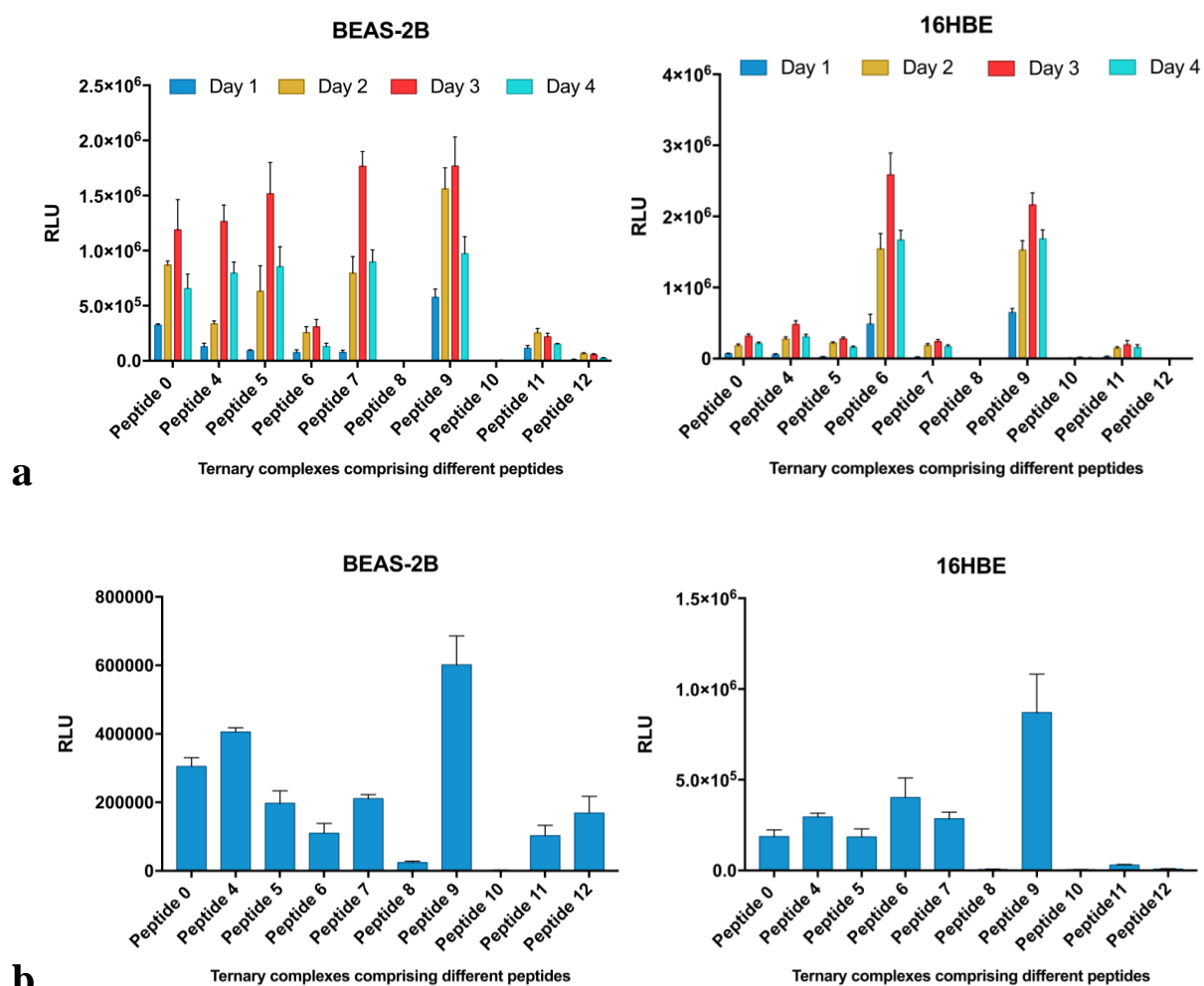


Figure 3.4-6 Comparisons of the transfection efficiency mediated by ternary complexes comprising different peptides in the optimum composition. (a) MetLuc-pDNA expression in BEAS-2B cells and 16HBE cells mediated by ternary complexes containing different peptides. Luciferase activity was measured on day 1, day 2, day 3 and day 4 after transfection. The concentration of T704 in ternary complexes treated for BEAS-2B cells was 50 (w/w), and which for 16HBE cells was 63 (w/w); **(b)** MetLuc-mRNA expression in BEAS-2B cells and 16HBE cells mediated by ternary complexes containing different peptides. Luciferase activity was assayed 24 h after transfection. The concentration of T704 in ternary complexes fixed at 63 (w/w). Data represent the mean \pm SD ($n > 5$).

3.5 Comparisons between the ternary complexes and other nonviral transfection reagents

In this chapter, we evaluated and compared the transfection efficiency of the ternary complex with other excellent nonviral transfection reagents using luciferase and enhanced green fluorescent protein (EGFP) as reporters. Lipofectamine2000 is a well-known commercial available reagent that has been commonly used as a standard for *in vitro* nucleic acid transfection in a wide variety of cells. In a previous study, we found Lipofectamine2000 was very efficient in the delivery of mRNA into cultured airway epithelial cells¹³⁹. As a result, Lipofectamine2000 was used as a lipoplex (complex formed by lipids and nucleic acids) control in the current study. Branched polyethyleneimine (brPEI, 25kDa) is a widely-used cationic polymer that is regarded as the “gold-standard” for nucleic acid delivery in the past few decades and was used as polyplex (complex formed by polymers and nucleic acids) control in current study¹⁵¹.

3.5.1 In vitro luciferase expression mediated by different carrier systems

We first identified the optimal composition of Lipofectamine2000 lipoplex and brPEI polyplex showing maximum transfection efficiency in airway epithelia (**Supplementary Figure 1** and **Supplementary Figure 2**), then compared with that of peptide 9 based ternary complex. As shown in **Figure 3.5-1a**, MetLuc-pDNA expression in ternary complex and Lipofectamine2000 lipoplex were at the same level in BEAS-2B cells, whereas the luciferase expression on day 3 and day 4 mediated by ternary complex was significantly higher than that mediated by Lipofectamine2000 in 16HBE cells. Furthermore, ternary complex brought about more than 5-times higher (in BEAS-2B cells) or 7-times better (in 16HBE cells) pDNA

transfection than brPEI counterparts (**Figure 3.5-1a**). In contrast, mRNA based ternary complex was less efficient than Lipofectamine2000 lipoplex in both cell lines (**Figure 3.5-1b**). Compared with brPEI polyplex, mRNA expression induced by ternary complex was 10-times in BEAS-2B cells and 36-times in 16HBE cells as efficient as that mediated by brPEI polyplex (**Figure 3.5-1b**). These results demonstrated that ternary complex was more efficient in delivering pDNA into cultured epithelial cells compared with the lipoplex and polyplex controls, while mRNA expression mediated by ternary complex was lower than that mediated by the lipoplex control.

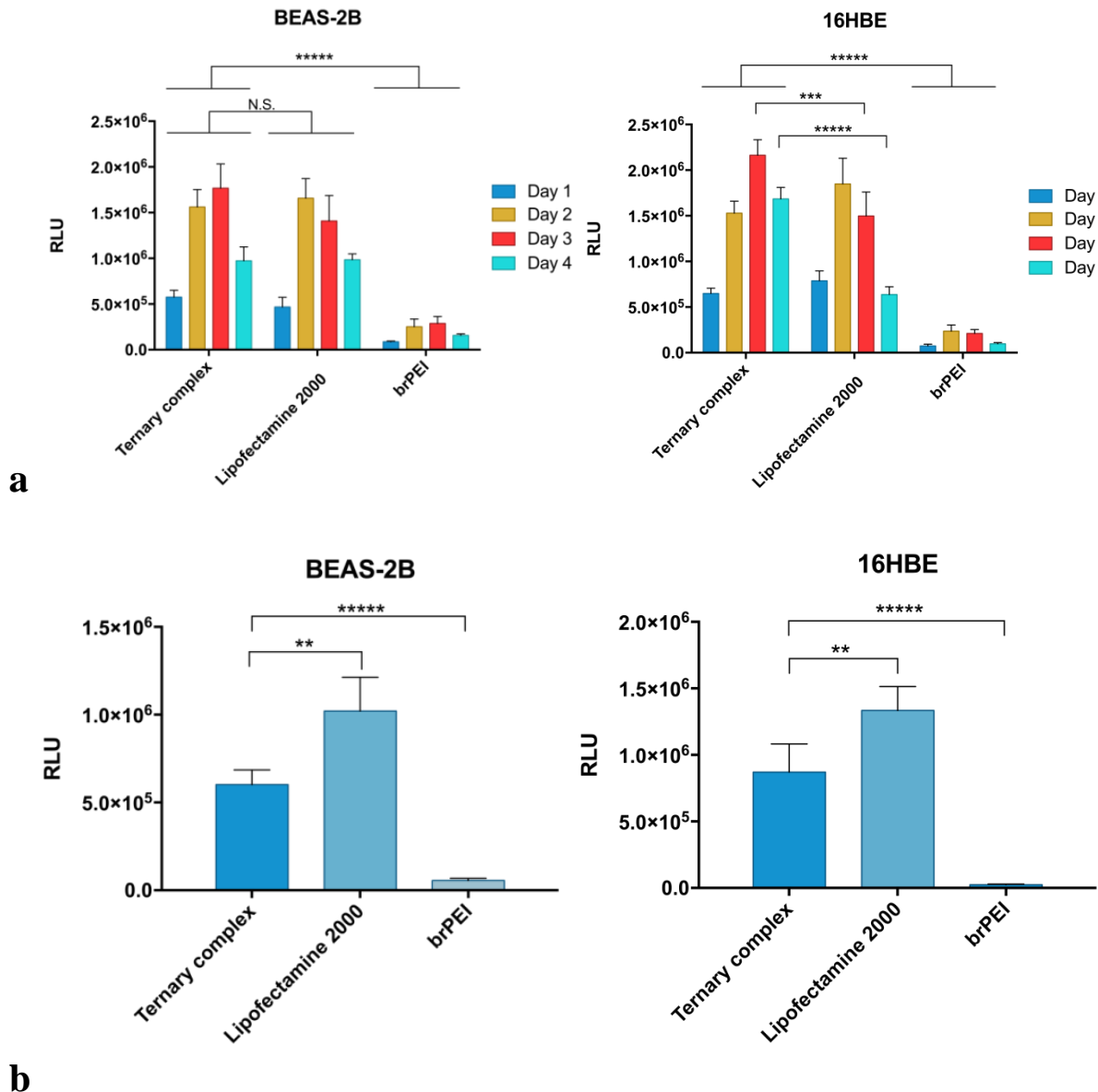


Figure 3.5-1 Comparisons of the *in vitro* transfection efficiency mediated by ternary complexes (T704 + Peptide 9 + pDNA or mRNA) and other nonviral vectors. (a) Optimum MetLuc-pDNA expression mediated by ternary complex, Lipofectamine2000 lipoplex and brPEI polyplex in BEAS-2B and 16HBE cells. Luciferase activity was measured on day 1, day 2, day 3 and day 4 after transfection. (b) MetLuc-mRNA expression (24 h after transfection) mediated by ternary complex, Lipofectamine2000 lipoplex and brPEI polyplex in BEAS-2B and 16HBE cells. All formulations were prepared at the optimum ratio to ensure their optimum performance on each cell line. The results represent the mean \pm SD of three independent experiments. Significant differences were defined as *: $p < 0.05$; **: $p < 0.01$; ***: $p < 0.005$; ****: $p < 0.001$; *****: $p < 0.0001$; N. S. meant not significant.

3.5.2 *In vitro* enhanced green fluorescent protein (EGFP) expression mediated by different carrier systems

Apart from the evaluation of the total levels of protein production, we also investigated the numbers of transfected cells using above-mentioned transfection reagents. BEAS-2B and 16HBE cells were transfected with mRNA or pDNA encoding EGFP. To visualize EGFP-mRNA transfected cells, fluorescent microscope pictures were acquired (**Figure 3.5-2**). Results revealed that the transfection efficiency of ternary complexes comprising peptide 9 was much better than that achieved with brPEI-based formulation and similar to the one achieved with Lipofectamine2000 counterpart.

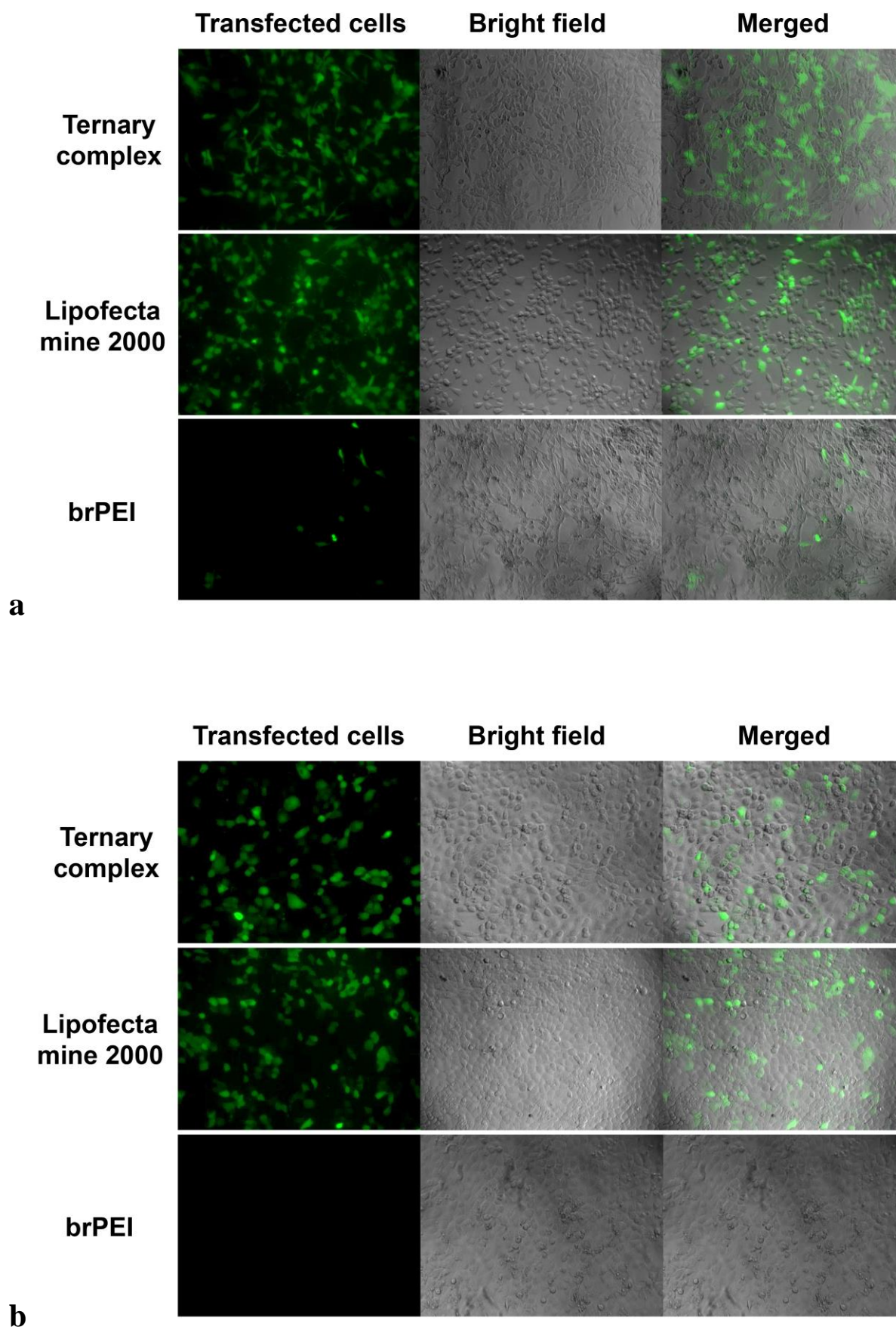


Figure 3.5-2 EGFP-mRNA expression mediated by different formulations. Representative expression of EGFP-mRNA mediated by ternary complex, Lipofectamine2000 based lipoplex and brPEI based polyplex in **(a)** BEAS-2B cells and **(b)** 16HBE cells determined by fluorescent microscope.

Afterward, the number of EGFP-mRNA or -pDNA transfected cells was quantitatively calculated by flow cytometry. As illustrated in **Figure 3.5-3**, EGFP-mRNA successfully expressed in $40.3\% \pm 4\%$ and $29.2\% \pm 3\%$ of BEAS-2B cells transfected by Lipofectamine2000 lipoplex and ternary complex respectively, whereas only $4.0\% \pm 2\%$ of BEAS-2B cells showed signals in brPEI group. Notably, the fluorescence intensity of ternary complex group was comparable to that of Lipofectamine2000 group. A similar profile could be observed in EGFP-mRNA transfected 16HBE cells wherein $42.5\% \pm 3\%$, $25.8\% \pm 5\%$ and $1.9\% \pm 1\%$ cells were transfected by Lipofectamine 2000 lipoplex, ternary complex and brPEI polyplex, respectively (**Figure 3.5-3**). In terms of EGFP-pDNA transfection, the rate of successfully transfected cells was significantly lower than that of EGFP-mRNA transfected counterpart, only 10%-20% BEAS-2B or 16HBE cells were successfully transfected by ternary complex and Lipofectamine2000 lipoplex (**Figure 3.5-3**). The culprit for this phenomenon would be the barrier posed by the nuclear membrane which is insurmountable for pDNA expression but irrelevant for mRNA expression¹⁴¹. However, the fluorescence intensity (per cell) expressed from EGFP-pDNA transfected cells was at a similar level with that expressed from EGFP-mRNA transfected counterparts. The number of EGFP-pDNA successfully transfected cells mediated by ternary complex was comparable to that mediated by Lipofecamine2000 lipoplex but was significantly higher than that mediated by brPEI polyplex in BEAS-2B and 16HBE cells (**Figure 3.5-3**).

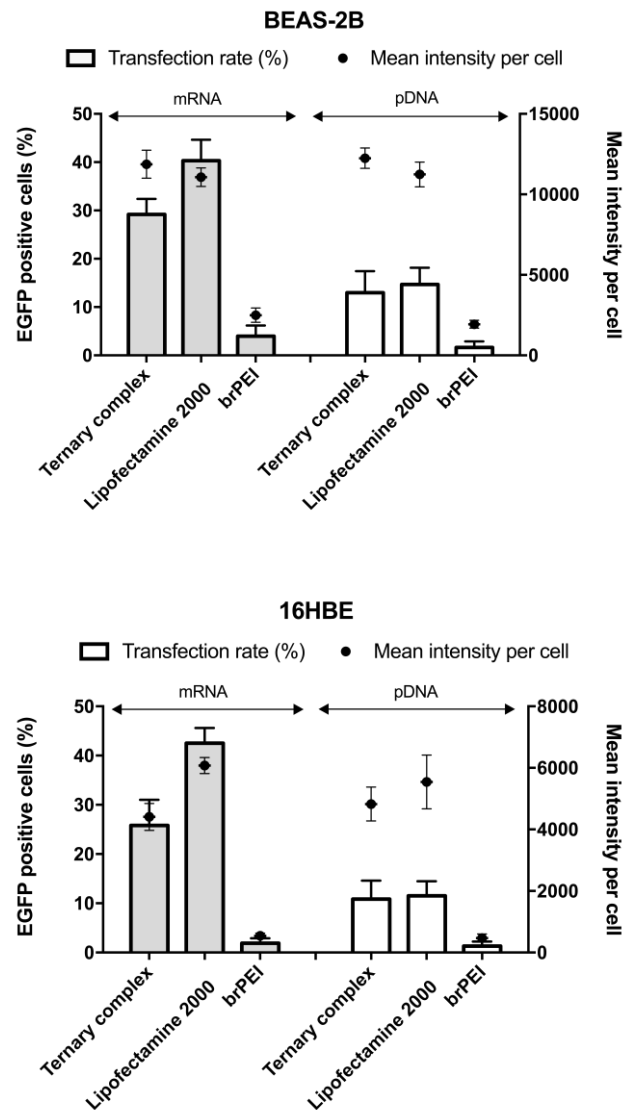


Figure 3.5-3 Quantitative investigations on the EGFP positive cells and their mean fluorescence intensity in EGFP-mRNA or EGFP-pDNA based formulations transfected BEAS-2B and 16HBE cells via flow cytometry analysis. Bars represent the rate of EGFP-positive cells (grey-mRNA, white-pDNA), individual dots refer to the mean fluorescence intensity per cell.

3.6 Cytotoxicity

3.6.1 Cytotoxicity of formulations based on ternary complexes, Lipofectamine2000 lipoplex and brPEI polyplex in the optimum composition

The potential of the ternary complex for therapeutic purposes can be appropriately interpreted only if impending toxic effects are taken into account. As a result, the cytotoxicity of the ternary complex (prepared under conditions showing highest transgene expression) was investigated and compared with Lipofectamine2000-based and brPEI-based counterparts. As shown in **Figure 3.6-1**, both BEAS-2B and 16HBE cells transfected by ternary complex survived most among all the groups. Similarly, brPEI polyplex induced mild toxicity to both cell lines. However, severe toxicity was observed in Lipofectamine2000 groups, which resulted in as much as 50%-70% cell death.

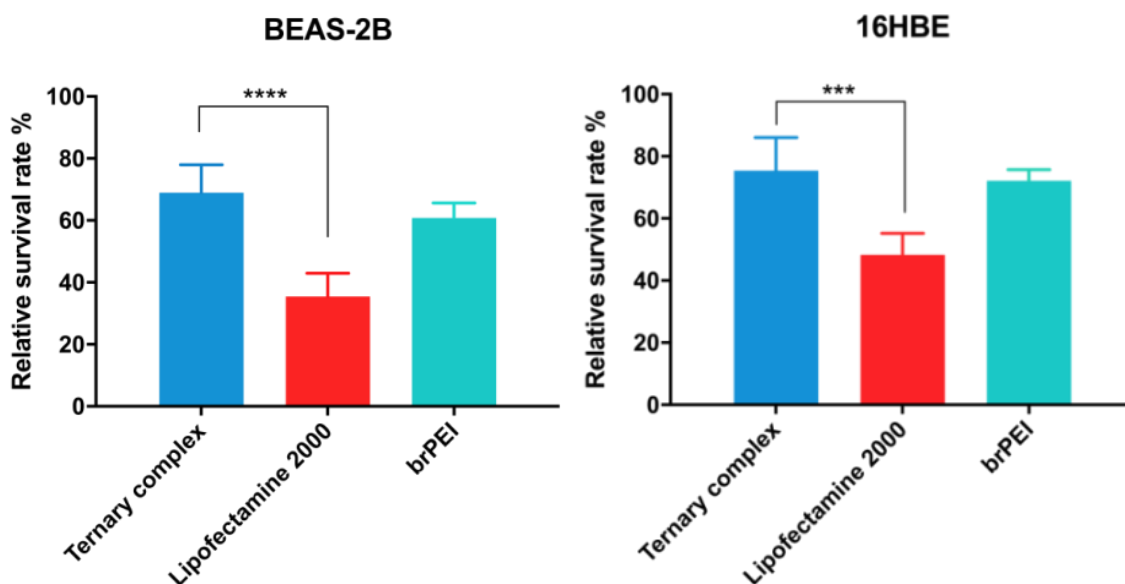


Figure 3.6-1 The cytotoxicity of pDNA based ternary complex, Lipofectamine2000 based lipoplex and brPEI based polyplex. BEAS-2B and 16HBE cells were incubated with above formulations for 4 h at 37 °C in a humidified atmosphere, then fresh cell culture media as recommended were added to substitute above samples.

An MTT assay was performed 24 h post transfection. The data are given as the mean \pm SD (n>5). Significant differences were defined as ***: $p < 0.005$; ****: $p < 0.001$;

3.6.2 Cytotoxicity of T704, peptide 9, Lipofectamine2000 and brPEI

The cytotoxicity of above formulations could be explained when the cytotoxic effect induced by T704, peptide 9, Lipofectamine2000 and brPEI alone in a wide concentration range (normalized to the weight of dosing per well) was revealed. The half maximal inhibitory concentration (IC_{50}) of each candidate in both cell lines was in the following order: $IC_{50}(\text{Lipofectamine2000}) < IC_{50}(\text{brPEI}) < IC_{50}(\text{peptide 9}) < IC_{50}(\text{T704})$, implying that the components of the ternary complex were safe and well-tolerated materials (**Figure 3.6-2**).

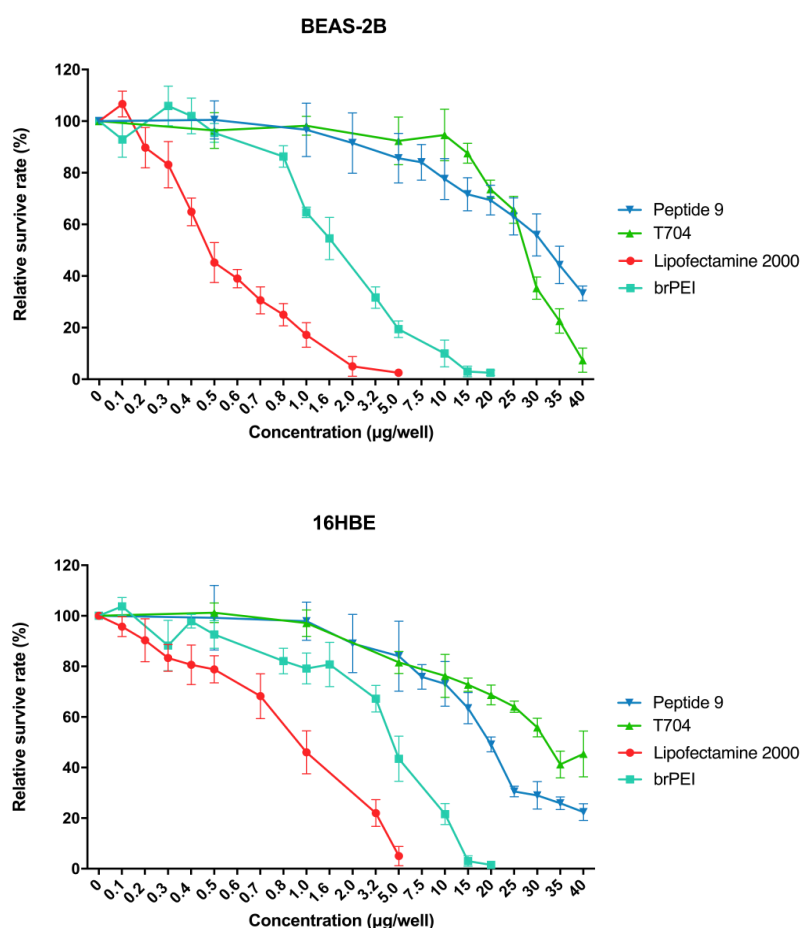


Figure 3.6-2 The cytotoxicity of T704, peptide 9, Lipofectamine2000 and brPEI at different concentrations (normalized to $\mu\text{g/well}$). BEAS-2B cells and 16HBE cells were incubated with different concentrations of peptide 9 (0.5 to 40 $\mu\text{g/well}$), T704 (0.5 to 40 $\mu\text{g/well}$), Lipofectamine2000 (0.1 to 20 $\mu\text{g/well}$) for 4 h at 37 °C in a humidified atmosphere, then fresh cell culture media as recommended were added to substitute above samples. An MTT assay was performed 24 h post transfection. The data are given as the mean \pm SD (n>5).

3.7 In vivo evaluation of ternary complexes

3.7.1 In vivo mRNA expression mediated by ternary complex

For *in vivo* evaluation of ternary complexes, we first investigated the mRNA delivery efficiency via the intratracheal application. We used *in vivo* bioluminescence imaging to compare the transgene expression induced by intratracheal dosing of following fLUC-mRNA based formulations in the lungs of mice: 1) T704-based binary complex in Tyrode's solution; 2) Peptide 9/T704-based ternary complex in NF-water; 3) NF-water served as a negative control formulation. 24 h post transfection, the luciferase expression was measured. Bioluminescence signals were generally too weak to be detected in live mice. Lungs were excised from mice to detect the luciferase expression by bioluminescence imaging (**Figure 3.7-1a**). Quantitative analysis of the data was performed by drawing regions of interest around the area displaying signals in the lungs, and the intensity of the signal in these regions was calculated. Using this method of quantification, signals from excised lungs indicated that mRNA expression mediated by Peptide 9/T704-based ternary complex was significantly higher than that mediated by the binary counterpart (**Figure 3.7-1b**).

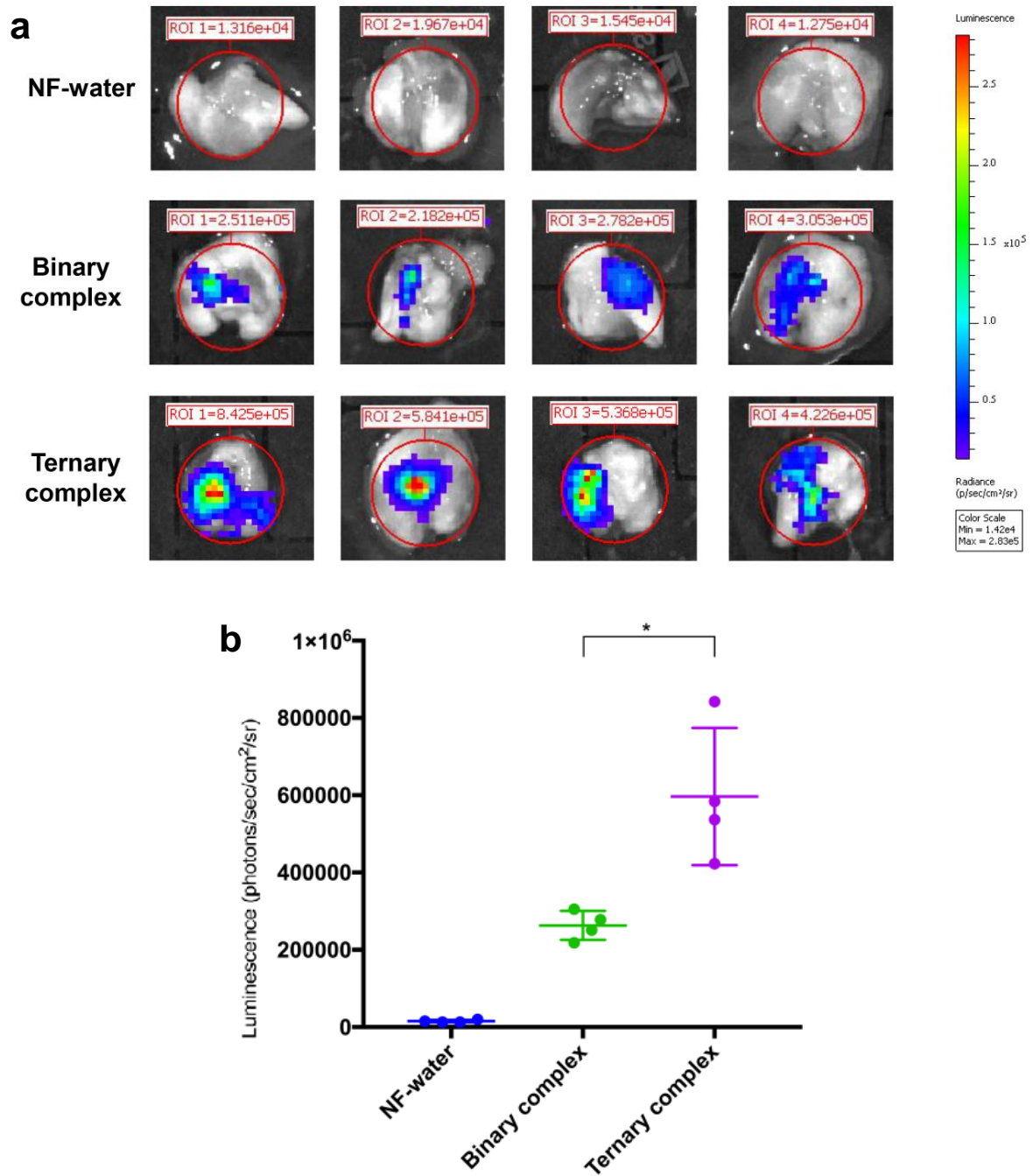


Figure 3.7-1 *In vivo* evaluation of mRNA transfection efficiency mediated by the ternary complex. (a) Transgene expression in the lungs of mice (24 h post transfection) following fLUC-mRNA transfections mediated by T704-based binary and ternary complex, (b) with a quantitative comparison of their signal intensities. Mice treated with NF-water served as negative controls. The lungs were excised prior to bioluminescence imaging. Significant differences were defined as * = $p < 0.05$;

3.7.2 *In vivo* evaluation of pDNA transfection efficiency mediated by ternary complex

The ternary complex has shown its superiority in the delivery of pDNA into cultured cells compared with other prominent transfection reagents as described above. In order to further prove its promising in *in vivo* applications, *in vivo* bioluminescence imaging was applied to compare the transgene expression induced by intratracheal dosing of following pGM206-fLUC-CFTR/T2 based formulations in CF-mice: 1) T704-based binary complex in Tyrode's solution; 2) T704- peptide 9 based ternary complex in NF-water; 3) Cationic lipids (DOTAP) based lipoplex. DOTAP was chosen as a lipoplex control because it is highly efficient for pDNA transfection and has been successfully used for several *in vivo* applications^{152–154}. Meanwhile, NF-water served as a negative control formulation. The expression of luciferase reporter gene obtained 48 h after intratracheal administration of above-mentioned formulations is presented in **Figure 3.7-2a**. Apart from NF-water group, discrete spots of signals are present in the area of lungs of mice. Similar to the previous report¹³⁰, T704 based binary complex led to brighter signals compared with that of DOTAP based lipoplex. Mice transfected by ternary complex showed the strongest signals among all the groups (**Figure 3.7-2a**). It is worth noting that the area expressing signals in the ternary complex group was more expanded and dispersed than that of the binary complex group. The epithelium targeting ligand which presents in the ternary complex may explain this phenomenon. Statistical analysis of the bioluminescence intensity showed that a highly significant difference in luciferase expression induced by ternary complex versus binary complex or DOTAP-based lipoplexes (**Figure 3.7-2b**). Transgene expression with ternary complex was nearly doubled than that with the binary complex.

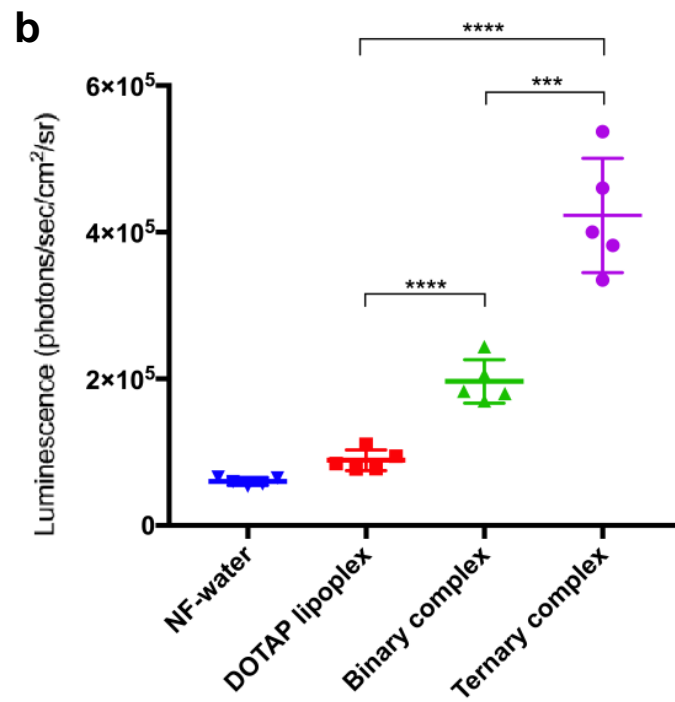
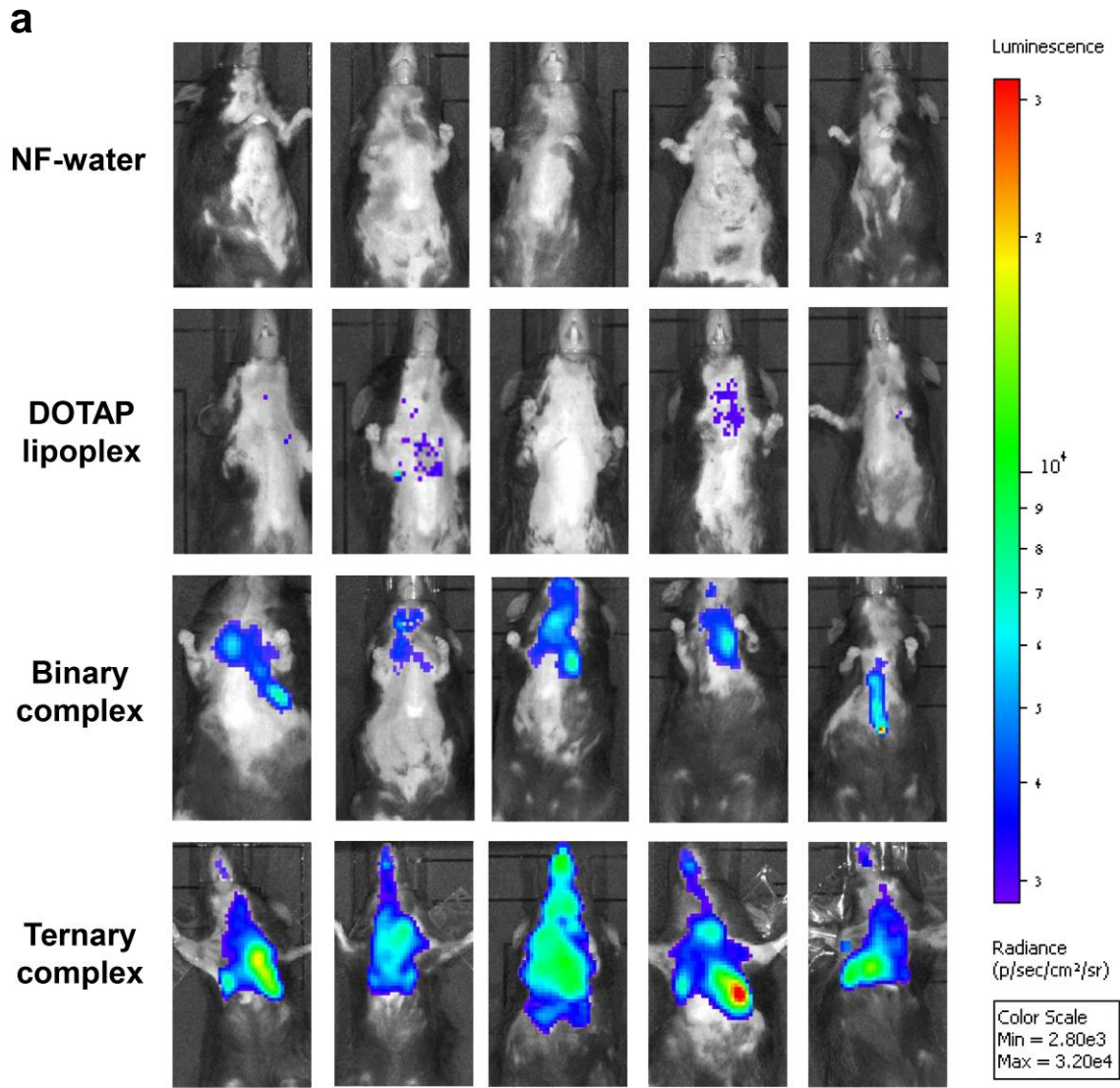


Figure 3.7-2 *In vivo* evaluation of pDNA transfection efficiency of the ternary complex. (a) Bioluminescence imaging (48 h after transfection) of pGM206-fLUC-CFTR/T2 expression mediated by DOTAP based lipoplex, T704 based binary and ternary complex in live mice. Mice treated with NF-water served as negative controls. (b) The signal intensity from each sample was measured and quantitatively compared. Significant differences were defined as ***: $p < 0.005$; ****: $p < 0.001$;

3.7.3 *In vivo* toxicity of ternary complex

To study *in vivo* toxicity and inflammation, pathohistological analysis of lung sections from mice treated with NF-water, DOTAP based lipoplex, binary and ternary complexes was performed. Lungs of mice treated with NF-water showed no signs of interstitial edema or cellular infiltration, and similar histology was observed in mice that were treated with binary complex and ternary complex (**Figure 3.7-3**). In contrast, lungs of mice that received DOTAP based lipoplex exhibited thickened alveolar walls and patchy inflammation which was predominantly of a macrophage/monocyte nature (**Figure 3.7-3b**). The trachea sections of mice treated with the binary complex and the ternary complex also showed no signs of inflammation (**Figure 3.7-4**).

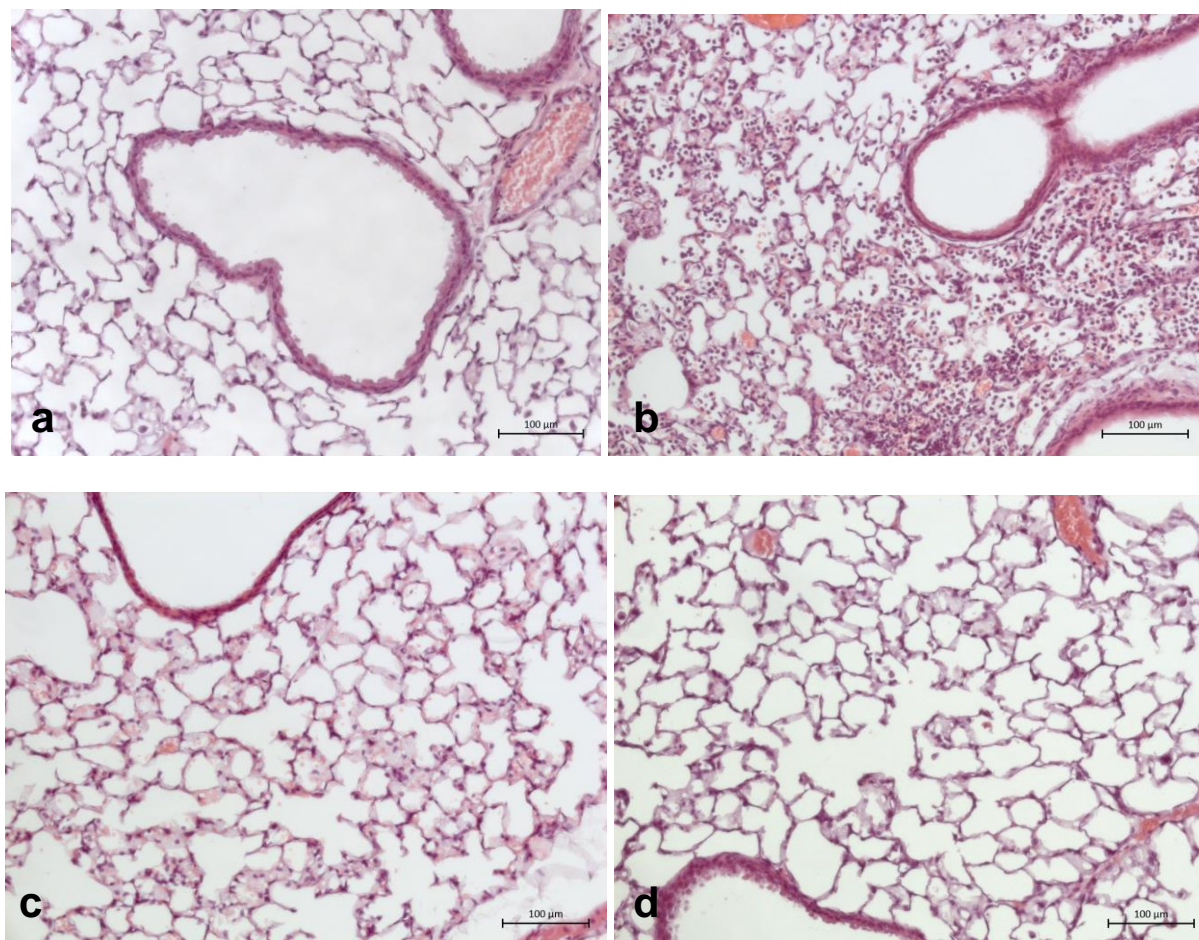


Figure 3.7-3 *In vivo* toxicity of different formulations. Histopathologic analysis of lung sections from (a) NF-water, (b) DOTAP-based lipoplex, (c) binary and (d) ternary complex treated mice obtained 48 h after dosing. Haematoxylin-Eosin (H&E) staining, $\times 20$ magnification.

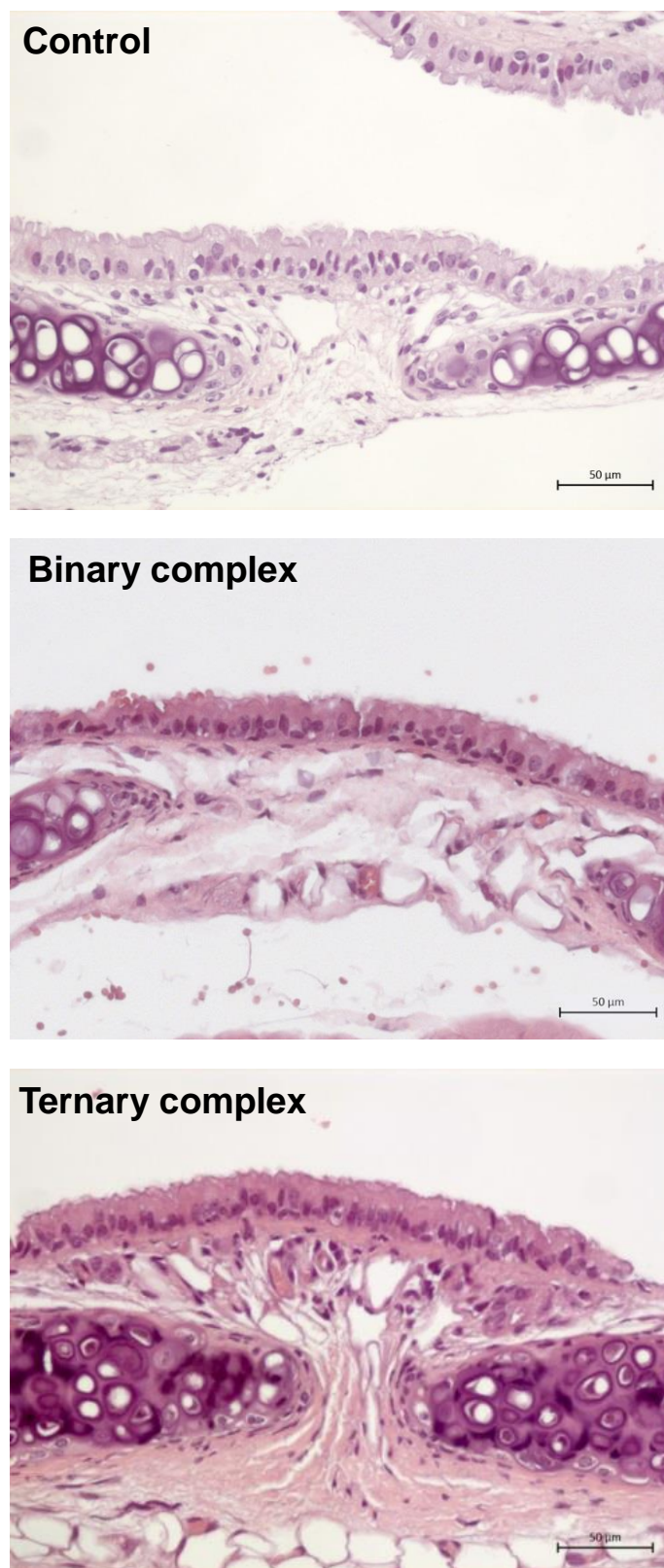


Figure 3.7-4 Representative histopathologic analysis of trachea sections. Samples were obtained from mice treated with NF-water, T704 based binary and ternary complex 48 h after dosing. Haematoxylin-Eosin (H&E) staining, $\times 40$ magnification.

3.8 In vivo long-term transgene expression mediated by ternary complexes containing SleepingBeauty (SB) transposon system

3.8.1 In vivo long-term luciferase expression

To determine if ternary complex could mediate *in vivo* long-term transgene expression, pGM206-fLUC-CFTR/T2 and SB100X-mRNA were formulated and administered to mice intratracheally. Two days after dosing, pGM206-fLUC-CFTR/T2 treated and (pGM206-fLUC-CFTR/T2+SB100X-mRNA) co-transfected mice showed strong luciferase expression in the area of lungs (**Figure 3.8-1**). Only a background-level signal could be observed in SB100X-mRNA treated mice in the whole study (**Figure 3.8-1**). The luciferase expression in (pGM206-fLUC-CFTR/T2+SB100X-mRNA) co-treated mice varied between 30-61% relative to day 2 in the following investigated periods, whereas the luciferase signal from pGM206-fLUC-CFTR/T2 treated mice was hardly detectable since 2 weeks post transfection (**Figure 3.8-1**). At the pre-determined end (7 weeks) of this investigation, strong bioluminescence signals still could be observed in the excised lungs of (pGM206-fLUC-CFTR/T2+SB100X-mRNA) co-treated group, while lungs from other groups showed no signal (**Figure 3.8-1**).

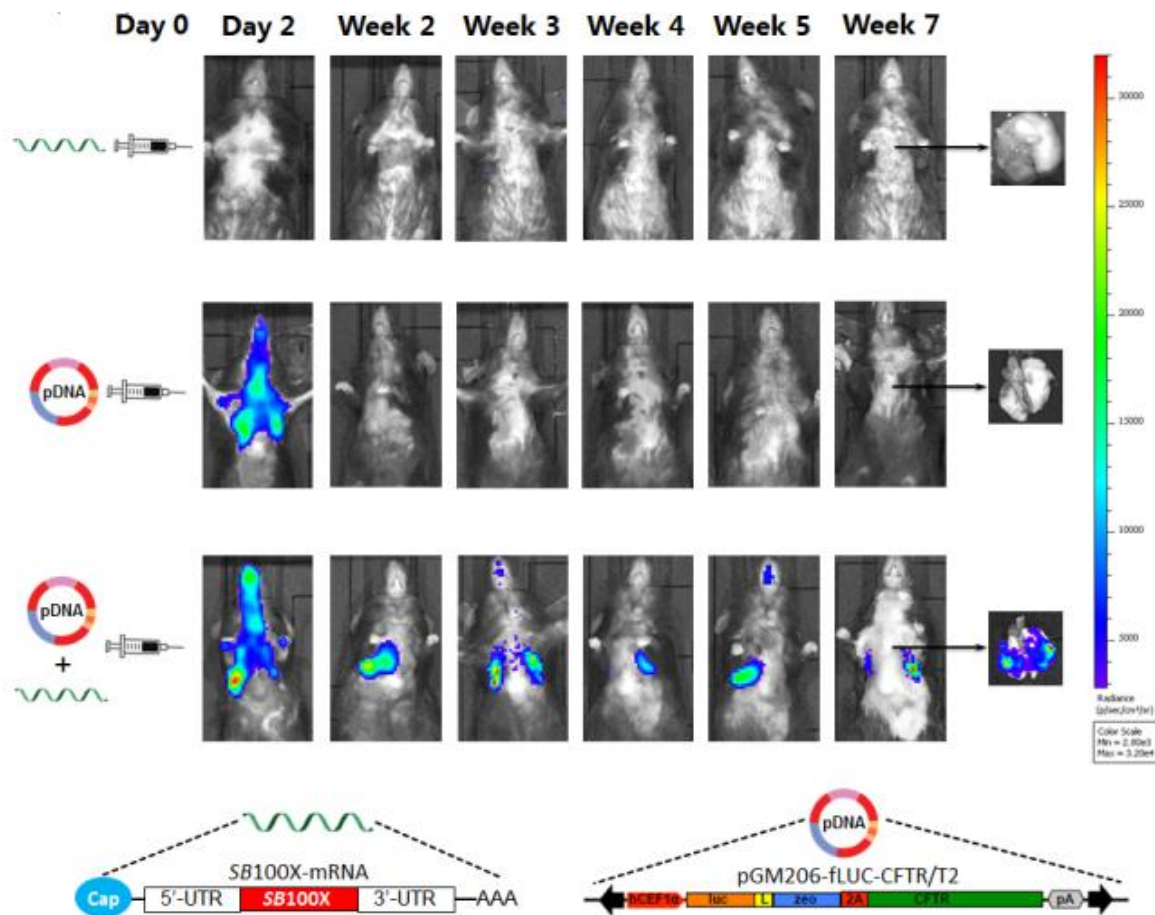


Figure 3.8-1 *In vivo* stable and long-term luciferase expression mediated by the ternary complex containing *SB* transposon system. Exemplary bioluminescence images were taken at indicated time points after dosing. Mice treated with a single formulation containing *SB100X* mRNA or fLUC-CFTR/T2 pDNA were applied as controls.

3.8.2 *In vivo* long-term CFTR expression

In order to confirm if there was long-term expression of CFTR in above (pGM206-fLUC-CFTR/T2+*SB100X*-mRNA) co-transfected group, CFTR immune-staining study was performed and revealed a clear and consistent CFTR expression at the apical side of the superficial epithelium of bronchial airways, which was similar to the CFTR signal observed in wildtype (WT) group, while only residual CFTR expression ($\sim 10\%^{155}$) was observed in the sample from untreated CF mice (**Fig.3.8-2**).

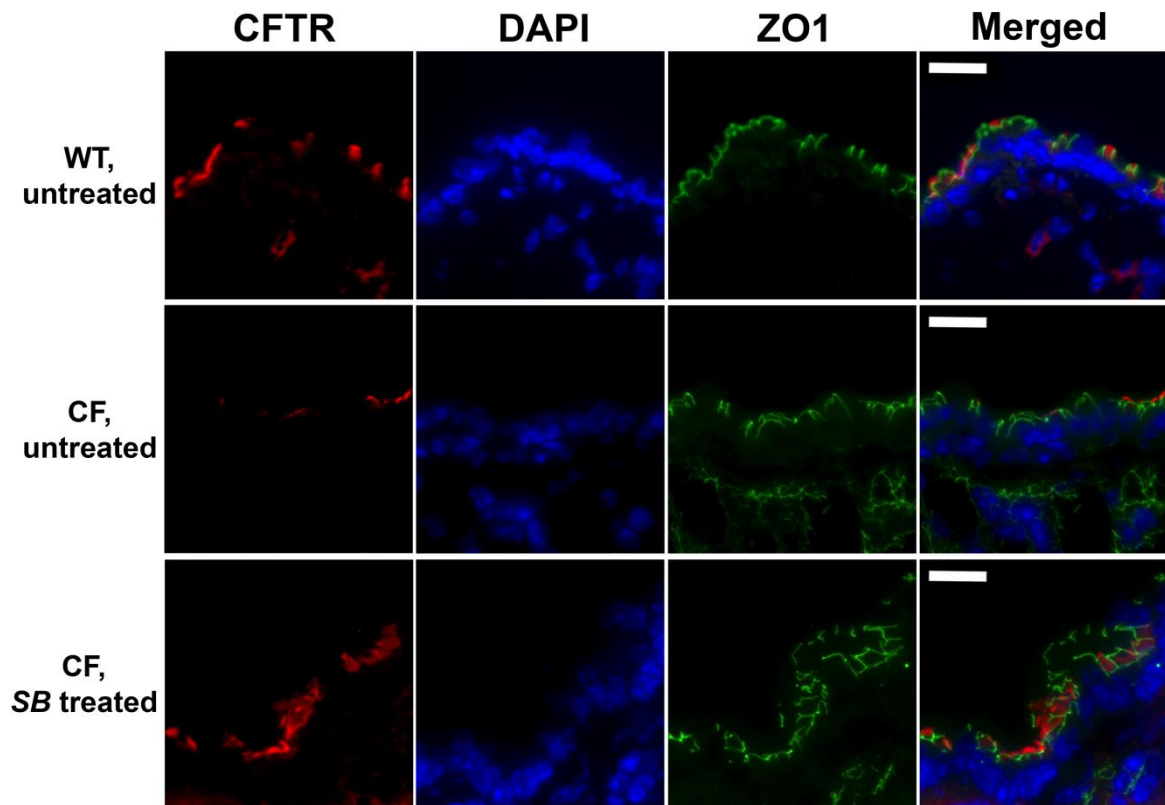


Figure 3.8-2 *In vivo* long-term CFTR expression. Restored long-term (7 weeks after dosing) CFTR expression in the bronchial epithelium of mice treated with the ternary complex containing *SB* transposon system detected by histochemical staining assay. The lung sections from untreated CF mice and wildtype (WT) mice were used as the negative and positive control, respectively. Scale bar: 10 μ m.

3.9 Preliminary evaluation of ternary complexes comprising other poloxamines or poloxamers

After establishing and optimizing peptide-T704 ternary complexes, it is interesting to determine if “ternary complex” strategy endowed by synthetic peptides could generalize to other poloxamines or poloxamers. To this end, poloxamine304 (T304), poloxamine904 (T904), poloxamine90R4 (T90R4) and poloxamer184 (L64) were employed to form ternary complexes with synthetic peptides and MetLuc-mRNA. Their transfection efficiency in 16HBE cells was evaluated. In order to standardize the transfection procedure, we fixed the following parameters for all transfections: i) the concentration of mRNA in ternary complex was fixed at 400 ng/well (relative to 96-well plates); ii) ternary complex was prepared by first mixing equal volume of poloxamine or poloxamer and peptide stock solution, followed by adding equal volume of mRNA stock solution; iii) ternary complex was consistently prepared in NF-water; iv) ternary complex was incubated with 16HBE cells for 4 h. Similar to T704 based binary complex, mRNA expression mediated by binary complexes comprising T304, T904, T90R4 or L64 were at the background level (Data not shown).

3.9.1 In vitro evaluation of ternary complexes consisting of T304

3.9.1.1 The influence of T304 concentration within ternary complex

In order to find out the optimum concentration of T304 within the ternary complex, we started from peptide 6 at the N/P ratio of 5 to investigate the influence of T304 concentration on the transfect efficiency of mRNA/T304/peptide 6 ternary complexes. As shown in **Figure 3.9-1**, ternary complexes showed a background level of transfection when T304 in the concentration range of 10-100 (w/w). The mRNA expression increased with the concentration of T304 from 250 (w/w), reaching maximum when the concentration of T304 was at 2045 (w/w). Then the

mRNA expression remained in the plateau at the higher T304 concentration (2045-2500 (w/w)).

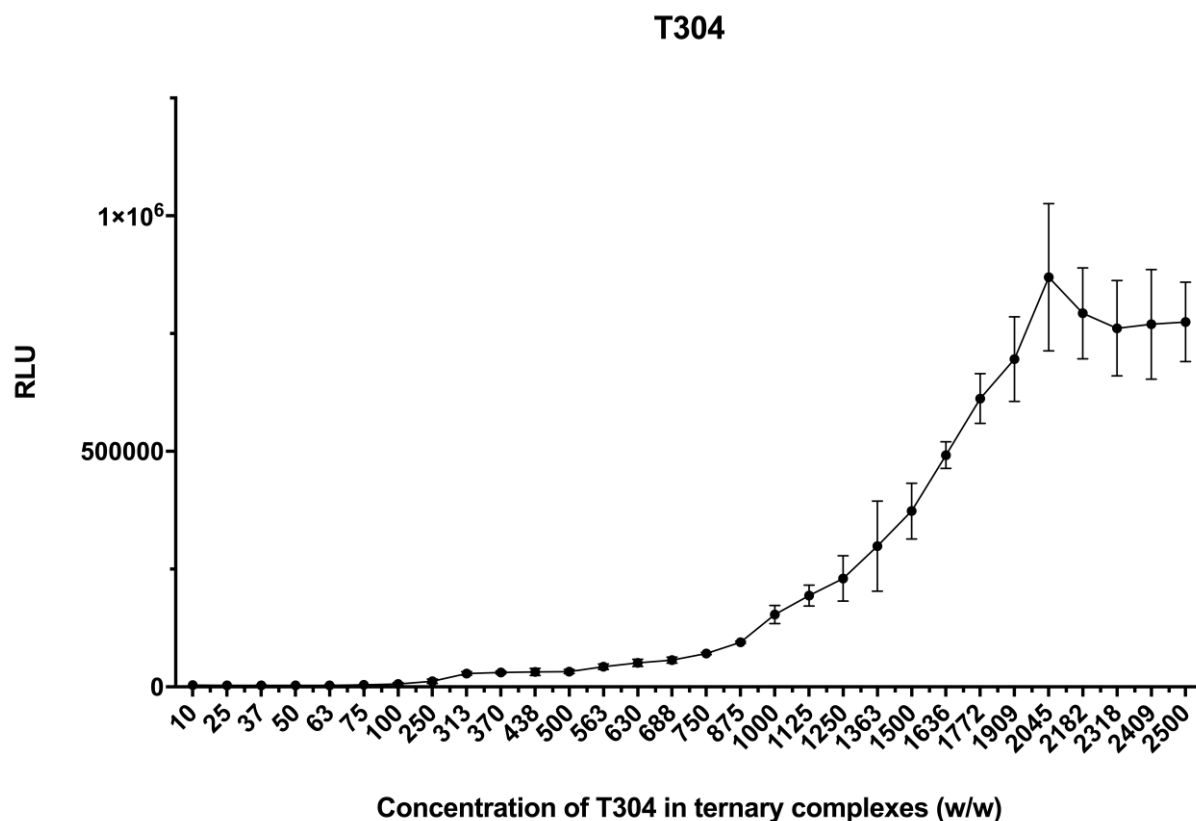


Figure 3.9-1 *In vitro* transfection efficiency of MetLuc-mRNA/peptide 6/T304 ternary complexes comprising T304 at different concentrations. T304 in the concentration range of 10-2500 (w/w, relative to mRNA) were complexed with peptide 6 at N/P ratio of 5 and MetLuc-mRNA. The same transfection procedure as described in the peptide-T704 ternary complex was applied. Luciferase activity was expressed in RLU. The data are given as the mean \pm SD ($n > 5$).

3.9.1.2 The influence of peptide component within T304 based ternary complex

To further optimize T304 based ternary complex, T304 at the concentration of 2000 (w/w) were used to formulate ternary complex with mRNA and different peptides at various N/P ratios. The transfection efficiency of resulting ternary complexes was displayed in **Figure 3.9-2**. The comparison of mRNA expression mediated by ternary complexes in the optimum composition was displayed in **Figure 3.9-3**. Peptide 0, Peptide 6, peptide 7 and peptide 8

based ternary complex showed a high level of mRNA expression among all the groups, with peptide 0-T304 ternary complex being the most potent one.

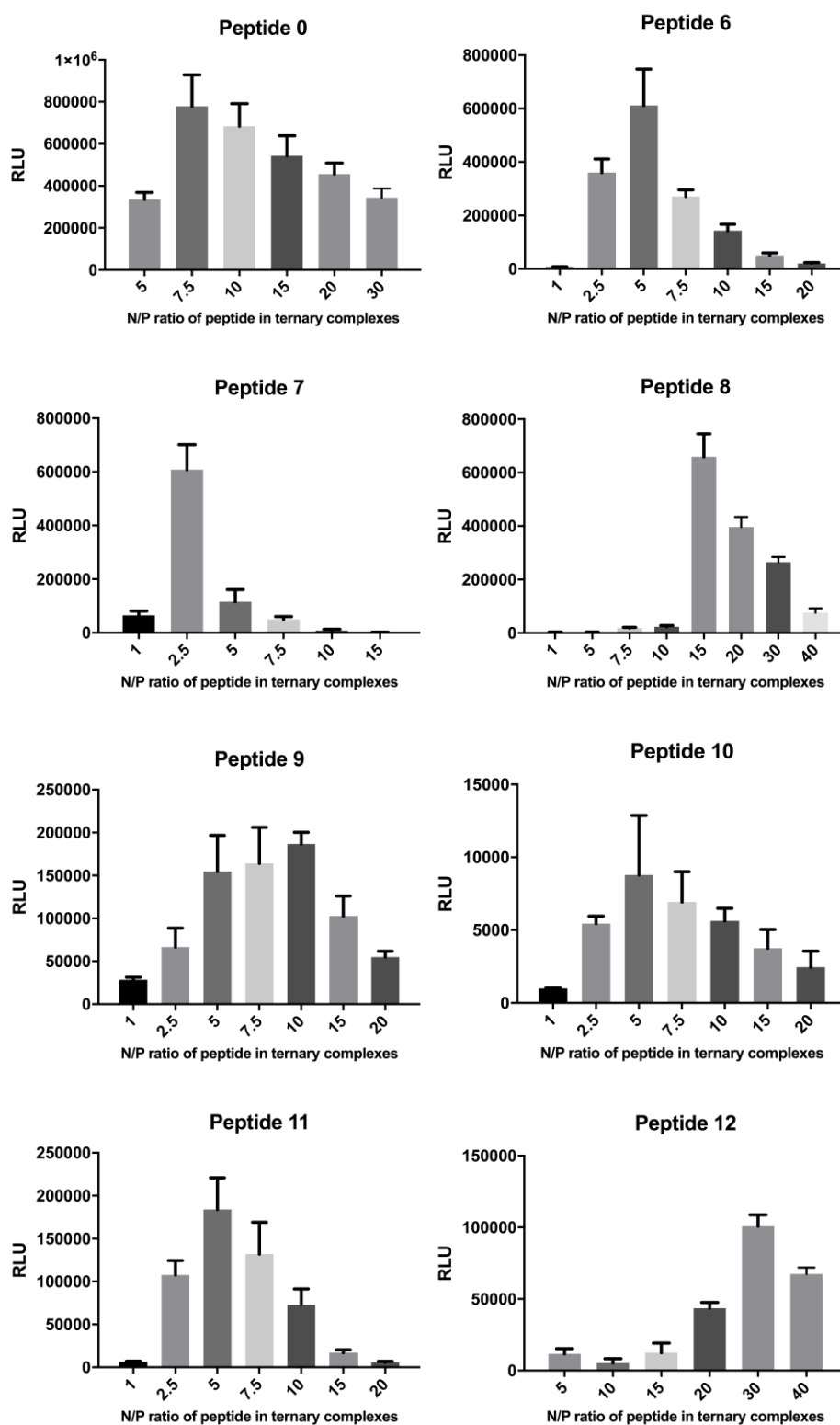


Figure 3.9-2 *In vitro* transfection efficiency of MetLuc-mRNA-T304 based ternary complexes comprising different peptides in 16HBE cells. Peptide0, Peptide 6 to peptide 12 at various N/P ratios were complexed with T304 at a concentration of 2000 (w/w) and MetLuc-mRNA. Luciferase activity was expressed in RLU. The data are given as the mean \pm SD (n > 5).

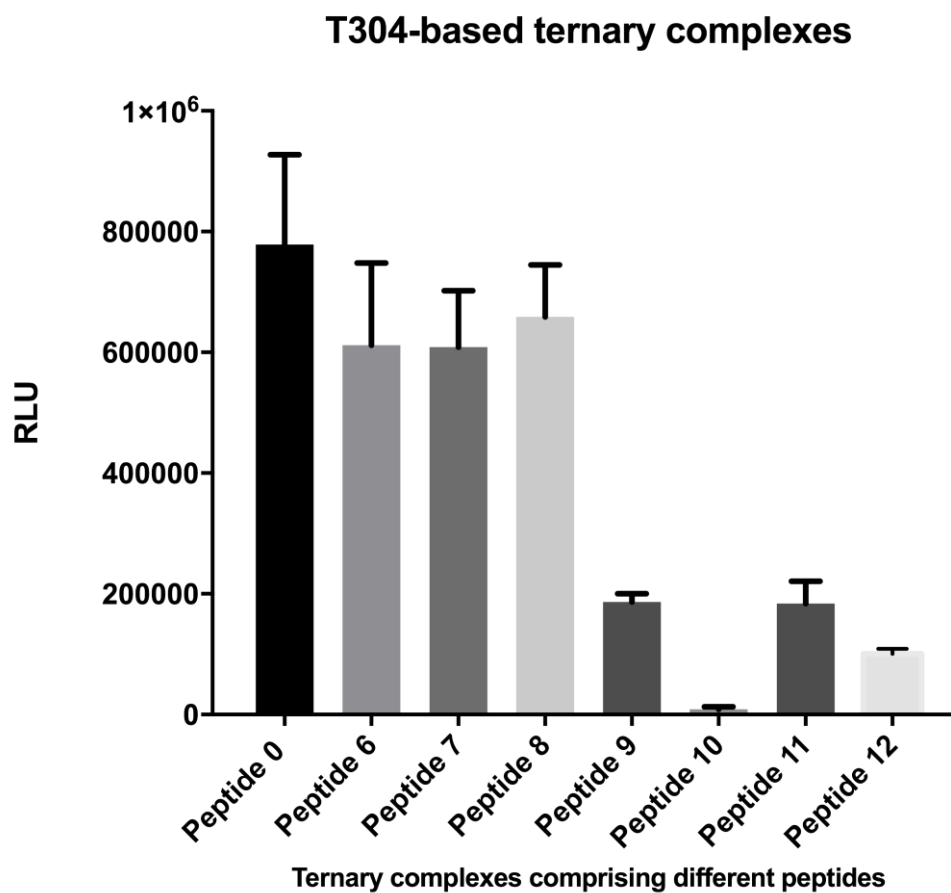


Figure 3.9-3 Comparisons of the optimum *in vitro* transfection efficiency mediated by MetLuc-mRNA-T304 based ternary complexes comprising different peptides in 16HBE cells. The concentration of T304 in ternary complexes was 2000 (w/w). The N/P ratio of the peptide in certain ternary complexes was as following: peptide12 at 30; peptide 8 at 15; peptide 9 at 10; peptide 0 at 7.5; peptide 6, 10 and 11 at 5; peptide7 at 2.5. Luciferase activity was expressed in RLU. The data are given as the mean \pm SD (n >5).

3.9.2 *In vitro* evaluation of T904 based ternary complexes

3.9.2.1 The influence of T904 concentration within ternary complex

To evaluate peptide-T904 ternary complex, we used peptide 6 at the N/P ratio of 5 to form the ternary complex with T904. As shown in **Figure 3.9-4**, the mRNA expression mediated by T904 based ternary complex showed its maximum expression when the concentration of T904 was 100 (w/w), which was similar to that of T704 based ternary complexes. Then the mRNA expression gradually declined at higher T904 concentration, reaching a plateau since the T904 concentration was above 350 (w/w).

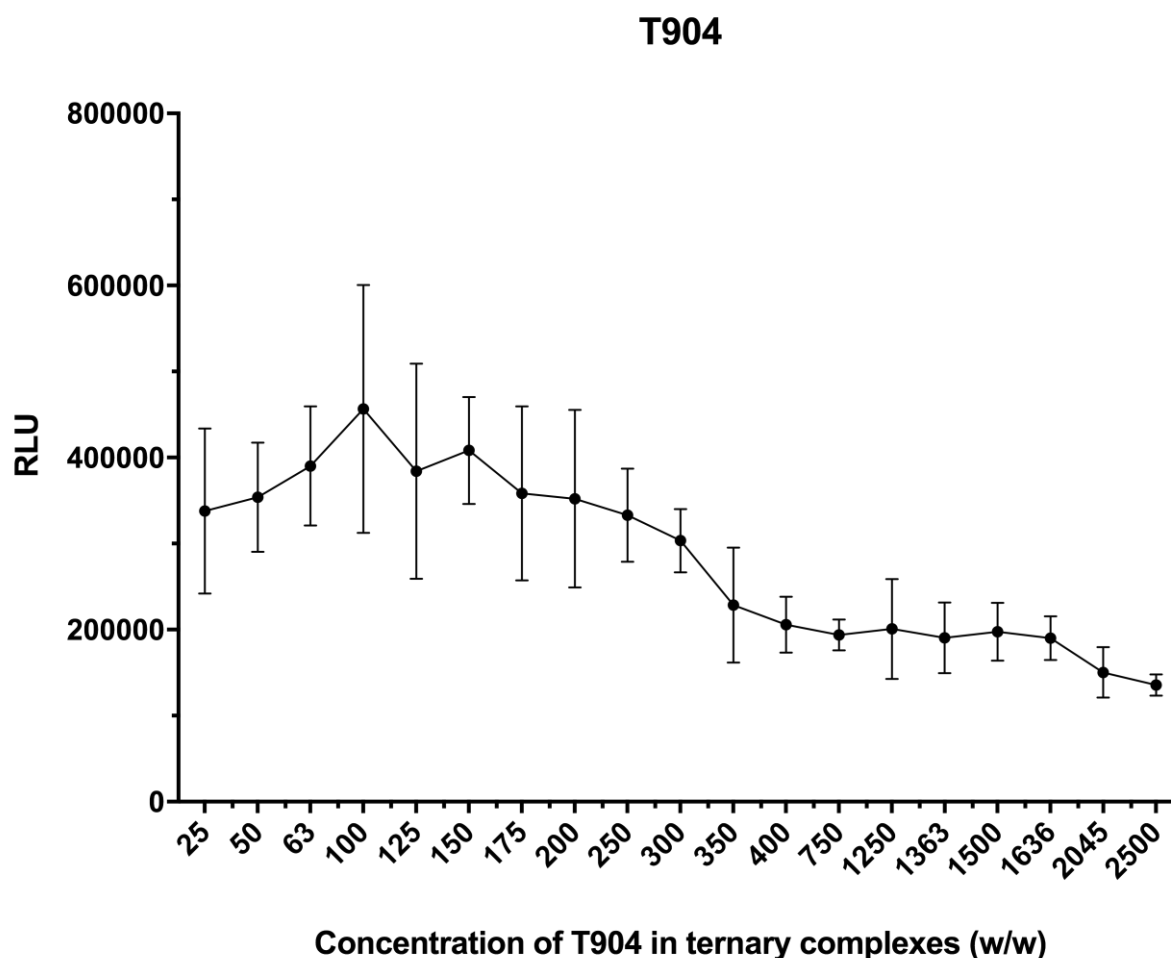


Figure 3.9-4 *In vitro* transfection efficiency of MetLuc-mRNA/peptide 6/T904 ternary complexes comprising T904 at different concentrations. T904 in the concentration range of 25-2500 (w/w, relative to mRNA) were complexed with peptide 6 at N/P ratio of 5 and MetLuc-mRNA. Luciferase activity was expressed in RLU. The data are given as the mean \pm SD (n >5).

3.9.2.2 The influence of peptide component within T904 based ternary complex

To further optimize T904 based ternary complex, T904 at the concentration of 100 (w/w) was used to formulate ternary complex with mRNA and different peptides at various N/P ratios.

The transfection efficiency of resulting ternary complexes was displayed in **Figure 3.9-5**.

The comparison of mRNA expression mediated by ternary complexes in optimum composition was displayed in **Figure 3.9-6**. Similar to T704 based ternary complexes, peptide

0, peptide 6, peptide 7 and peptide 9 based ternary complexes showed a high level of mRNA expression among all the groups, with peptide 9-T904 ternary complex being the highest one.

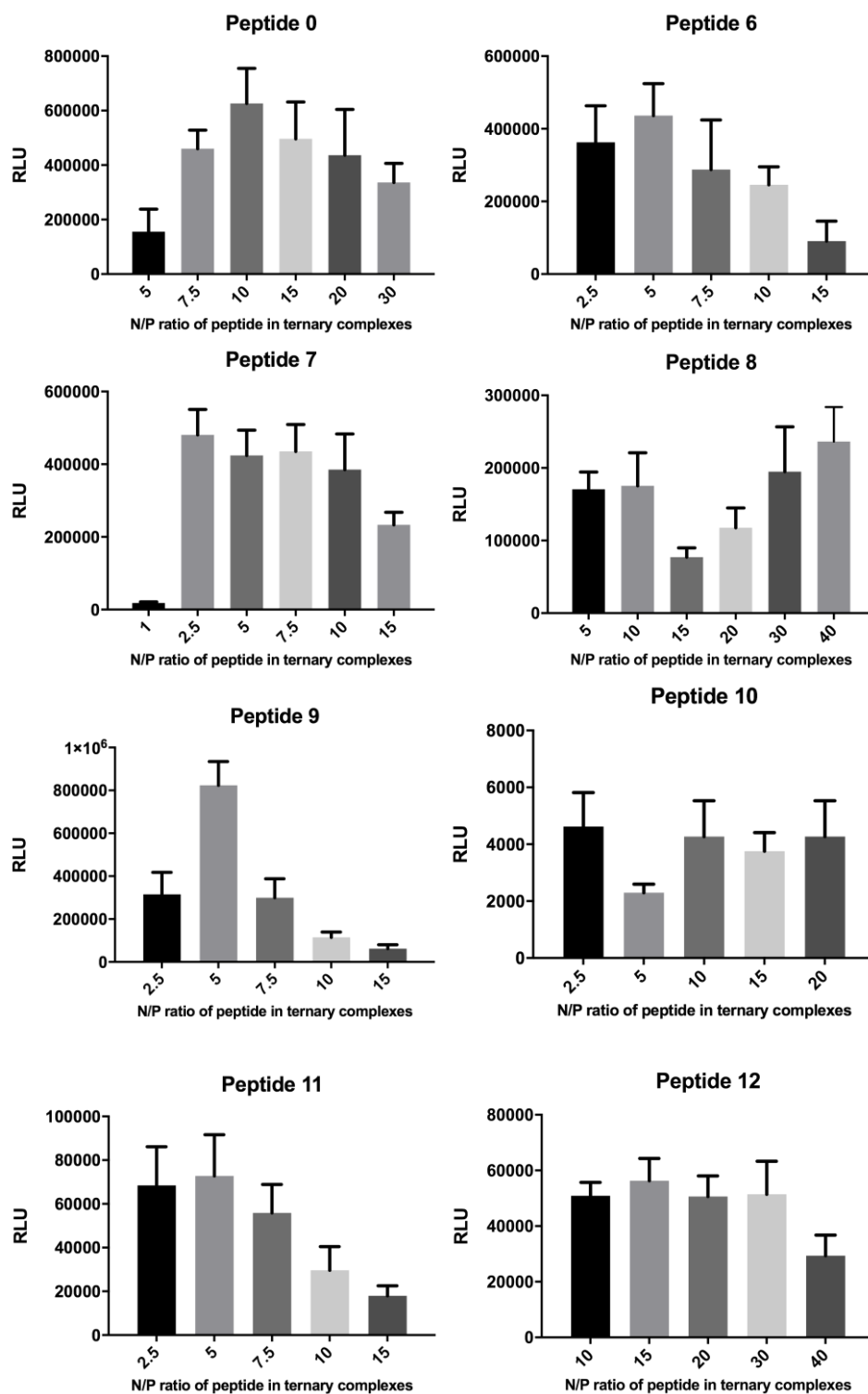


Figure 3.9-5 *In vitro* transfection efficiency of MetLuc-mRNA-T904 based ternary complexes comprising different peptides in 16HBE cells. Peptide0, Peptide 6 to peptide 12 at various N/P ratios were complexed with T904 at a concentration of 100 (w/w) and MetLuc-mRNA. Luciferase activity was expressed in RLU. The data are given as the mean \pm SD (n > 5).

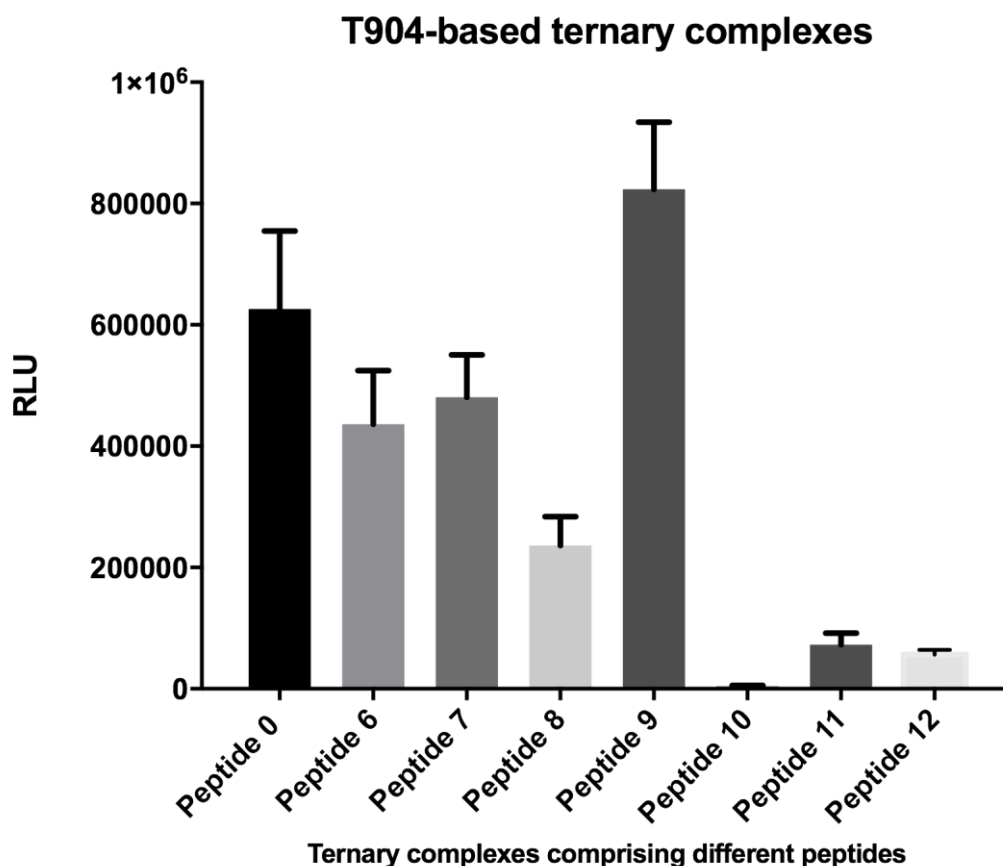


Figure 3.9-6 Comparisons of the optimum *in vitro* transfection efficiency mediated by MetLuc-mRNA/T904 based ternary complexes comprising different peptides in 16HBE cells. The concentration of T904 in ternary complexes was 100 (w/w). The N/P ratio of the peptide in certain ternary complexes was as following: peptide 8 at 40; peptide 12 at 15; peptide 0 at 10; peptide 6, 9 and 11 at 5; peptide 7 and 10 at 2.5. Luciferase activity was expressed in RLU. The data are given as the mean \pm SD (n >5).

3.9.3 *In vitro* evaluation of ternary complexes consisting of T90R4

3.9.3.1 The influence of T90R4 concentration within ternary complex

T90R4 represents a reverse-sequential poloxamine. In contrast to T904, the ethylenediamine molecule first reacted with ethylene oxide (EO) precursors and afterward with propylene oxide (PO), leading to tetrafunctional block copolymers displaying poly(propylene oxide) (PPO) terminal segments. Peptide 6 at the N/P ratio of 5 was applied to formulate ternary complex with T90R4 and mRNA. The mRNA expression mediated by T90R4 based ternary

complex progressively raised at low concentration of T90R4 (10-438 (w/w) and drastically boosted from T90R4 at the concentration 438 (w/w), reaching the maximum expression at a T90R4 concentration of 1636 (w/w) (**Figure 3.9-7**). Afterward, the mRNA expression gradually decreased to half of the maximum when T90R4 was at the concentration of 2500 (w/w).

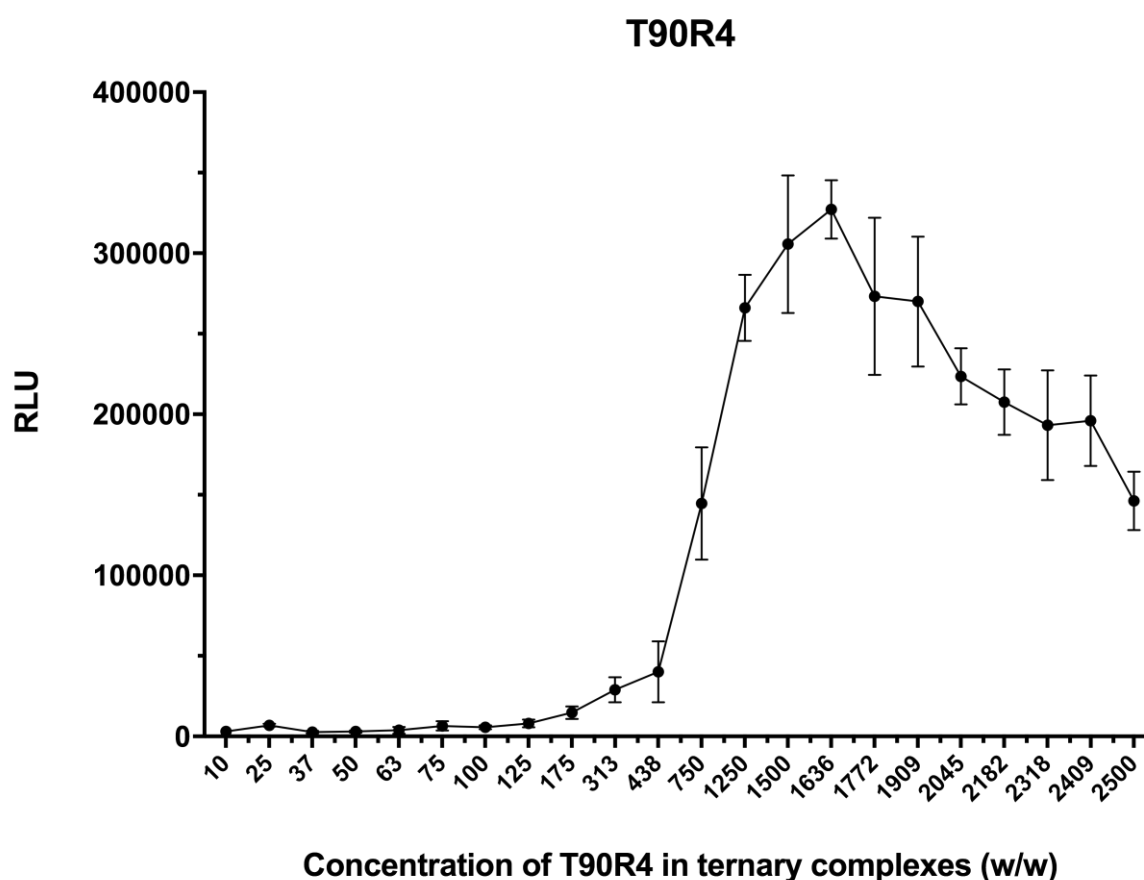
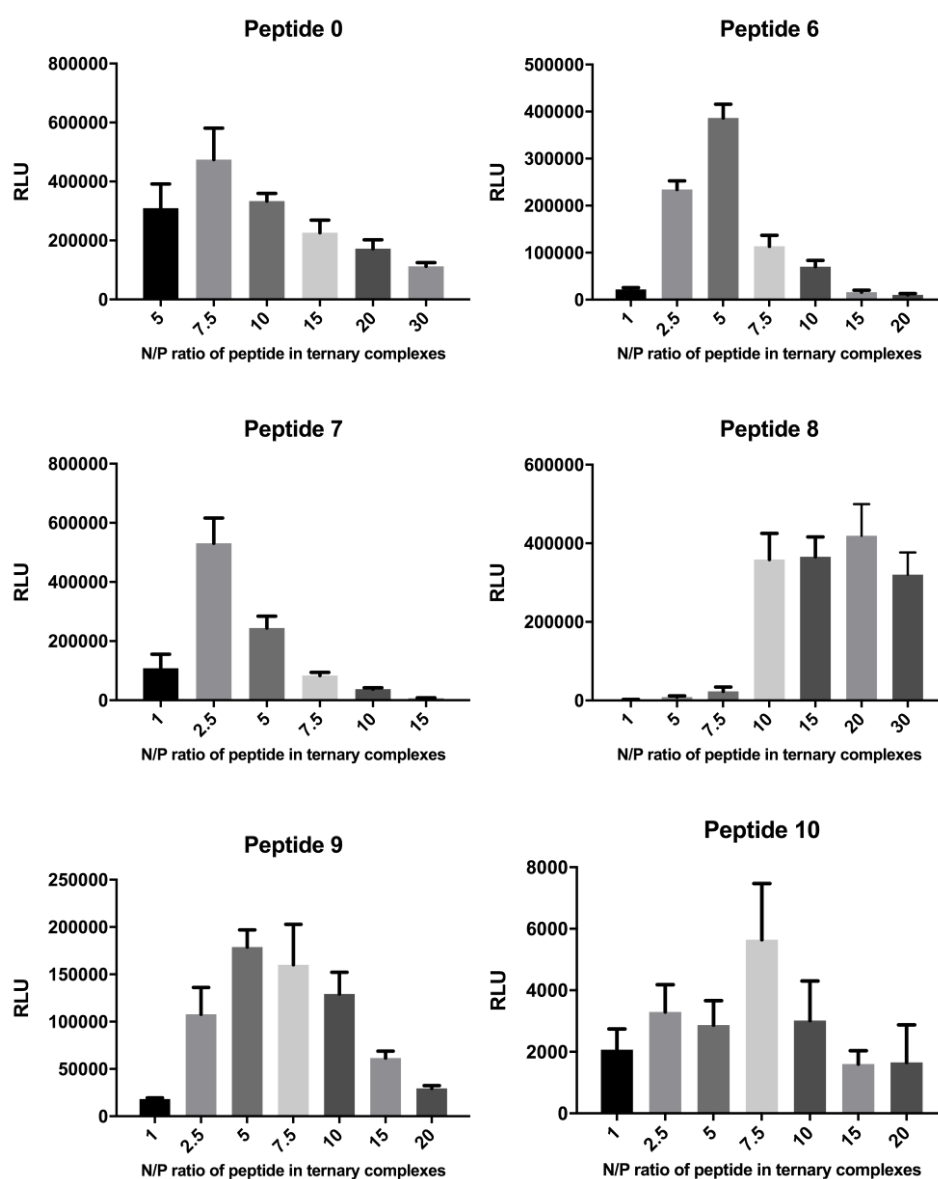


Figure 3.9-7 *In vitro* transfection efficiency of MetLuc-mRNA/peptide 6/T90R4 ternary complexes comprising T90R4 at different concentrations. T90R4 in the concentration range of 10-2500 (w/w, relative to mRNA) were complexed with peptide 6 at N/P ratio of 5 and MetLuc-mRNA. Luciferase activity was expressed in RLU. The data are given as the mean \pm SD ($n > 5$).

3.9.3.2 The influence of peptide component within T90R4 based ternary complex

To further investigate the influence of peptide component towards the transfection efficiency of T90R4 based ternary complex, T90R4 was fixed at the concentration of 1600 (w/w) to form ternary complexes with mRNA and different peptides at various N/P ratios. The

transfection efficiency of resulting ternary complexes was displayed in **Figure 3.9-8**. The maximum mRNA expression mediated by ternary complexes containing different peptides was compared (**Figure 3.9-9**). The results showed that peptide 0, peptide 6, peptide 7 and peptide 8 based ternary complex were potent candidates, with peptide 7-T90R4 ternary complex being the most efficient one.



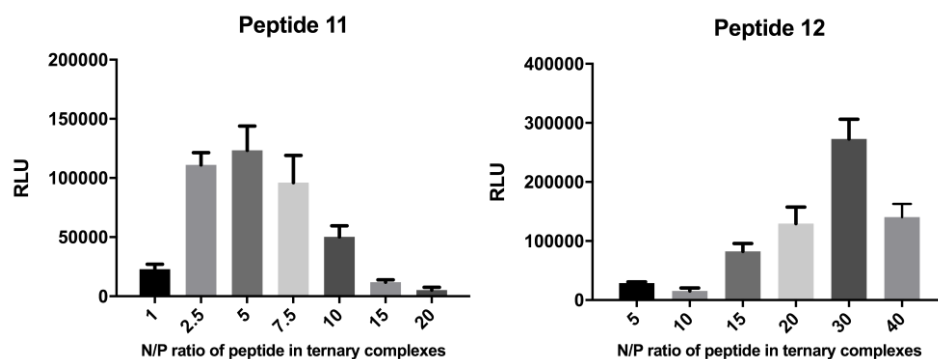


Figure 3.9-8 *In vitro* transfection efficiency of MetLuc-mRNA/T90R4 based ternary complexes comprising different peptides in 16HBE cells. Peptide0, Peptide 6 to peptide 12 at various N/P ratios were complexed with T90R4 at a concentration of 1600 (w/w) and MetLuc-mRNA. Luciferase activity was expressed in RLU. The data are given as the mean \pm SD ($n > 5$).

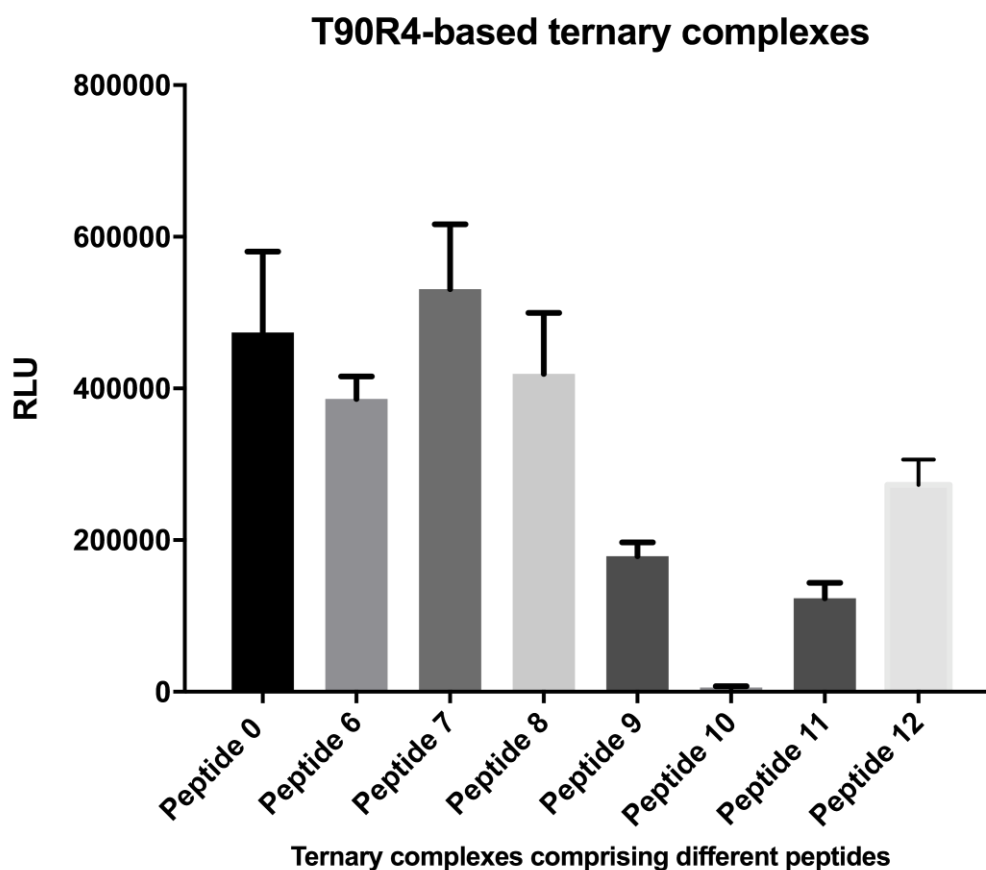


Figure 3.9-9 Comparisons of the optimum *in vitro* transfection efficiency mediated by MetLuc-mRNA/T90R4 based ternary complexes comprising different peptides in 16HBE cells. The concentration of T90R4 in ternary complexes was 1600 (w/w). The N/P ratio of the peptides in certain ternary complexes was as following: peptide 12 at 30; peptide 8 at 10; peptide 0 and 10 at 7.5; peptide 6, 9 and 11 at 5; peptide 7 at 2.5. Luciferase activity was expressed in RLU. The data are given as the mean \pm SD ($n > 5$).

3.9.4 *In vitro* evaluation of ternary complexes consisting of L64

3.9.4.1 The influence of L64 concentration within ternary complex

Poloxamer based block copolymers, consisting of EO and PO blocks arranged in a linear triblock structure (EO_x-PO_y-EO_x), are biocompatible amphiphilic copolymers which have been approved by FDA for the use of *in vivo* drug delivery¹⁵⁶. Poloxamer based block copolymers are recognized pharmaceutical excipients listed in the US and British Pharmacopoeia. Poloxamers have proven to be useful gene transfer vehicles in many *in vivo* studies. Poloxamer184 (L64) is one of the frequently used candidates within this chemical family. To evaluate peptide-L64 ternary complex, peptide 6 at the N/P ratio of 5 were formulated with MetLuc-mRNA and L64 in the concentration range of 50-2500 (w/w). The mRNA expression showed a sharp growth with the increased concentration of L64, reaching maximum at the concentration of 300 (w/w) (**Figure 3.9-10**). A descent of mRNA expression could be observed when the concentration of L64 within the ternary complex was above 400 (w/w) (**Figure 3.9-10**). This decline of mRNA expression may result from cytotoxic effects of highly concentrated materials. As revealed by the MTT assay, more than half of the cells were dead when the concentration of L64 within the ternary complex was above 500 (w/w) (data not shown).

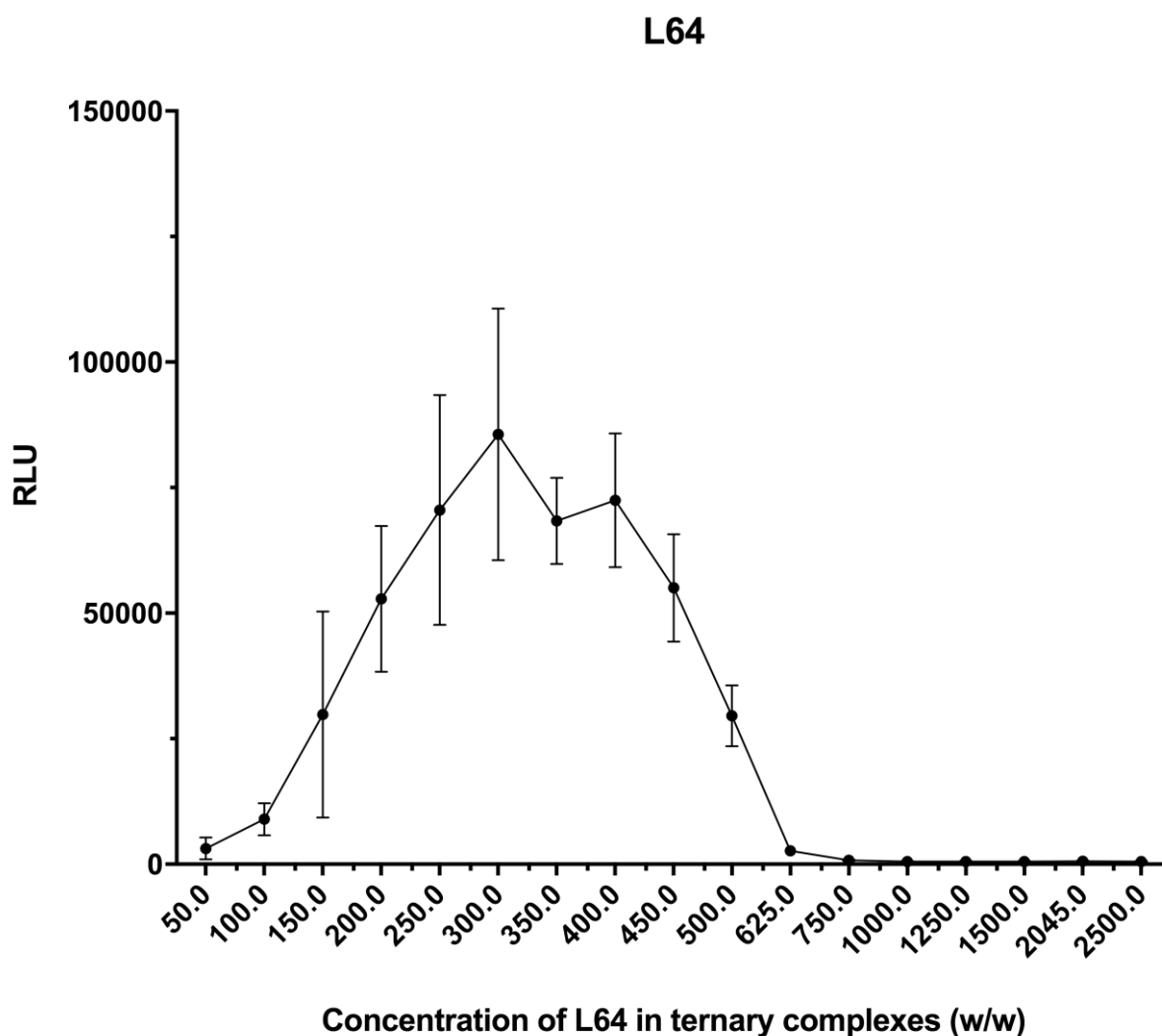


Figure 3.9-10 *In vitro* transfection efficiency of MetLuc-mRNA/peptide 6/L64 ternary complexes comprising L64 at different concentrations. L64 in the concentration range of 50-2500 (w/w, relative to mRNA) were complexed with peptide 6 at N/P ratio of 5 and MetLuc-mRNA. Luciferase activity was expressed in RLU. The data are given as the mean \pm SD ($n > 5$).

3.9.4.2 The influence of peptide component within L64 based ternary complex

To further investigate the impact of peptide component towards the transfection efficiency of L64 based ternary complex, L64 was fixed at the concentration of 300 (w/w) to form ternary complexes with mRNA and different peptides at various N/P ratios. The transfection efficiency of resulting ternary complexes was displayed in **Figure 3.9-11**.

The maximum mRNA expression mediated by ternary complexes containing different peptides was compared (**Figure 3.9-12**). The overall transfection efficiency of poloxamer-

based ternary complexes was lower than that of poloxamine counterparts. Among all the investigated groups, Peptide 0, 7 and 9 based ternary complexes were relatively more potent, with peptide 0-L64 ternary complex showing the highest transfection.

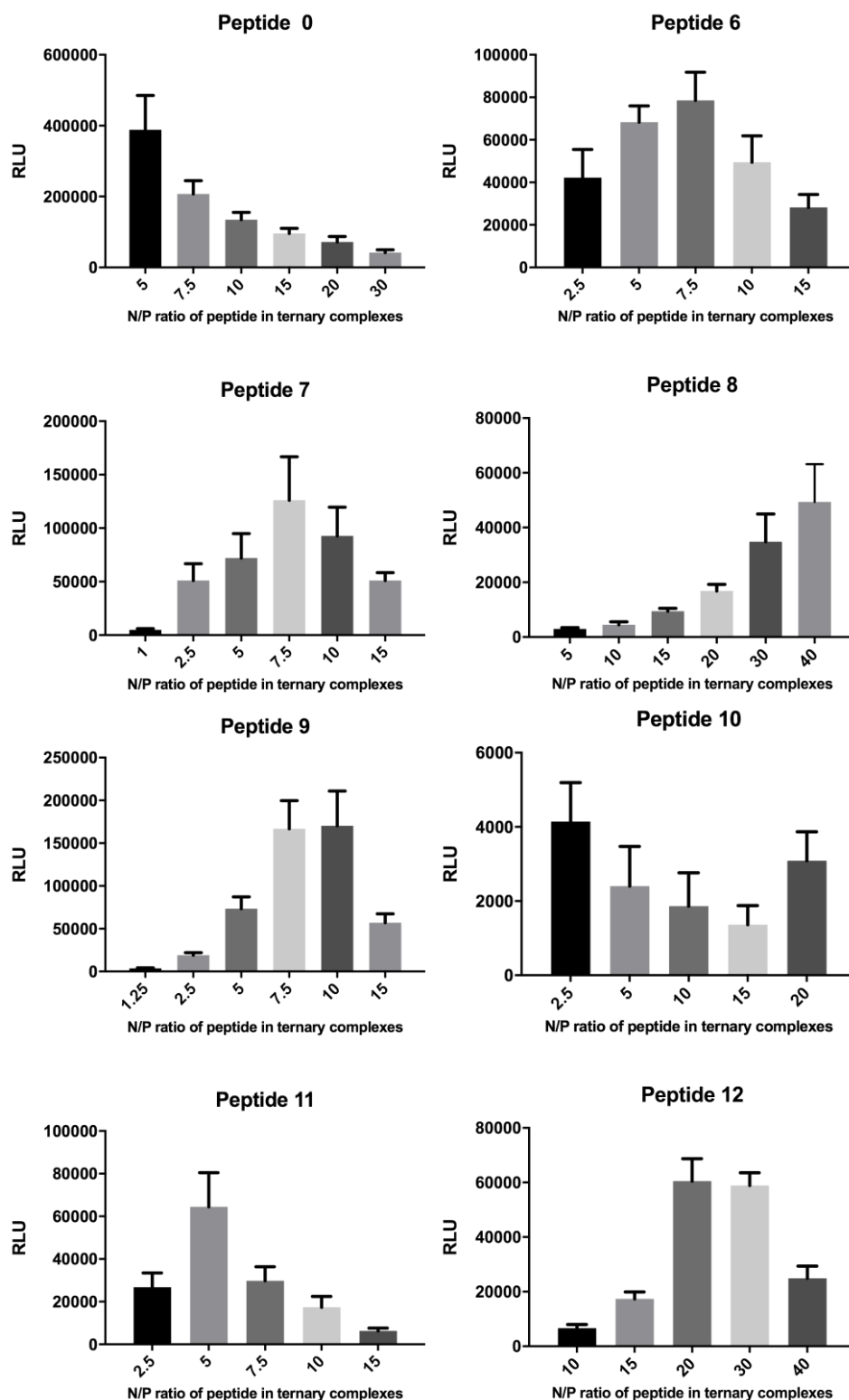


Figure 3.9-11 *In vitro* transfection efficiency of MetLuc-mRNA/L64 based ternary complexes comprising different peptides in 16HBE cells. Peptide 0, peptide 6 to peptide 12 at various N/P ratios were complexed with L64 at a concentration of 300 (w/w) and MetLuc-mRNA. Luciferase activity was expressed in RLU. The data are given as the mean \pm SD ($n > 5$).

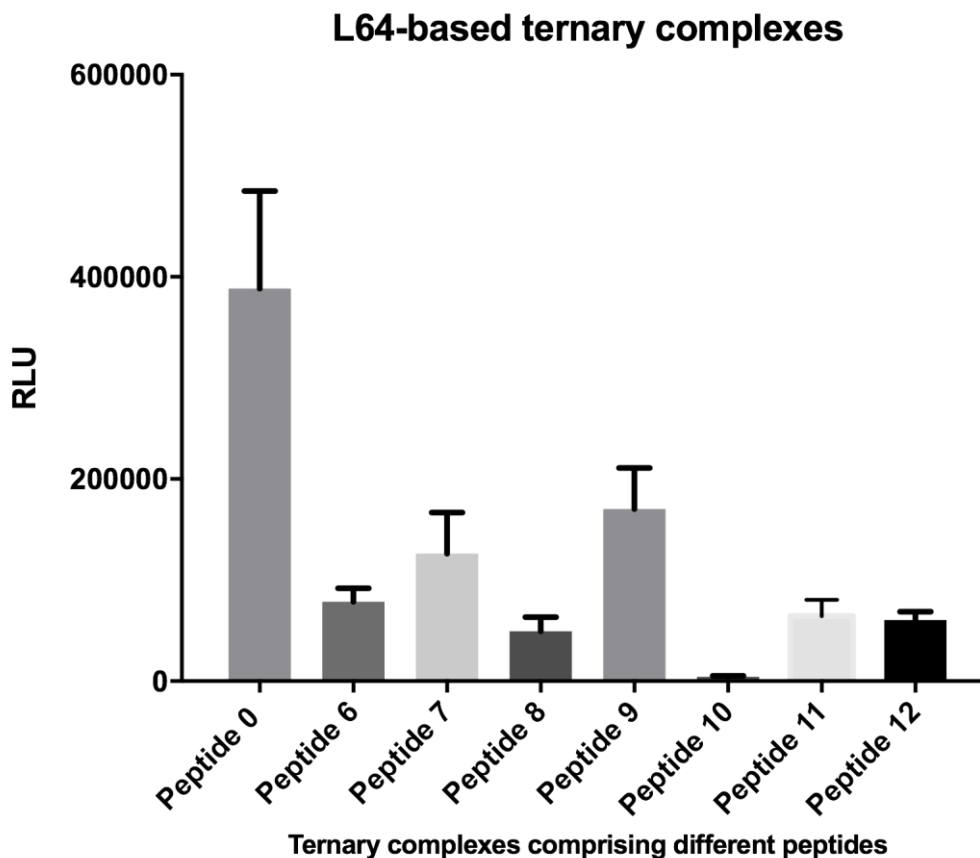


Figure 3.9-12 Comparisons of the optimum *in vitro* transfection efficiency mediated by MetLuc-mRNA/L64 based ternary complexes comprising different peptides in 16HBE cells. The concentration of L64 in ternary complexes was 300 (w/w). The N/P ratio of the peptides in certain ternary complexes was as following: peptide 8 at 40; peptide 12 at 20; peptide 9 at 10; peptide 6 and 7 at 7.5; peptide 0 and 11 at 5; peptide 10 at 2.5. Luciferase activity was expressed in RLU. The data are given as the mean \pm SD ($n > 5$).

4 DISCUSSION

Successful gene therapy requires the gene delivery system to efficiently overcome various biochemical and physiological barriers. Therefore, a versatile delivery vehicle is needed to achieve efficient and safe nucleic acids delivery. Among various non-viral gene delivery systems, peptide-based formulations have gained considerable attention because of the ease of synthesis and chemical modification, the versatility of side-chain groups, and biodegradability etc.¹⁵⁷. Nevertheless, there are few reports on the successful *in vivo* therapeutic nucleic acids delivery with peptide-based delivery vectors, which mainly due to the vulnerable and unstable properties of these complexes, leaving them therapeutically less potent¹⁵⁸. In the majority of applications, synthetic peptides were employed to conjugate with lipid or polymer-based carriers to formulate hybrid nanoparticles for gene delivery^{159,160}. However, the key challenges in hybrid nanoparticles development are the multistep syntheses, complicated purification, and distinct characterization in numerous steps prior to evaluation of their performance, which leads to the low efficiency, tedious chemical synthesis, time consumption, and expensiveness¹⁶¹. In the current study, we developed a synthetic peptide based platform to form compact and homogenized nanoparticles with poloxamine-based copolymers. The resulting nanoparticle represents a novel class of gene delivery vehicle which is self-assembled via noncovalent interaction between peptide and block copolymer component. Such peptide-poloxamine nanoparticle is easy to prepare and could be tailor designed for different therapeutic purposes (e.g., targeting to different tissues or organelles). The peptide-poloxamine nanoparticle could integrate advantages afforded by peptide and poloxamine components while excluding their inherent disadvantages. Considering the fact that GMP-grade poloxamine and synthetic peptide are commercially available with low costs, the peptide-poloxamine based formulations as a result hold promising in clinical applications.

4.1 Establishing and characterization of ternary complexes

Apart from some important parameters such as the concentration of components, the medium used for preparation, transfected cell line and incubation time, we found that the method for preparing the peptide-T704 ternary complexes had an enormous impact on gene transfection efficiency. While ternary complexes prepared by packing mRNA with T704 first and adding peptide component afterward (the “T704 first” method) or condensing mRNA with pre-mixed peptide-T704 solution (the “mRNA last” method) showed efficient gene expression, the complexes generated by mixing mRNA with peptide first and adding T704 copolymer afterward (the “peptide first” method) produced significant lower transgene expression in comparison. It is possible that the “T704 first” and the “mRNA last” methods possibly lead to the formation of a compact micelle-like structure consisting of a condensed hydrophobic core (comprising polypropyleneoxide (PPO) building blocks of T704 and peptide where nucleic acid payloads bind) and a hydrophilic shell that is composed of polyethyleneoxide (PEO) blocks from T704 with the presence of targeting ligand from peptide. The targeting ligand in such nanoparticles could easily take effect. On the other hand, the targeting ligand from the synthetic peptide in ternary complexes prepared by the “peptide first” method might have been masked by T704 copolymer that was added subsequently, thus resulting in lower transfection efficiency. Another possible reason for this phenomenon may result from a stronger binding between the peptide component and mRNA molecules prepared by “peptide first” method, more details were elaborated in chapter“4.4”.

In addition, the hydrophilic outer corona has important functions in prohibiting nanoparticles aggregation and increasing the stability of ternary complexes, this was partially confirmed by the colloidal stability studies. All these features of ternary complex help to meet the criteria of

efficient inhaled gene vectors which must be small enough to diffuse through the mucus mesh while possessing a muco-inert surface to avoid adhesion to mucus constituents¹⁶².

4.2 Investigations of the underlying mechanism of the superior transfection efficiency of ternary complex compared with the binary counterpart

Investigations of the cellular uptake and subcellular location of binary and ternary complexes revealed that ternary complex is able to overcome most of the challenges associated with successful *in vitro* gene transfer including the cellular uptake, intracellular transport, endosome escape and nucleus import, while none of which could be conquered by the binary complex. This would be the reason why binary complex showed background level transfection as described above. The seemingly-contradictory facts between efficient *in vivo* gene transfer profile and poor *in vitro* gene transfer profile of binary complex suggested that T704-based copolymers possessed characteristics to conquer various extracellular barriers in lung tissue whereas these features probably excluded them from overcoming barriers at cellular level, similar to the case of “polyethyleneglycol (PEG) modification dilemma”¹⁶³. On the other hand, we can also infer that the *in vivo* gene expression of binary complex resulted from the very low portion of nucleic acid payloads that passively diffused into cells and localized to the final target site, emphasizing the huge unexplored spaces existed in the *in vivo* transfection efficiency mediated by T704-based copolymers.

As already shown in many studies, cell-penetrating-peptides, which comprise short peptide sequences rich in basic amino acids, could utilize “direct translocation” pathway which is independent of energy consumption¹⁶⁴. Several differences were observed between the internalization of unconjugated cell-penetrating-peptides and conjugates that consist of cell-penetrating-peptides and high molecular-weight molecules (normally proteins and DNA),

suggesting the distinct internalization mechanism utilized by the same peptide, depending on the absence or presence of a linked cargo¹⁶⁵. In terms of peptide 0 in the current study, it shares a similar arginine and lysine rich peptide structure with cell-penetrating-peptides. The cellular internalization of peptide 0 based ternary complex was completely abolished by low temperature (4 °C), indicating the absence of “direct translocation” pathway in the cellular uptake of peptide 0 based ternary complex. Based on this information, it could be inferred that the cellular uptake pathway of cell-penetrating-peptides may also be influenced or altered when they noncovalently interact with cargo molecules.

4.3 Optimizing peptide structure with different candidate modules

The significantly decreased transfection efficiency of peptide 1, peptide 2 and peptide 3 based ternary complexes compared with peptide 0 based ternary complex indicated that anchor moiety, cationic moiety and targeting moiety are indispensable to the efficient *in vitro* transfection of ternary complexes. Among all these moieties, the cationic part is particularly important. This was in agreement with previous studies which indicate that positive charge in the carrier system is not only helpful in condensing nucleic acids payload to avoid nuclease degradation but also plays important roles in overcoming various membrane-based barriers^{166,167}. Heparan sulfate proteoglycans on the cell surface may play an important role in the peptide internalization process¹⁶⁸. On the one hand, the binding of the cationic moiety to cell surface proteoglycans could promote the interaction of the synthetic peptide with the cellular membranes, facilitating the subsequent interactions necessary to the translocation process. On the other hand, the same binding step could lead to certain endocytic mechanism which results in the internalization of synthetic peptide. According to a previous study, the cellular internalization of the arginine based peptide was shown to be mediated by an endocytic mechanism dependent on peptide binding to heparan sulfate proteoglycans¹⁶⁹. The

authors of this study also indicated that the heparan sulfate chains would be degraded by heparanase once inside the endosome, leading to dissociation of the peptides and consequent interaction of the arginine oligomers with the endosomal membrane, thus promoting its endosome escape and subsequent release into the cytoplasm¹⁶⁹.

In the screening of ternary complexes containing peptide 4 to peptide 12, it is particularly interesting to compare peptide 4 and peptide 9. Apart from the same cationic moiety and targeting moiety inherited from peptide 4, peptide 9 specifically contained an enlarged hydrophobic area made by a quadruple tryptophan-rich sequence in anchor moiety. An attractive hypothesis for the superiority of peptide 9 would be that the expanded hydrophobic moiety may increase its capacity for docking the PPO groups of T704, thus resulting in a more compact and stable structure than other counterparts. This could be partially confirmed via size measurement showing that the particle size of peptide 9 based ternary complex was slightly smaller than other counterparts (**Table 2**). Meanwhile, we also evaluated the gene transfer ability of peptide 9 (as a single component to form a complex with pDNA). As shown in **Supplementary Figure 3**, peptide 9 alone could just mediate a MetLuc-pDNA expression to a level that less than 200000 RLU in both investigated cell lines, which represents less than 10% of the pDNA expression mediated by peptide9-T704 ternary complex, emphasizing again the superiority of ternary complex. In the evaluation of targeting moiety, different candidates had their own advantages in different aspects, but ligand S exceeded others in transfecting 16HBE cells which better mimic the *in vivo* status. Another advantage of ligand S is that it was completely functional at a rather low concentration compared with NLS, thereby decreasing the positive charge and toxicity of ternary complex. It is worth to note that ternary complexes formed by peptide 10 which possess “short” cationic moiety were not capable of mediating efficient mRNA or pDNA transfection in both cultured cells, highlighting the importance of cationic moiety. One possible explanation for this phenomenon is that limited

numbers of lysine/arginine might not be sufficient to trigger an efficient intracellular uptake and endosome escape of nucleic acid payloads¹⁵⁷. When comparing the transfection efficiency of peptide 4 and peptide 6 based ternary complexes in 16HBE cells, arginine residues were more efficient in mediating mRNA and pDNA transfection compared with lysine residues, and there seemed to be an optimal number of arginine residues (> 8) for them to be effective in the ternary complex.

4.4 Comparison of the transfection efficiency of ternary complexes with other nonviral transfection reagents

Ternary complexes were more efficient compared with 25kDa brPEI polyplexes in all aspects, but they were still inferior to Lipofectamine2000 lipoplex in mediating mRNA delivery, this is consistent with previous studies implying the superiority of lipid-based carriers compared with other nonviral vectors in mRNA delivery^{81,82}. We found this phenomenon did not result from the differences between the amount of nucleic acid payloads delivered into cells by these carriers, as ternary complex could efficiently mediate the uptake of nucleic acid payloads by almost 70% 16HBE cells whereas the Lipofectamine2000 counterpart was internalized by only 22% 16HBE cells (**Supplementary Figure 3**). The binding strength represents a critical parameter in mRNA expression because the mRNA molecules should be released from the delivery vehicles to facilitate subsequent translation process¹⁷⁰. We performed a heparan sulfate (HS) competition assay to see if there is any difference between the binding strength of pDNA within the ternary complex and that of mRNA. As shown in **Supplementary Figure 4**, pDNA could be released from the ternary complex when the HS/pDNA ratio (w/w) reached at 50, whereas mRNA could not be released from the ternary complex at the same HS/mRNA ratio. Only partial mRNA release could be observed in the ternary complex at the highest HS/mRNA = 100 (w/w) ratio. Results also showed that mRNA within Lipofectamine2000 lipoplex could not be retarded (**Supplementary Figure 5**, lane “mRNA Lipoplex”), revealing

the weak affinity between mRNA and Lipofectamine2000. Therefore, one possible reason for the inferior mRNA transfection efficiency of the ternary complex compared with that of lipoplex most likely resulted from the strong binding between mRNA molecules and the cationic moiety of the peptide. Further efforts to improve the transfection efficiency of the ternary complex containing mRNA will be focused on the adjustments of the cationic moiety of peptide in order to obtain a balance between the affinity to mRNA molecules and ability to overcome cellular barriers.

4.5 Cytotoxicity

The cytotoxicity of peptide-poloxamine nanoparticles is another important parameter for their application as nucleic acid delivery vehicles. MTT assay showed that T704 was not cytotoxic *in vitro* at low and moderate concentrations. However, T704 at high concentration may destabilize the cell membrane and subsequently induces cell death according to the previous investigation¹¹¹. In addition, although showing severe toxicity at high concentration, peptide 9 is actually rather safe when considering that peptide 9 already exerts its maximal function in the ternary complex at a very low concentration (around 2.0 µg/well) at which only negligible cytotoxicity could be observed. Degradation of peptides by intracellular trypsin-like protease would be one of the reasons accounting for their alleviated cytotoxicity. Trypsin-like protease predominantly cleaves the carboxyl side of the arginine and lysine residues within peptide sequence¹⁷¹, and peptide 9 is composed of multiple lysine and arginine residues. The safety profile of peptide-poloxamine nanoparticles was further confirmed in the *in vivo* application. T704 based binary complexes and T704-peptide ternary complexes did not cause inflammation in the lungs of CF mice, whereas severe inflammation was observed in the lungs of DOTAP lipoplex treated mice. These results are consistent with that observed in the previous study¹³⁰. However, there was a study showing that PPO building blocks from

poloxamines sometimes elicits mild immunogenic response¹⁷². As a result, it is important to investigate the safe concentration range of poloxamine used for different therapeutic applications.

4.6 In vivo long-term restoration of CFTR deficiency

The most common approach for CF gene therapy relies on the transfer of a functional copy of the wildtype CFTR gene into deficient cells so that the channel activity could be corrected. The disadvantage of this approach is the transient gene expression profile that is not qualified for CF treatment in which repeated dosing is required due to the turnover of slowly dividing cells. Recently, genome editing tools have emerged, such as clustered regularly interspaced short palindromic repeats associated to Cas9 nucleases (CRISPR/Cas9), transcription activator-like effector nucleases and zinc-finger nucleases. These genome correction strategies are designed to correct the mutant gene within its original genome with low off-target effect. However, in terms of CF gene therapy using these genome editing systems, only a few preliminary *in vitro* investigations have been reported up to date^{173,174}. The deficiency of potent delivery systems critically hindered the *in vivo* translation process of these genome editing systems for CF applications.

An alternative approach has been reported up to date. The approach is mediated by synthetic oligonucleotide analogs, namely triplex forming peptide nucleic acids that are able to induce DNA repair on the sequence-specific triplex formation at targeted genomic sites^{175,176}. Intranasal delivery of poly(lactic-co-glycolic) acid (PLGA) based nanoparticles containing triplex-forming peptide nucleic acids and donor DNA in CF mice induced a response to cyclic adenosine monophosphate (cAMP)-stimulated chloride efflux in the nasal epithelium potential difference assay¹⁷⁷, which is a sign of corrected CFTR function. Furthermore, a deep

sequencing analysis suggested that a correct gene editing of the Phe508del mutation in ~1 % of mouse lung cells was detected¹⁷⁷.

In the present study, we utilized a *SleepingBeauty* (SB) transposon system for long-term correction of CFTR deficiency. SB transposon system contains two components: (i) a transposon element containing a gene-expression cassette and (ii) a genetic element encoding SB transposase enzyme which catalyzes the transposition of transposon element from one genomic locus to another¹⁷⁸. When transposing the expression cassette from a plasmid into the genome, long-term expression of the gene cassette can be achieved¹⁷⁹. This system combines the advantages of viral vectors (directed integration of single copies of a therapeutic gene) with the advantages of nonviral vectors (the absence of protein factors that can elicit adverse reactions)¹⁸⁰. The feasibility of the SB transposon system for *in vivo* applications was first demonstrated by Yant et al. who showed long-term expression of clotting Factor IX in clotting Factor IX-deficient hemophilic mice model and of α 1-antitrypsin in normal mice¹⁸¹. This initial work was followed by the successful treatment of other mouse models of genetic disease, including mucopolysaccharidosis (MPS) types I and VII^{182,183}, hemophilia A^{184–186} and inherited tyrosinemia¹⁸⁷. Apart from that, SB transposons system has also been applied for the *in vivo* treatment of B-cell lymphoma^{188–190}, sickle cell anemia¹⁹¹, glioblastoma multiforme¹⁹² and epidermolysis bullosa¹⁹³. Moreover, SB transposons system has been reported to treat jaundice¹⁹⁴ and pulmonary hypertension¹⁹⁵ in the rat model.

Up to date, SB transposon system has been successfully delivery to the liver of mice via intravenous route (both by hydrodynamic injection of naked plasmid and by injection of plasmid complexed with linear polyethyleneimine) in many investigations. Studies focusing on lung as the target tissue of SB transposon system are also available. By intravenous injection of SB transposon system complexed with linear polyethyleneimine, Belur et al.

demonstrate sustained expression of luciferase transposons in the mouse lung¹⁹⁶. Immunohistochemistry analysis revealed that the majority of the transduced cells were type-2 alveolar pneumocytes¹⁹⁶. This is mainly because of vector entrapment in the alveolar capillaries of the pulmonary circulation, the first capillary bed encountered after intravenous administration¹³⁸. Liu et al. subsequently proved that such expression can be targeted to endothelial cells of the lung using the endothelial-1 promoter to regulate transgene expression in the SB transposon system¹⁹⁷. Systemic delivery of SB transposon system is potentially advantageous in the treatment of diseases such as cancer, for which both primary and metastatic tumors are located deep in the lung. However, if SB transposon system based gene therapy for CF is to be effective, genetic payloads have to be targeted to the airway epithelial cells which are the primary expression sites of CFTR¹⁹⁸.

Airway delivery of SB transposon system was first reported by Lawton et al. who intranasally administered SB transposon system in liposome complexes to BALB/c mice¹⁹⁹. Although a significantly higher level of luciferase expression could be observed in SB transposon system transfected mice compared with the control group (treated with pDNA expressing inactive transposase) at 84 days after dosing, integration site analysis within the lung cell genome suggested that no integration events could be rescued within samples from SB transposon system transfected mice¹⁹⁹. The authors also revealed that the number of lung epithelial cells transfected using this protocol was very low (around 1 in 500000) via parallel studies using the EGFP reporter¹⁹⁹. These results indicated that an improvement in the delivery efficiency of SB transposon system to the lung epithelium is required in order to demonstrate SB mediated integration in the airway epithelial genome. In a recent study, Cooney et al. demonstrated a sustained reporter gene (luciferase) expression after intranasal delivery of viral vectors containing *piggyBac* DNA transposon to mice²⁰⁰. They also showed a persistent correction of Cl⁻ current in differentiated primary cultures of human airway epithelia derived

from CF patients using viral vectors containing *piggyBac* encoding CFTR²⁰⁰. However, the authors of this study did not show a long-term correction of CFTR in *in vivo* conditions, which presumably resulted from the viral vector size limitation to integrate an efficient *piggyBac* DNA transposon that is qualified for *in vivo* applications. Although nonviral delivery of transposon system was thought to be inefficient in somatic cells for the *in vivo* therapeutic application of transposon systems²⁰⁰, *SB*-transposon/T704/peptide nanoparticles in the current study were able to facilitate long-term restoration of the CFTR deficiency in CF mice. However, further investigations in large animal models are still necessary.

It is worth to note that the potential cytotoxicity of transposases needs careful considerations. As the transposase providing source has always been a co-delivered DNA molecule in the majority of previous SB mediated genome modification studies. Using DNA molecule as the transposase-encoding sequence may be problematic and cause unexpected toxicity. Continued expression and potential integration of transposase-encoding DNA may lead to transposon re-mobilization and re-integration, increasing the risk of genotoxicity. On the other hand, it has been revealed that SB transposase, including conventional one and the newly developed codon-optimized SB100X, may trigger apoptosis and premitotic arrest²⁰¹. So the SB transposase itself is toxic to the recipient cells. In the current study, we addressed such potential safety concern by using *in vitro* transcribed messenger RNA (IVT-mRNA) as a source of SB transposase²⁰². Because of its safe and transient protein expression profile, IVT-mRNA represents a promising candidate in the development of novel therapeutics for genetic diseases, vaccines or genome editing strategies, especially when its inherent shortcomings (e.g., instability and immunogenicity) have been partially addressed via structural modifications.

4.7 Distinct behaviors of ternary complexes comprising different poloxamines

In the evaluation of T704 based ternary complexes comprising different peptides, T704-peptide 9 ternary complexes mediated the most potent mRNA and pDNA expression from day 1 to day 4 among all the tested groups in two cell lines of airway epithelia. All these results suggested that peptide 9 was the best performing candidate in the formation of the ternary complex with T704. Peptide 9 was also the best candidate for poloxamine904 (T904) based ternary complexes, this might result from the fact that T704 and T904 share a similar structure and physicochemical property (**Figure 1.4-1** and **Supplementary Table 1**). However, the story was completely different when it comes to the ternary complex comprising other poloxamines. When peptide 9 formed the ternary complex with poloxamine304 (T304) or poloxamine90R4 (T90R4), the maximum mRNA expression mediated by the resulting T304-peptide 9 or T90R4-peptide 9 ternary complexes was less than 200000 RLU in 16HBE cells, which represented just one fifth of the mRNA expression mediated by T704-peptide 9 ternary complex. On the other hand, peptide 8 works surprisingly perfect with T304 and T90R4. mRNA/T304/peptide 8 ternary complexes in optimum composition could reach to comparable gene transfection with that of mRNA/T704/peptide 9 counterpart. When comparing mRNA/T304/peptide 8 and mRNA/T704/peptide 8 ternary complexes, mRNA expression mediated by the former was more than 100-fold higher than mediated by the latter. All these results indicated that different peptides interact distinctively with different poloxamines. The resulting ternary complexes may show completely different transfection profiles. The underlying mechanism of this phenomenon probably resulted from distinct interacting behaviors between peptides and poloxamines. The resultant ternary complex conformation is dependent on i) the proportion and the size of both the PPO and PEO segments within a certain poloxamine; as well as on ii) forces including the electrostatic interactions, hydrogen bonding and hydrophobic forces between the PPO block in poloxamines and the anchor

moieties in peptide; and on iii) nanoparticle-solvent interactions. All these factors determine the final structure of the peptide-poloxamine ternary complex and subsequently influence the transfection profiles of the resulting peptide-poloxamine ternary complex.

5 SUMMARY

In my dissertation, a synthetic peptide-based platform which makes efficient *in vitro* transfection of poloxamine-based block copolymers possible was developed. When spontaneously forming compact and homogenized ternary complex with T704 and therapeutic nucleic acids via a simple self-assembly, the peptide component can mediate efficient *in vitro* and *in vivo* gene transfection. mRNA expression mediated by peptide-T704 nanoparticles could be drastically increased from the background level to 870000 relative light units which is 35-times higher than that mediated by 25kDa brPEI, while pDNA expression was dramatically boosted from background level to a level that was comparable with Lipofectamine2000 mediated one but with less cytotoxicity. Particularly, the superiority of ternary complex compared with the binary counterpart and the lipid-based formulation was further validated in CF mice.

The ternary complex holds several unique features that are able to overcome various extracellular and intracellular barriers. By preventing non-specific interactions with extracellular matrix components, T704 in ternary complex affords the ability to overcome biological barriers formed in the lung tissue, enabling ternary complex efficiently penetrated the adhesive mucus gel layer through nanoporous to reach the underlying epithelium. Subsequently, the synthetic peptide in ternary complex provides the possibility of specific and efficient delivery of genetic payloads into the target cell and target organelle, rather than the passive diffusion manner of binary counterpart which is similar to that of naked nucleic acids. Importantly, the ternary complex demonstrated favorable safety profiles in both *in vitro* and *in vivo* applications. The biodegradability of synthetic peptides is an additional beneficial factor when the repeated dosing is required. By virtue of these advantages, ternary complex is able

to efficiently transfect cultured epithelial cells as well as airway epithelia of mice, indicating their great potential for pulmonary gene delivery.

Although nonviral delivery of transposon system was previously thought to be inefficient in somatic cells for *in vivo* therapeutic application²⁰⁰, *SB*-transposon/T704/peptide 9 nanoparticles are able to facilitate long-term restoration of the CFTR deficiency in CF mice. While zinc-finger nucleases and CRISPR/Cas9 systems have previously been evaluated for CF genome editing *in vitro*^{173,174}, modification frequencies were low and delivery systems for *in vivo* translation were absent. Peptide-poloxamine nanoparticles in the present study could potentially be competent *in vivo* carriers for these genome editing tools.

In addition, preliminary studies indicated that ternary complex strategy is also generalizable to other amphiphilic block copolymers, including poloxamine 304, 904 and 90R4 as well as poloxamer L64. Considering that poloxamine and poloxamer-based copolymers also mediate efficient *in vivo* gene transfer in skeletal muscle and myocardial tissues, and a poloxamer-based delivery vehicle (poloxamer CRL1005) has progressed into clinical trials^{75,203,204}, the modular design approach of synthetic peptide platform also allows the flexible exchange of targeting moieties showing high affinity to these tissues. As a result, the platform in current study holds great promising in the gene therapy of related diseases within these tissues.

5 ZUSAMMENFASSUNG

Ich habe in meiner Dissertation die Grundlagen gelegt für die Etablierung einer Plattformtechnologie, die eine effiziente *in vitro* Transfektion von Nukleinsäuren mittels Poloxamin-basierter Blockcopolymere in Kombination mit synthetischen Peptiden ermöglicht. Die Peptidkomponente vermittelt in Anwesenheit von T704 und Nukleinsäuren die Ausbildung kompakter ternärer Komplexe über eine einfache Selbstorganisation und ermöglicht somit eine effiziente *in vitro*- und *in vivo*-Gen-Transfektion. Der Transfer von mRNA durch Peptid-T704-Nanopartikel führte zu einer 35-mal höheren Transgenexpression im Vergleich zu 25 kDa brPEI. Der Transfer von pDNA- durch Peptid-T704-Nanopartikel führte zu einer vergleichbar hohen Transgenexpression wie dies bei Lipofectamin2000 gemessen werden konnte, allerdings war die Peptid-T704-Nanopartikel vermittelte Transfektion weniger zytotoxisch. In Transfektionsstudien bei CF-Mäusen wurde die Überlegenheit der Peptid-T704-Nanopartikel gegenüber den binären Komplexen und den lipidbasierten Formulierung weiter validiert.

Der ternäre Komplex enthält mehrere unterschiedliche Abschnitte, wodurch verschiedene extrazelluläre und intrazelluläre Barrieren überwunden werden können. T704 als wesentlicher Bestandteil der ternären Komplexe zeigt weniger unspezifische Wechselwirkungen mit extrazellulären Matrixkomponenten, wodurch biologische Barrieren besser überwunden werden können und das Epithel der Atemwege erreicht werden kann. Anschließend ermöglicht das synthetische Peptid im ternären Komplex die Bindung mit den Zielzellen, was dann zu einer effizienten Abgabe der genetischen Nutzlast in die Zielzelle und Zielorganellen ermöglicht. Wichtig ist, dass der ternäre Komplex sowohl *in vitro* als auch in *in vivo* Anwendungen ein geringes Nebenwirkungsprofil zeigte. Die biologische Abbaubarkeit von

synthetischen Peptiden ist ein zusätzlicher vorteilhafter Faktor, wenn wiederholte Applikationen erforderlich sind. Aufgrund dieser Vorteile ist der ternäre Komplex in der Lage, kultivierte Epithelzellen sowie Atemwegsepithelien von Mäusen effizient zu transfizieren, dies unterstreicht das große Anwendungspotential ternärer Komplexe für den pulmonalen Gentransfer.

Obwohl die nichtvirale Applikation des Transposonsystems bisher als ineffizient in somatischen Zellen für die *in vivo* therapeutische Anwendung angesehen wurde²⁰⁰, konnte im Rahmen dieser Arbeit gezeigt werden, dass durch SB-Transposon/T704/Peptid 9 Nanopartikel eine langfristige Wiederherstellung einer CFTR--Expression bei CF-Mäusen erreicht werden konnte. Für Zinkfinger-Nukleasen und CRISPR/Cas9-Systeme liegen erste Ergebnisse für die CF-Genom-Modifikation *in vitro* vor^{173,174}; die Effizienz dieser Ansätze war niedrig und *in vivo* Daten fehlen. Peptid-Poloxamin-Nanopartikel könnten potentiell effiziente *in vivo* Träger für das Verfahren des Genom-Editierens sein.

Darüber hinaus zeigten vorläufige Studien, dass die ternäre Komplexformulierungsstrategie auch für andere amphiphile Blockcopolymere, einschließlich Poloxamin 304, 904 und 90R4 sowie Poloxamer L64, verwendbar ist. In Anbetracht der Tatsache, dass Poloxamin- und Poloxamer-basierte Copolymere auch einen effizienten *in vivo* Gentransfer im Skelettmuskel- und Myokardgewebe vermitteln und ein Poloxamer-basiertes Carrier-System (Poloxamer CRL1005) in klinischen Studien erprobt wird^{75,203,204}, ermöglicht der modulare Designansatz der synthetischen Peptidplattform auch einen flexiblen Austausch von Targeting-Liganden mit hoher Affinität zu diesen Geweben. Zusammenfassend kann festgestellt werden, dass die in dieser Dissertation entwickelte Plattformtechnologie ein vielversprechender Ansatz für eine Reihe von Gentransfer-Verfahren in unterschiedliche Gewebe und Zielzellen sein kann.

6 APPENDIX

6.1 Abbreviations

16HBE: Human bronchial epithelial cell line

7-AAD: 7-Aminoactinomycin D

AAVs: Adeno-associated viruses

ATP: Adenosine triphosphate

BCs: Binary complexes formed by poloxamine 704 and nucleic acids

BEAS-2B: Human bronchial epithelia cell line

brPEI: Branched polyethyleneimine

cAMP: Cyclic adenosine monophosphate

cDNA: Complementary DNA

CF: Cystic fibrosis

CFBE-delF: Cells contain the most common CF phenotype causing mutation (Phe508del)

CFBE-WT: Cells express wild type CFTR

CFTR: *Cystic fibrosis transmembrane conductance regulator*

Cl⁻: Chloride ion

CLSM: Confocal laser scanning microscope

CpG: Cytosine-phosphate-guanine motifs

CPPs: Cell penetrating peptides

CRISPR/Cas9: Clustered regularly interspaced short palindromic repeats/Cas9 nuclease

DAPI: 4,6-diamidino-2-phenylindole

DIPEA: N,N-diisopropylethylamine

DLS: Dynamic light scattering

DOPE: 1,2-dioleoyl-sn-glycero-3-phosphoethanolamine

DOTAP: 1,2-dioleoyl-3-trimethylammoniumpropane

EDMPC:Chol: *p*-ethyl-dimyristoylphosphatidyl choline cholesterol liposomes

EDTA: Ethylenediaminetetraacetic acid

EGFP: Enhanced green fluorescent protein

ER: Endoplasmic reticulum

FACS: Flow cytometry

FBS: Fetal bovine serum

FCS: Fetal bovine serum

fLUC: Firefly luciferase

Fluo-pDNA: Fluorescein labelled plasmid DNA

GL67A: Cationic lipids based nonviral gene transfection formulation

HCO₃⁻: Bicarbonate ion

HCTU: 2-(6-chloro-1H-benzotriazole-1-yl)-1,1,3,3-tetramethylaminium hexafluorophosphate

H&E: Haematoxylin-Eosin staining

HPLC: High performance liquid chromatography

HS: Heparan sulfate

HSPG: Heparan sulfate proteoglycans

ICAM-1: Intercellular adhesion molecule-1

IC₅₀: Half maximal inhibitory concentration

IgG: Immunoglobulin G

IVIS: In Vivo Imaging System

IVT mRNA: *In vitro* transcribed messenger RNA

kDa: Kilo Dalton

L64: Poloxamer 184

LC/MS: Liquid chromatography-mass spectroscopy

ligand S: Short peptide sequence displays close similarity to receptor binding proteins of rhinovirus (sequence: SERSMNF)

ligand Y: Short peptide closely resembles part of a targeting protein expressed by the intracellular pathogen *Legionella pneumophila* (sequence: YGLPHKF)

lipoplex: Complex formed by cationic lipids and nucleic acids

MetLuc: Metridia luciferase

mM: Millimolar

mRNA: Messenger RNA

MTT: 3-(4,5- Dimethyl-2-tetrazolyl)-2,5-diphenyl-2Htetrazolium bromide

MW: Molecular weight

NF-water: Nuclease-free water

NLS: Nuclear localization signal

N/P ratio: The ratio between nitrogen residues in peptide and nucleic acids phosphate groups

PBS: Phosphate buffer saline

PDI: polydispersity index

pDNA: Plasmid DNA

PEG: Polyethylenglycol

PEO: Poly(ethylene oxide)

pGM206-fLUC-CFTR/T2: Plasmid containing a T2 *SB* transposon encoding both firefly luciferase and *Cystic Fibrosis Transmembrane Conductance Regulator*

pH: Potentia Hydrogenii

Phe508del: The most common CF phenotype causing mutation which originates from the deletion of three nucleotides inducing a deletion of phenylalanine within the protein

PLGA: Poly (lactic-co-glycolic acid)

Poloxamers: Nonionic triblock copolymers composed of a central hydrophobic chain of polyoxypropylene (poly(propylene oxide)) flanked by two hydrophilic chains of polyoxyethylene (poly(ethylene oxide))

Poloxamines: A subgroup of the poloxamers and structurally composed of an ethylene diamine core whose amino groups are substituted with copolymers of variable length polyoxyethylene and polyoxypropylene blocks

Polyplex: Complex formed by cationic polymer and nucleic acids

PPO: Poly(propylene oxide)

RLU: Relative light units

RT: Room temperature

SB: *Sleeping Beauty* based transposon system

SB100X: *Sleeping Beauty* 100X transposase

SD: Standard deviation

SNIM mRNA: Stabilized, non-immunogenic messenger RNA

siRNA: Short interfering RNA

T304: poloxamine 304

T704: poloxamine 704

T904: poloxamine 904

T90R4: poloxamine 90R4

TAE: Tris-acetate-EDTA buffer

TCs: Ternary complexes formed by T704, peptide and nucleic acids

TEM: Transmission electron microscopy

TFA: Trifluoroacetic acid

TLR: Toll-like receptor

v/v: Volume percent

wtCFTR: Wild type CFTR

w/v: Mass concentration

w/w: Weight to weight ratio

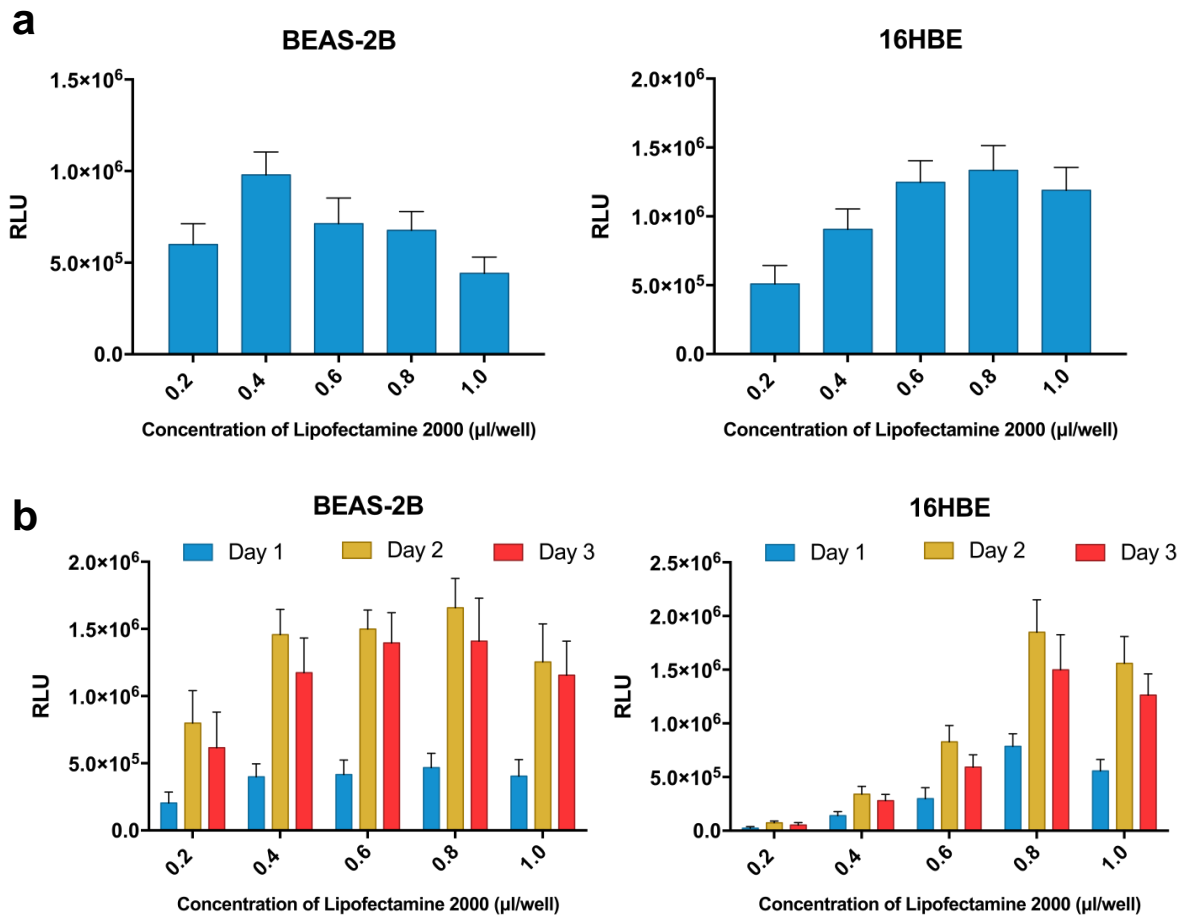
6.2 Supporting figures and tables

Supplementary Table 1. Currently available poloxamine varieties commercialized by BASF under the trade name Tetronic® obtained from BASF web page

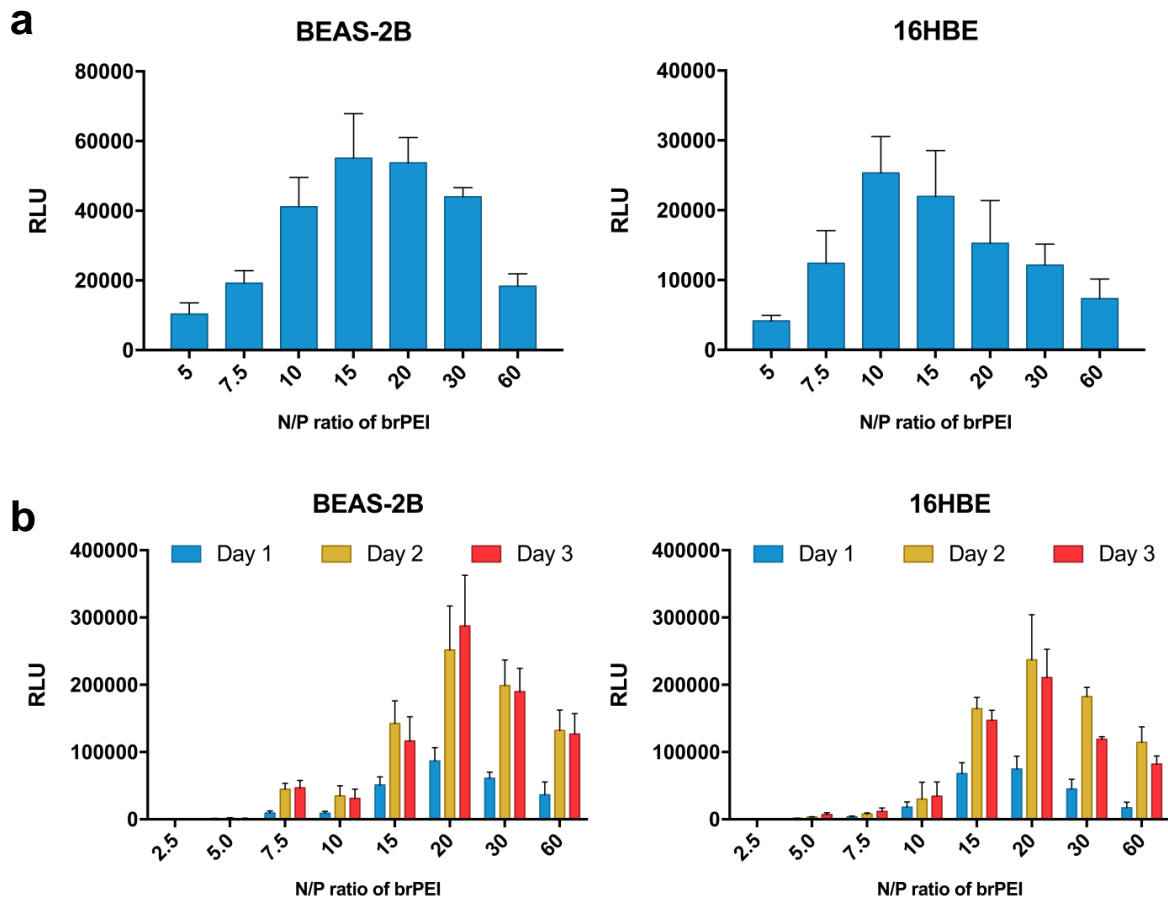
Tetronic	Mw (Da)	EO units per block	PO units per block	HLB	Solubility*	Cloud point**	pKa
304	1650	3.7	4.3	12-18	> 10	75	4.3; 8.1
701	3600	2.1	14.0	1-7	Insoluble	18	4.0; 7.9
901	4700	2.7	18.2	1-7	Insoluble	20	5.1; 7.6
904	6700	15	17	12-18	> 10	74	4.0; 7.8
908	25000	114	21	> 24	> 10	> 100	5.2; 7.9
1107	15000	60	20	18-23	> 10	> 100	5.6; 7.9
1301	6800	4	26	1-7	Insoluble	16	4.1; 6.2
1304	10500	21.4	27.1	12-18	> 10	---	---
1307	18000	72	23	> 24	> 10	> 100	4.6; 7.8
90R4	6900	16	18	1-7	> 10	43	---
150R1	8000	5	30	1-7	Insoluble	20	4.8; 7.5

*represents solubility in water at 25°C (w/w %)

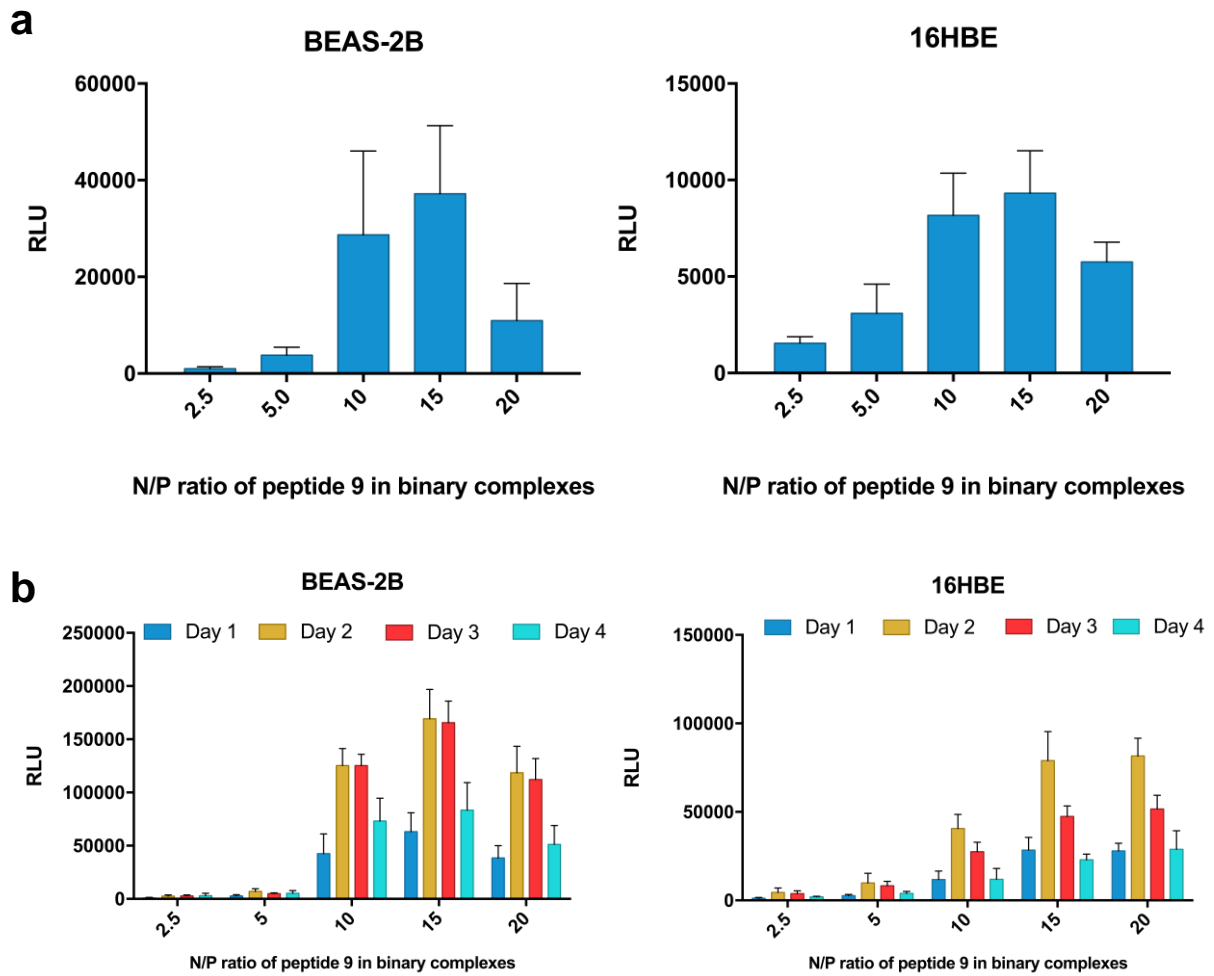
**represents cloud point of 1 % (°C)



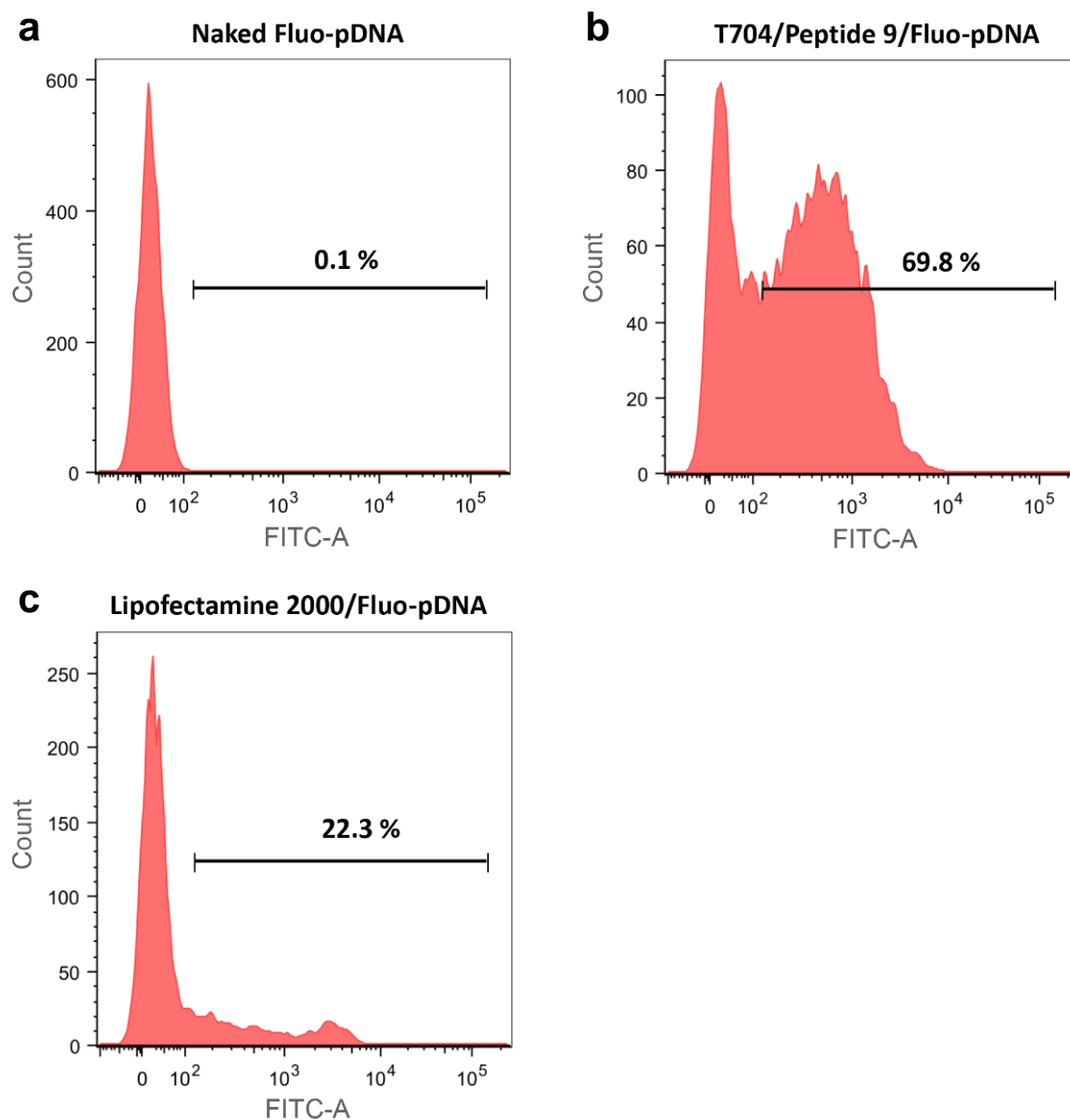
Supplementary Figure 1 *In vitro* transfection profile of Lipofectamine2000 based lipoplexes in cultured human bronchial epithelial cells (BEAS-2B and 16HBE). (a) 400 ng/well MetLuc-mRNA was complexed with Lipofectamine2000 at different concentrations from 0.2 to 1.0 µg/well (relative to 96-well plate) in OptiMEM. After 30 min incubation at room temperature (RT), samples were added into 96-well plate containing pre-seeded cells and incubated with cells in OptiMEM (without serum and antibiotics) for 4 h at 37 °C in a humidified atmosphere (95% air, 5% CO₂). Luciferase activity in 50 µl supernatants from transfected cells was assayed after 24 h and its activity was expressed in RLU. (b) MetLuc-pDNA/Lipofectamine 2000 lipoplexes were prepared in the same way of mRNA counterpart, luciferase activity was measured 24 h, 48 h and 72 h after transfection and its activity was expressed in RLU. All experiments were performed at least three times. Data represent the mean ± SD (n>5).



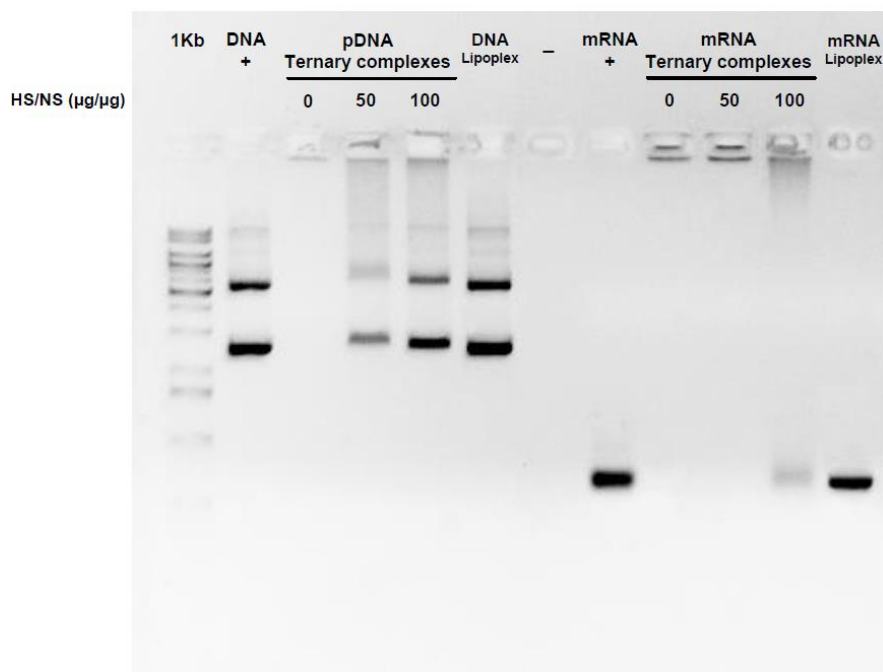
Supplementary Figure 2 *In vitro* transfection profile of 25kDa brPEI based polyplexes in cultured human bronchial epithelial cells (BEAS-2B and 16HBE). (a) 400 ng/well MetLuc-mRNA was complexed with brPEI at different N/P ratios from 5 to 60 (relative to nucleic acids) in nuclease-free water. After 30 min incubation at RT, samples were added into 96-well plate containing pre-seeded cells and incubated with cells in OptiMEM (without serum and antibiotics) for 4 h at 37 °C in a humidified atmosphere (95% air, 5% CO₂). Luciferase activity in 50 µl supernatants from transfected cells was assayed after 24 h and its activity was expressed in RLU. (b) MetLuc-pDNA/brPEI polyplexes were prepared in the same way of mRNA counterpart, luciferase activity was measured 24 h, 48 h and 72 h after transfection and its activity was expressed in RLU. All experiments were performed at least three times. The data are given as the mean \pm SD (n>5).



Supplementary Figure 3 *In vitro* transfection profile of peptide 9 based binary complexes in BEAS-2B and 16HBE cells. **(a)** 400 ng/well MetLuc-mRNA was complexed with peptide 9 at different N/P ratios from 2.5 to 20 in NF-water. After 30 min incubation at RT, samples were added into 96-well plate containing pre-seeded cells and incubated with cells in Opti-MEM (without serum and antibiotics) for 4 h at 37 °C in a humidified atmosphere (95% air, 5% CO₂). Luciferase activity in 50 µl supernatants from transfected in transfected BEAS-2B or 16HBE cells was measured after 24 h and its activity was expressed in RLU. **(b)** MetLuc-pDNA/peptide 9 binary complexes were prepared in the same way of mRNA counterpart, luciferase activity in 50 µl supernatants from transfected cells was measured 24 h, 48 h, 72h and 96 h after transfection and its activity was expressed in RLU. All experiments were performed at least three times. The data are given as the mean ± SD (n>5).



Supplementary Figure 4 Cellular uptake profiles of peptide 9 based ternary complex and Lipofectamine 2000 based lipoplex. The uptake of (a) naked fluorescein labelled pDNA (Fluo-pDNA), (b) Fluo-pDNA/T704/peptide 9 ternary complex and (c) Fluo-pDNA/Lipofectamine2000 lipoplex in 16HBE cells.



Supplementary Figure 5 Binding and condensation properties of ternary complexes containing pDNA or mRNA. Complexes were incubated with increasing amounts of heparan sulfate (HS) per µg nucleic acid (NS). Naked nucleic acid was used as a positive control (+) and NF-water as a negative control (-). “DNA Lipoplex” represents Lipofectamine2000 based lipoplex containing pDNA in optimum composition. “mRNA Lipoplex” represents Lipofectamine2000 based lipoplex containing mRNA in optimum composition.

7 REFERENCE

1. Griesenbach, U., Pytel, K. M. & Alton, E. W. F. W. Cystic Fibrosis Gene Therapy in the UK and Elsewhere. *Human gene therapy* **26**, 266–75 (2015).
2. Wang, Y., Wrennall, J. A., Cai, Z., Li, H. & Sheppard, D. N. Understanding how cystic fibrosis mutations disrupt CFTR function: from single molecules to animal models. *The international journal of biochemistry & cell biology* **52**, 47–57 (2014).
3. Kerem, B. & Kerem, E. The molecular basis for disease variability in cystic fibrosis. *European journal of human genetics : EJHG* **4**, 65–73 (1996).
4. Rowe, S. M., Miller, S. & Sorscher, E. J. Cystic fibrosis. *The New England journal of medicine* **352**, 1992–2001 (2005).
5. Stoltz, D. A., Meyerholz, D. K. & Welsh, M. J. Origins of cystic fibrosis lung disease. *The New England journal of medicine* **372**, 351–62 (2015).
6. Kerem, B. *et al.* Identification of the cystic fibrosis gene: genetic analysis. *Science (New York, N.Y.)* **245**, 1073–80 (1989).
7. Riordan, J. R. *et al.* Identification of the cystic fibrosis gene: cloning and characterization of complementary DNA. *Science (New York, N.Y.)* **245**, 1066–73 (1989).
8. Rommens, J. M. *et al.* Identification of the cystic fibrosis gene: chromosome walking and jumping. *Science (New York, N.Y.)* **245**, 1059–65 (1989).
9. Riordan, J. R. CFTR function and prospects for therapy. *Annual review of biochemistry* **77**, 701–26 (2008).
10. Amaral, M. D. Targeting CFTR: how to treat cystic fibrosis by CFTR-repairing therapies. *Current drug targets* **12**, 683–93 (2011).
11. Collawn, J. F. & Matalon, S. CFTR and lung homeostasis. *American journal of physiology. Lung cellular and molecular physiology* **307**, L917–23 (2014).
12. Boucher, R. C. Airway surface dehydration in cystic fibrosis: pathogenesis and therapy. *Annual review of medicine* **58**, 157–70 (2007).
13. Davies, J. C. *et al.* Potential difference measurements in the lower airway of children with and without cystic fibrosis. *American journal of respiratory and critical care medicine* **171**, 1015–9 (2005).
14. Naehrlich, L. *et al.* Nasal potential difference measurements in diagnosis of cystic fibrosis: an international survey. *Journal of cystic fibrosis : official journal of the European Cystic Fibrosis Society* **13**, 24–8 (2014).
15. Chen, J.-H. *et al.* Loss of anion transport without increased sodium absorption characterizes newborn porcine cystic fibrosis airway epithelia. *Cell* **143**, 911–23 (2010).
16. Pezzulo, A. A. *et al.* Reduced airway surface pH impairs bacterial killing in the porcine cystic fibrosis lung. *Nature* **487**, 109–13 (2012).
17. Goldstein, W. & Döring, G. Lysosomal enzymes from polymorphonuclear leukocytes and proteinase inhibitors in patients with cystic fibrosis. *The American review of respiratory disease* **134**, 49–56 (1986).
18. Nakamura, H., Yoshimura, K., McElvaney, N. G. & Crystal, R. G. Neutrophil elastase in respiratory epithelial lining fluid of individuals with cystic fibrosis induces interleukin-8 gene expression in a human bronchial epithelial cell line. *The Journal of clinical investigation* **89**, 1478–84 (1992).
19. Di, A. *et al.* CFTR regulates phagosome acidification in macrophages and alters bactericidal activity. *Nature cell biology* **8**, 933–44 (2006).
20. Haggie, P. M. & Verkman, A. S. Cystic fibrosis transmembrane conductance regulator-independent phagosomal acidification in macrophages. *The Journal of biological chemistry* **282**, 31422–8 (2007).

21. Mueller, C. *et al.* Lack of cystic fibrosis transmembrane conductance regulator in CD3+ lymphocytes leads to aberrant cytokine secretion and hyperinflammatory adaptive immune responses. *American journal of respiratory cell and molecular biology* **44**, 922–9 (2011).
22. Amaral, M. D. & Kunzelmann, K. Molecular targeting of CFTR as a therapeutic approach to cystic fibrosis. *Trends in pharmacological sciences* **28**, 334–41 (2007).
23. Amaral, M. D. CFTR and chaperones: processing and degradation. *Journal of molecular neuroscience : MN* **23**, 41–8 (2004).
24. Collins, F. S. Cystic fibrosis: molecular biology and therapeutic implications. *Science (New York, N.Y.)* **256**, 774–9 (1992).
25. Cheng, S. H. *et al.* Defective intracellular transport and processing of CFTR is the molecular basis of most cystic fibrosis. *Cell* **63**, 827–34 (1990).
26. Highsmith, W. E. *et al.* A novel mutation in the cystic fibrosis gene in patients with pulmonary disease but normal sweat chloride concentrations. *The New England journal of medicine* **331**, 974–80 (1994).
27. Amaral, M. D. *et al.* Cystic fibrosis patients with the 3272-26A>G splicing mutation have milder disease than F508del homozygotes: a large European study. *Journal of medical genetics* **38**, 777–83 (2001).
28. Goodier, J. L. & Mayer, J. PTC124 for cystic fibrosis. *Lancet (London, England)* **373**, 1426; author reply 1426–7 (2009).
29. Wilschanski, M. *et al.* Chronic ataluren (PTC124) treatment of nonsense mutation cystic fibrosis. *The European respiratory journal* **38**, 59–69 (2011).
30. Nudelman, I. *et al.* Repairing faulty genes by aminoglycosides: development of new derivatives of geneticin (G418) with enhanced suppression of diseases-causing nonsense mutations. *Bioorganic & medicinal chemistry* **18**, 3735–46 (2010).
31. Pedemonte, N. *et al.* Small-molecule correctors of defective DeltaF508-CFTR cellular processing identified by high-throughput screening. *The Journal of clinical investigation* **115**, 2564–71 (2005).
32. Clancy, J. P. *et al.* Results of a phase IIa study of VX-809, an investigational CFTR corrector compound, in subjects with cystic fibrosis homozygous for the F508del-CFTR mutation. *Thorax* **67**, 12–8 (2012).
33. Moran, O. & Zegarra-Moran, O. A quantitative description of the activation and inhibition of CFTR by potentiators: Genistein. *FEBS letters* **579**, 3979–83 (2005).
34. Van Goor, F. *et al.* Rescue of CF airway epithelial cell function in vitro by a CFTR potentiator, VX-770. *Proceedings of the National Academy of Sciences of the United States of America* **106**, 18825–30 (2009).
35. Ramsey, B. W. *et al.* A CFTR potentiator in patients with cystic fibrosis and the G551D mutation. *The New England journal of medicine* **365**, 1663–72 (2011).
36. De Boeck, K. *et al.* Efficacy and safety of ivacaftor in patients with cystic fibrosis and a non-G551D gating mutation. *Journal of cystic fibrosis : official journal of the European Cystic Fibrosis Society* **13**, 674–80 (2014).
37. Wainwright, C. E. *et al.* Lumacaftor-Ivacaftor in Patients with Cystic Fibrosis Homozygous for Phe508del CFTR. *The New England journal of medicine* **373**, 220–31 (2015).
38. Bell, S. C., De Boeck, K. & Amaral, M. D. New pharmacological approaches for cystic fibrosis: promises, progress, pitfalls. *Pharmacology & therapeutics* **145**, 19–34 (2015).
39. Griesenbach, U. & Alton, E. W. F. W. Moving forward: cystic fibrosis gene therapy. *Human Molecular Genetics* **22**, R52–R58 (2013).
40. Moss, R. B. *et al.* Repeated aerosolized AAV-CFTR for treatment of cystic fibrosis: a randomized placebo-controlled phase 2B trial. *Human gene therapy* **18**, 726–32 (2007).
41. Alton, E. W. F. W. *et al.* Repeated nebulisation of non-viral CFTR gene therapy in

- patients with cystic fibrosis: a randomised, double-blind, placebo-controlled, phase 2b trial. *The Lancet. Respiratory medicine* **3**, 684–91 (2015).
42. Rosenecker, J., Huth, S. & Rudolph, C. Gene therapy for cystic fibrosis lung disease: current status and future perspectives. *Current opinion in molecular therapeutics* **8**, 439–45 (2006).
 43. Zabner, J. *et al.* Adenovirus-mediated gene transfer transiently corrects the chloride transport defect in nasal epithelia of patients with cystic fibrosis. *Cell* **75**, 207–16 (1993).
 44. Crystal, R. G. *et al.* Administration of an adenovirus containing the human CFTR cDNA to the respiratory tract of individuals with cystic fibrosis. *Nature genetics* **8**, 42–51 (1994).
 45. Knowles, M. R. *et al.* A controlled study of adenoviral-vector-mediated gene transfer in the nasal epithelium of patients with cystic fibrosis. *The New England journal of medicine* **333**, 823–31 (1995).
 46. Hay, J. G., McElvaney, N. G., Herena, J. & Crystal, R. G. Modification of nasal epithelial potential differences of individuals with cystic fibrosis consequent to local administration of a normal CFTR cDNA adenovirus gene transfer vector. *Human gene therapy* **6**, 1487–96 (1995).
 47. Zabner, J. *et al.* Repeat administration of an adenovirus vector encoding cystic fibrosis transmembrane conductance regulator to the nasal epithelium of patients with cystic fibrosis. *The Journal of clinical investigation* **97**, 1504–11 (1996).
 48. Bellon, G. *et al.* Aerosol administration of a recombinant adenovirus expressing CFTR to cystic fibrosis patients: a phase I clinical trial. *Human gene therapy* **8**, 15–25 (1997).
 49. Harvey, B. G. *et al.* Airway epithelial CFTR mRNA expression in cystic fibrosis patients after repetitive administration of a recombinant adenovirus. *The Journal of clinical investigation* **104**, 1245–55 (1999).
 50. Zuckerman, J. B. *et al.* A phase I study of adenovirus-mediated transfer of the human cystic fibrosis transmembrane conductance regulator gene to a lung segment of individuals with cystic fibrosis. *Human gene therapy* **10**, 2973–85 (1999).
 51. Joseph, P. M. *et al.* Aerosol and lobar administration of a recombinant adenovirus to individuals with cystic fibrosis. I. Methods, safety, and clinical implications. *Human gene therapy* **12**, 1369–82 (2001).
 52. Perricone, M. A. *et al.* Aerosol and lobar administration of a recombinant adenovirus to individuals with cystic fibrosis. II. Transfection efficiency in airway epithelium. *Human gene therapy* **12**, 1383–94 (2001).
 53. Walters, R. W. *et al.* Basolateral localization of fiber receptors limits adenovirus infection from the apical surface of airway epithelia. *The Journal of biological chemistry* **274**, 10219–26 (1999).
 54. Koehler, D. R. *et al.* Aerosol delivery of an enhanced helper-dependent adenovirus formulation to rabbit lung using an intratracheal catheter. *The journal of gene medicine* **7**, 1409–20 (2005).
 55. Toietta, G. *et al.* Reduced inflammation and improved airway expression using helper-dependent adenoviral vectors with a K18 promoter. *Molecular therapy : the journal of the American Society of Gene Therapy* **7**, 649–58 (2003).
 56. Koehler, D. R. *et al.* Protection of Cftr knockout mice from acute lung infection by a helper-dependent adenoviral vector expressing Cftr in airway epithelia. *Proceedings of the National Academy of Sciences of the United States of America* **100**, 15364–9 (2003).
 57. Vetrini, F. & Ng, P. Gene therapy with helper-dependent adenoviral vectors: current advances and future perspectives. *Viruses* **2**, 1886–917 (2010).
 58. Wagner, J. A. *et al.* Safety and biological efficacy of an adeno-associated virus vector-

- cystic fibrosis transmembrane regulator (AAV-CFTR) in the cystic fibrosis maxillary sinus. *The Laryngoscope* **109**, 266–74 (1999).
59. Aitken, M. L. *et al.* A phase I study of aerosolized administration of tgAAVCF to cystic fibrosis subjects with mild lung disease. *Human gene therapy* **12**, 1907–16 (2001).
60. Wagner, J. A. *et al.* A phase II, double-blind, randomized, placebo-controlled clinical trial of tgAAVCF using maxillary sinus delivery in patients with cystic fibrosis with antrostomies. *Human gene therapy* **13**, 1349–59 (2002).
61. Flotte, T. R. *et al.* Phase I trial of intranasal and endobronchial administration of a recombinant adeno-associated virus serotype 2 (rAAV2)-CFTR vector in adult cystic fibrosis patients: a two-part clinical study. *Human gene therapy* **14**, 1079–88 (2003).
62. Moss, R. B. *et al.* Repeated adeno-associated virus serotype 2 aerosol-mediated cystic fibrosis transmembrane regulator gene transfer to the lungs of patients with cystic fibrosis: a multicenter, double-blind, placebo-controlled trial. *Chest* **125**, 509–21 (2004).
63. Flotte, T. R. *et al.* Expression of the cystic fibrosis transmembrane conductance regulator from a novel adeno-associated virus promoter. *The Journal of biological chemistry* **268**, 3781–90 (1993).
64. Li, W. *et al.* Generation of novel AAV variants by directed evolution for improved CFTR delivery to human ciliated airway epithelium. *Molecular therapy : the journal of the American Society of Gene Therapy* **17**, 2067–77 (2009).
65. Song, Y. *et al.* Functional cystic fibrosis transmembrane conductance regulator expression in cystic fibrosis airway epithelial cells by AAV6.2-mediated segmental trans-splicing. *Human gene therapy* **20**, 267–81 (2009).
66. Kaeppl, C. *et al.* A largely random AAV integration profile after LPLD gene therapy. *Nature medicine* **19**, 889–91 (2013).
67. Segura, M. M., Mangion, M., Gaillet, B. & Garnier, A. New developments in lentiviral vector design, production and purification. *Expert opinion on biological therapy* **13**, 987–1011 (2013).
68. Sinn, P. L. *et al.* Lentiviral vector gene transfer to porcine airways. *Molecular therapy. Nucleic acids* **1**, e56 (2012).
69. Sinn, P. L., Arias, A. C., Brogden, K. A. & McCray, P. B. Lentivirus vector can be readministered to nasal epithelia without blocking immune responses. *Journal of virology* **82**, 10684–92 (2008).
70. Mitomo, K. *et al.* Toward gene therapy for cystic fibrosis using a lentivirus pseudotyped with Sendai virus envelopes. *Molecular therapy : the journal of the American Society of Gene Therapy* **18**, 1173–82 (2010).
71. Griesenbach, U. *et al.* Assessment of F/HN-pseudotyped lentivirus as a clinically relevant vector for lung gene therapy. *American journal of respiratory and critical care medicine* **186**, 846–56 (2012).
72. Aiuti, A. *et al.* Lentiviral hematopoietic stem cell gene therapy in patients with Wiskott-Aldrich syndrome. *Science (New York, N.Y.)* **341**, 1233151 (2013).
73. Biffi, A. *et al.* Lentiviral hematopoietic stem cell gene therapy benefits metachromatic leukodystrophy. *Science (New York, N.Y.)* **341**, 1233158 (2013).
74. Palfi, S. *et al.* Long-term safety and tolerability of ProSavin, a lentiviral vector-based gene therapy for Parkinson's disease: a dose escalation, open-label, phase 1/2 trial. *Lancet (London, England)* **383**, 1138–46 (2014).
75. Yin, H. *et al.* Non-viral vectors for gene-based therapy. *Nature reviews. Genetics* **15**, 541–55 (2014).
76. Kanasty, R., Dorkin, J. R., Vegas, A. & Anderson, D. Delivery materials for siRNA therapeutics. *Nature materials* **12**, 967–77 (2013).

77. Kormann, M. S. D. *et al.* Expression of therapeutic proteins after delivery of chemically modified mRNA in mice. *Nature Biotechnology* **29**, 154–157 (2011).
78. Weide, B. *et al.* Results of the first phase I/II clinical vaccination trial with direct injection of mRNA. *Journal of immunotherapy (Hagerstown, Md. : 1997)* **31**, 180–8
79. Midoux, P. & Pichon, C. Lipid-based mRNA vaccine delivery systems. *Expert review of vaccines* **14**, 221–34 (2015).
80. Wang, W., Li, W., Ma, N. & Steinhoff, G. Non-viral gene delivery methods. *Current pharmaceutical biotechnology* **14**, 46–60 (2013).
81. Zou, S., Scarfo, K., Nantz, M. H. & Hecker, J. G. Lipid-mediated delivery of RNA is more efficient than delivery of DNA in non-dividing cells. *International journal of pharmaceutics* **389**, 232–43 (2010).
82. Rejman, J., Tavernier, G., Bavarsad, N., Demeester, J. & De Smedt, S. C. mRNA transfection of cervical carcinoma and mesenchymal stem cells mediated by cationic carriers. *Journal of controlled release : official journal of the Controlled Release Society* **147**, 385–91 (2010).
83. Gul-Uludağ, H. *et al.* Polymeric nanoparticle-mediated silencing of CD44 receptor in CD34+ acute myeloid leukemia cells. *Leukemia research* **38**, 1299–308 (2014).
84. Menon, J. U. *et al.* Polymeric nanoparticles for pulmonary protein and DNA delivery. *Acta biomaterialia* **10**, 2643–52 (2014).
85. Jarzębińska, A. *et al.* A Single Methylene Group in Oligoalkylamine-Based Cationic Polymers and Lipids Promotes Enhanced mRNA Delivery. *Angewandte Chemie (International ed. in English)* (2016). doi:10.1002/anie.201603648
86. Caplen, N. J. *et al.* Liposome-mediated CFTR gene transfer to the nasal epithelium of patients with cystic fibrosis. *Nature medicine* **1**, 39–46 (1995).
87. Gill, D. R. *et al.* A placebo-controlled study of liposome-mediated gene transfer to the nasal epithelium of patients with cystic fibrosis. *Gene therapy* **4**, 199–209 (1997).
88. Porteous, D. J. *et al.* Evidence for safety and efficacy of DOTAP cationic liposome mediated CFTR gene transfer to the nasal epithelium of patients with cystic fibrosis. *Gene therapy* **4**, 210–8 (1997).
89. Zabner, J. *et al.* Comparison of DNA-lipid complexes and DNA alone for gene transfer to cystic fibrosis airway epithelia in vivo. *The Journal of clinical investigation* **100**, 1529–37 (1997).
90. Alton, E. W. *et al.* Cationic lipid-mediated CFTR gene transfer to the lungs and nose of patients with cystic fibrosis: a double-blind placebo-controlled trial. *Lancet (London, England)* **353**, 947–54 (1999).
91. Noone, P. G. *et al.* Safety and biological efficacy of a lipid-CFTR complex for gene transfer in the nasal epithelium of adult patients with cystic fibrosis. *Molecular therapy : the journal of the American Society of Gene Therapy* **1**, 105–14 (2000).
92. Ruiz, F. E. *et al.* A clinical inflammatory syndrome attributable to aerosolized lipid-DNA administration in cystic fibrosis. *Human gene therapy* **12**, 751–61 (2001).
93. McLachlan, G. *et al.* Pre-clinical evaluation of three non-viral gene transfer agents for cystic fibrosis after aerosol delivery to the ovine lung. *Gene therapy* **18**, 996–1005 (2011).
94. Konstan, M. W. *et al.* Compacted DNA nanoparticles administered to the nasal mucosa of cystic fibrosis subjects are safe and demonstrate partial to complete cystic fibrosis transmembrane regulator reconstitution. *Human gene therapy* **15**, 1255–69 (2004).
95. Hyde, S. C. *et al.* Repeat administration of DNA/liposomes to the nasal epithelium of patients with cystic fibrosis. *Gene therapy* **7**, 1156–65 (2000).
96. Read, M. L. *et al.* A versatile reducible polycation-based system for efficient delivery of a broad range of nucleic acids. *Nucleic acids research* **33**, e86 (2005).
97. Wasungu, L. & Hoekstra, D. Cationic lipids, lipoplexes and intracellular delivery of

- genes. *Journal of controlled release : official journal of the Controlled Release Society* **116**, 255–64 (2006).
98. Ballarín-González, B. & Howard, K. A. Polycation-based nanoparticle delivery of RNAi therapeutics: Adverse effects and solutions. *Advanced Drug Delivery Reviews* **64**, 1717–1729 (2012).
99. Novo, L., van Gaal, E. V. B., Mastrobattista, E. & van Nostrum, C. F. Decationized crosslinked polyplexes for redox-triggered gene delivery. *Journal of Controlled Release* **169**, 246–256 (2013).
100. Lemieux, P. *et al.* A combination of poloxamers increases gene expression of plasmid DNA in skeletal muscle. *Gene therapy* **7**, 986–91 (2000).
101. Pitard, B. *et al.* A nonionic amphiphile agent promotes gene delivery in vivo to skeletal and cardiac muscles. *Human gene therapy* **13**, 1767–75 (2002).
102. Pitard, B. *et al.* Negatively charged self-assembling DNA/poloxamine nanospheres for in vivo gene transfer. *Nucleic acids research* **32**, e159 (2004).
103. Alvarez-Lorenzo, C., Rey-Rico, A., Sosnik, A., Taboada, P. & Concheiro, A. Poloxamine-based nanomaterials for drug delivery. *Frontiers in bioscience (Elite edition)* **2**, 424–40 (2010).
104. Dong, J., Chowdhry, B. Z. & Leharne, S. A. Solubilisation of polyaromatic hydrocarbons in aqueous solutions of poloxamine T803. *Colloids and Surfaces A: Physicochemical and Engineering Aspects* **246**, 91–98 (2004).
105. Alvarez-Lorenzo, C., Gonzalez-Lopez, J., Fernandez-Tarrio, M., Sandez-Macho, I. & Concheiro, A. Tetronic micellization, gelation and drug solubilization: Influence of pH and ionic strength. *European journal of pharmaceuticals and biopharmaceutics : official journal of Arbeitsgemeinschaft fur Pharmazeutische Verfahrenstechnik e.V* **66**, 244–52 (2007).
106. Fernandez-Tarrio, M., Alvarez-Lorenzo, C. & Concheiro, A. Calorimetric approach to tetronic/water interactions. *Journal of Thermal Analysis and Calorimetry* **87**, 171–178 (2007).
107. Subbaraman, L. N. *et al.* Rewetting drops containing surface active agents improve the clinical performance of silicone hydrogel contact lenses. *Optometry and vision science : official publication of the American Academy of Optometry* **83**, 143–51 (2006).
108. Tonge, S., Jones, L., Goodall, S. & Tighe, B. The ex vivo wettability of soft contact lenses. *Current eye research* **23**, 51–9 (2001).
109. Mansur, C. R. E., Barboza, S. P., González, G. & Lucas, E. F. PLURONIC x TETRONIC polyols: study of their properties and performance in the destabilization of emulsions formed in the petroleum industry. *Journal of colloid and interface science* **271**, 232–40 (2004).
110. Wu, J., Xu, Y., Dabros, T. & Hamza, H. Effect of EO and PO positions in nonionic surfactants on surfactant properties and demulsification performance. *Colloids and Surfaces A: Physicochemical and Engineering Aspects* **252**, 79–85 (2005).
111. Moghimi, S. M. & Hunter, A. C. Poloxamers and poloxamines in nanoparticle engineering and experimental medicine. *Trends in biotechnology* **18**, 412–20 (2000).
112. Takáts, Z., Vékey, K. & Hegedüs, L. Qualitative and quantitative determination of poloxamer surfactants by mass spectrometry. *Rapid Communications in Mass Spectrometry* **15**, 805–810 (2001).
113. Al-Hanbali, O. *et al.* Modification of the Stewart biphasic colorimetric assay for stable and accurate quantitative determination of Pluronic and Tetronic block copolymers for application in biological systems. *Analytical biochemistry* **361**, 287–93 (2007).
114. Jones, D. S. *et al.* Moisture-activated rheological structuring of nonaqueous poloxamine-poly(acrylic acid) systems designed as novel biomedical implants. *Journal*

- of pharmaceutical sciences* **99**, 1838–54 (2010).
115. Ciucurel, E. C. & Sefton, M. V. A Poloxamine–Polylysine Acrylate Scaffold for Modular Tissue Engineering. *Journal of Biomaterials Science, Polymer Edition* **22**, 2515–2528 (2011).
116. Cellesi, F. & Tirelli, N. A new process for cell microencapsulation and other biomaterial applications: Thermal gelation and chemical cross-linking in “tandem”. *Journal of materials science. Materials in medicine* **16**, 559–65 (2005).
117. Sosnik, A., Leung, B., McGuigan, A. P. & Sefton, M. V. Collagen/poloxamine hydrogels: cytocompatibility of embedded HepG2 cells and surface-attached endothelial cells. *Tissue engineering* **11**, 1807–16 (2005).
118. Sosnik, A. & Sefton, M. V. Poloxamine hydrogels with a quaternary ammonium modification to improve cell attachment. *Journal of biomedical materials research. Part A* **75**, 295–307 (2005).
119. Sosnik, A. & Sefton, M. V. Semi-synthetic collagen/poloxamine matrices for tissue engineering. *Biomaterials* **26**, 7425–35 (2005).
120. Cappel, M. J. & Kreuter, J. Effect of nonionic surfactants on transdermal drug delivery: II. Poloxamer and poloxamine surfactants. *International Journal of Pharmaceutics* **69**, 155–167 (1991).
121. McIlroy, D. *et al.* DNA/amphiphilic block copolymer nanospheres promote low-dose DNA vaccination. *Molecular therapy : the journal of the American Society of Gene Therapy* **17**, 1473–81 (2009).
122. Rolland-Debord, C. *et al.* Block copolymer/DNA vaccination induces a strong allergen-specific local response in a mouse model of house dust mite asthma. *PloS one* **9**, e85976 (2014).
123. Beilvert, F. *et al.* DNA/amphiphilic block copolymer nanospheres reduce asthmatic response in a mouse model of allergic asthma. *Human gene therapy* **23**, 597–608 (2012).
124. Zou, W., Liu, C., Chen, Z. & Zhang, N. Studies on bioadhesive PLGA nanoparticles: A promising gene delivery system for efficient gene therapy to lung cancer. *International journal of pharmaceutics* **370**, 187–95 (2009).
125. Lai, T. C., Kataoka, K. & Kwon, G. S. Pluronic-based cationic block copolymer for forming pDNA polyplexes with enhanced cellular uptake and improved transfection efficiency. *Biomaterials* **32**, 4594–603 (2011).
126. Prokop, A., Kozlov, E., Moore, W. & Davidson, J. M. Maximizing the in vivo efficiency of gene transfer by means of nonviral polymeric gene delivery vehicles. *Journal of pharmaceutical sciences* **91**, 67–76 (2002).
127. Richard, P. *et al.* Amphiphilic block copolymers promote gene delivery in vivo to pathological skeletal muscles. *Human gene therapy* **16**, 1318–24 (2005).
128. Biliczki, P. *et al.* Trafficking-deficient long QT syndrome mutation KCNQ1-T587M confers severe clinical phenotype by impairment of KCNH2 membrane localization: evidence for clinically significant IKr-IKs alpha-subunit interaction. *Heart rhythm* **6**, 1792–801 (2009).
129. Richard-Fiardo, P. *et al.* Effect of fractalkine-Fc delivery in experimental lung metastasis using DNA/704 nanospheres. *Cancer gene therapy* **18**, 761–72 (2011).
130. Richard-Fiardo, P. *et al.* Evaluation of tetrafunctional block copolymers as synthetic vectors for lung gene transfer. *Biomaterials* **45**, 10–7 (2015).
131. Csaba, N., Sánchez, A. & Alonso, M. J. PLGA: Poloxamer and PLGA: Poloxamine blend nanostructures as carriers for nasal gene delivery. *Journal of Controlled Release* **113**, 164–172 (2006).
132. Zhang, J., Bae, S., Lee, J. S. & Webb, K. Efficacy and mechanism of poloxamine-

- assisted polyplex transfection. *The journal of gene medicine* **15**, 271–81 (2013).
133. Zhang, J., Sen, A., Cho, E., Lee, J. S. & Webb, K. Poloxamine/fibrin hybrid hydrogels for non-viral gene delivery. *Journal of Tissue Engineering and Regenerative Medicine* **11**, 246–255 (2017).
134. Wang, T., Upponi, J. R. & Torchilin, V. P. Design of multifunctional non-viral gene vectors to overcome physiological barriers: dilemmas and strategies. *International journal of pharmaceutics* **427**, 3–20 (2012).
135. van Gaal, E. V. B. *et al.* How to screen non-viral gene delivery systems in vitro? *Journal of Controlled Release* **154**, 218–232 (2011).
136. Podetz-Pedersen, K. M. *et al.* Gene expression in lung and liver after intravenous infusion of polyethylenimine complexes of Sleeping Beauty transposons. *Human gene therapy* **21**, 210–20 (2010).
137. Lin, E.-H. *et al.* Lifelong reporter gene imaging in the lungs of mice following polyethyleneimine-mediated sleeping-beauty transposon delivery. *Biomaterials* **32**, 1978–85 (2011).
138. Belur, L. R., Podetz-Pedersen, K., Frandsen, J. & McIvor, R. S. Lung-directed gene therapy in mice using the nonviral Sleeping Beauty transposon system. *Nature protocols* **2**, 3146–52 (2007).
139. Johler, S. M., Rejman, J., Guan, S. & Rosenecker, J. Nebulisation of IVT mRNA Complexes for Intrapulmonary Administration. *PloS one* **10**, e0137504 (2015).
140. Guan, S. & Rosenecker, J. Nanotechnologies in delivery of mRNA therapeutics using nonviral vector-based delivery systems. *Gene Therapy* (2017). doi:10.1038/gt.2017.5
141. Sahin, U., Karikó, K. & Türeci, Ö. mRNA-based therapeutics — developing a new class of drugs. *Nature Reviews Drug Discovery* **13**, 759–80 (2014).
142. Zhong, Y. *et al.* Reversibly crosslinked hyaluronic acid nanoparticles for active targeting and intelligent delivery of doxorubicin to drug resistant CD44+ human breast tumor xenografts. *Journal of Controlled Release* **205**, 144–154 (2015).
143. Wang, F. *et al.* Recent progress of cell-penetrating peptides as new carriers for intracellular cargo delivery. *Journal of controlled release : official journal of the Controlled Release Society* **174**, 126–36 (2014).
144. Gilleron, J. *et al.* Image-based analysis of lipid nanoparticle-mediated siRNA delivery, intracellular trafficking and endosomal escape. *Nature biotechnology* **31**, 638–46 (2013).
145. ur Rehman, Z., Hoekstra, D. & Zuhorn, I. S. Mechanism of polyplex- and lipoplex-mediated delivery of nucleic acids: real-time visualization of transient membrane destabilization without endosomal lysis. *ACS nano* **7**, 3767–77 (2013).
146. Kalderon, D., Richardson, W. D., Markham, A. F. & Smith, A. E. Sequence requirements for nuclear location of simian virus 40 large-T antigen. *Nature* **311**, 33–8
147. Writer, M. J. *et al.* Targeted gene delivery to human airway epithelial cells with synthetic vectors incorporating novel targeting peptides selected by phage display. *Journal of drug targeting* **12**, 185–93 (2004).
148. Manunta, M. D. I. *et al.* Nebulisation of receptor-targeted nanocomplexes for gene delivery to the airway epithelium. *PloS one* **6**, e26768 (2011).
149. Tagalakakis, A. D. *et al.* PEGylation improves the receptor-mediated transfection efficiency of peptide-targeted, self-assembling, anionic nanocomplexes. *Journal of controlled release : official journal of the Controlled Release Society* **174**, 177–87 (2014).
150. Tagalakakis, A. D. *et al.* Multifunctional, self-assembling anionic peptide-lipid nanocomplexes for targeted siRNA delivery. *Biomaterials* **35**, 8406–15 (2014).
151. Aied, A., Greiser, U., Pandit, A. & Wang, W. Polymer gene delivery: overcoming the obstacles. *Drug Discovery Today* **18**, 1090–1098 (2013).

152. Fletcher, S. *et al.* In vivo studies of dialkynoyl analogues of DOTAP demonstrate improved gene transfer efficiency of cationic liposomes in mouse lung. *Journal of medicinal chemistry* **49**, 349–57 (2006).
153. Eliyahu, H. *et al.* Characterization and in vivo performance of dextran-spermine polyplexes and DOTAP/cholesterol lipoplexes administered locally and systemically. *Biomaterials* **28**, 2339–49 (2007).
154. Gjetting, T. *et al.* In vitro and in vivo effects of polyethylene glycol (PEG)-modified lipid in DOTAP/cholesterol-mediated gene transfection. *International journal of nanomedicine* **5**, 371–83 (2010).
155. Charizopoulou, N. *et al.* Spontaneous rescue from cystic fibrosis in a mouse model. *BMC genetics* **7**, 18 (2006).
156. Adams, M. L., Lavasanifar, A. & Kwon, G. S. Amphiphilic block copolymers for drug delivery. *Journal of Pharmaceutical Sciences* **92**, 1343–1355 (2003).
157. Qin, B., Chen, Z., Jin, W. & Cheng, K. Development of cholesteryl peptide micelles for siRNA delivery. *Journal of controlled release : official journal of the Controlled Release Society* **172**, 159–68 (2013).
158. Cerrato, C. P., Lehto, T. & Langel, Ü. Peptide-based vectors: recent developments. *Biomolecular Concepts* **5**, 479–88 (2014).
159. Nam, H. Y. *et al.* Cell penetrating peptide conjugated bioreducible polymer for siRNA delivery. *Biomaterials* **32**, 5213–5222 (2011).
160. Dey, D. *et al.* Efficient gene delivery of primary human cells using peptide linked polyethylenimine polymer hybrid. *Biomaterials* **32**, 4647–4658 (2011).
161. Qiao, Z.-Y. *et al.* A General Strategy for Facile Synthesis and In Situ Screening of Self-Assembled Polymer-Peptide Nanomaterials. *Advanced materials (Deerfield Beach, Fla.)* **28**, 1859–67 (2016).
162. Suk, J. S. *et al.* Lung gene therapy with highly compacted DNA nanoparticles that overcome the mucus barrier. *Journal of Controlled Release* **178**, 8–17 (2014).
163. Knop, K., Hoogenboom, R., Fischer, D. & Schubert, U. S. Poly(ethylene glycol) in drug delivery: pros and cons as well as potential alternatives. *Angewandte Chemie (International ed. in English)* **49**, 6288–308 (2010).
164. Madani, F., Lindberg, S., Langel, Ü., Futaki, S. & Gräslund, A. Mechanisms of Cellular Uptake of Cell-Penetrating Peptides. *Journal of Biophysics* **2011**, 1–10 (2011).
165. Trabulo, S., Cardoso, A. L., Mano, M. & De Lima, M. C. P. Cell-Penetrating Peptides-Mechanisms of Cellular Uptake and Generation of Delivery Systems. *Pharmaceuticals (Basel, Switzerland)* **3**, 961–993 (2010).
166. Plank, C., Tang, M. X., Wolfe, A. R. & Szoka, F. C. Branched cationic peptides for gene delivery: role of type and number of cationic residues in formation and in vitro activity of DNA polyplexes. *Human gene therapy* **10**, 319–32 (1999).
167. Huang, Y. *et al.* Curb challenges of the “Trojan Horse” approach: smart strategies in achieving effective yet safe cell-penetrating peptide-based drug delivery. *Advanced drug delivery reviews* **65**, 1299–315 (2013).
168. Belting, M. Heparan sulfate proteoglycan as a plasma membrane carrier. *Trends in Biochemical Sciences* **28**, 145–151 (2003).
169. Fuchs, S. M. & Raines, R. T. Pathway for polyarginine entry into mammalian cells. *Biochemistry* **43**, 2438–44 (2004).
170. Li, J. *et al.* Structurally Programmed Assembly of Translation Initiation Nanoplex for Superior mRNA Delivery. *ACS Nano* acsnano.6b08447 (2017). doi:10.1021/acsnano.6b08447
171. Futaki, S. *et al.* Arginine-rich Peptides: AN ABUNDANT SOURCE OF MEMBRANE-PERMEABLE PEPTIDES HAVING POTENTIAL AS CARRIERS FOR INTRACELLULAR PROTEIN DELIVERY. *Journal of Biological Chemistry*

- 276, 5836–5840 (2001).
172. Huang, K., Lee, B. P., Ingram, D. R. & Messersmith, P. B. Synthesis and Characterization of Self-Assembling Block Copolymers Containing Bioadhesive End Groups. *Biomacromolecules* **3**, 397–406 (2002).
 173. Lee, C. M., Flynn, R., Hollywood, J. A., Scallan, M. F. & Harrison, P. T. Correction of the $\Delta F508$ Mutation in the Cystic Fibrosis Transmembrane Conductance Regulator Gene by Zinc-Finger Nuclease Homology-Directed Repair. *BioResearch open access* **1**, 99–108 (2012).
 174. Schwank, G. *et al.* Functional repair of CFTR by CRISPR/Cas9 in intestinal stem cell organoids of cystic fibrosis patients. *Cell stem cell* **13**, 653–8 (2013).
 175. Majumdar, A. *et al.* Targeted gene knockout mediated by triple helix forming oligonucleotides. *Nature Genetics* **20**, 212–214 (1998).
 176. Rogers, F. A., Vasquez, K. M., Egholm, M. & Glazer, P. M. Site-directed recombination via bifunctional PNA-DNA conjugates. *Proceedings of the National Academy of Sciences of the United States of America* **99**, 16695–700 (2002).
 177. McNeer, N. A. *et al.* Nanoparticles that deliver triplex-forming peptide nucleic acid molecules correct F508del CFTR in airway epithelium. *Nature Communications* **6**, 6952 (2015).
 178. Ivics, Z., Hackett, P. B., Plasterk, R. H. & Izsvák, Z. Molecular reconstruction of Sleeping Beauty, a Tc1-like transposon from fish, and its transposition in human cells. *Cell* **91**, 501–10 (1997).
 179. Fernando, S. & Fletcher, B. S. Sleeping beauty transposon-mediated nonviral gene therapy. *BioDrugs : clinical immunotherapeutics, biopharmaceuticals and gene therapy* **20**, 219–29 (2006).
 180. Hackett, P. B., Ekker, S. C., Largaespada, D. A. & McIvor, R. S. in *Advances in genetics* **54**, 189–232 (2005).
 181. Yant, S. R. *et al.* Somatic integration and long-term transgene expression in normal and haemophilic mice using a DNA transposon system. *Nature genetics* **25**, 35–41 (2000).
 182. Aronovich, E. L. *et al.* Prolonged expression of a lysosomal enzyme in mouse liver after Sleeping Beauty transposon-mediated gene delivery: implications for non-viral gene therapy of mucopolysaccharidoses. *The journal of gene medicine* **9**, 403–15 (2007).
 183. Aronovich, E. L. *et al.* Systemic correction of storage disease in MPS I NOD/SCID mice using the sleeping beauty transposon system. *Molecular therapy : the journal of the American Society of Gene Therapy* **17**, 1136–44 (2009).
 184. Ohlfest, J. R. *et al.* Phenotypic correction and long-term expression of factor VIII in hemophilic mice by immunotolerization and nonviral gene transfer using the Sleeping Beauty transposon system. *Blood* **105**, 2691–8 (2005).
 185. Liu, L., Mah, C. & Fletcher, B. S. Sustained FVIII Expression and Phenotypic Correction of Hemophilia A in Neonatal Mice Using an Endothelial-Targeted Sleeping Beauty Transposon. *Molecular Therapy* **13**, 1006–1015 (2006).
 186. Kren, B. T. *et al.* Nanocapsule-delivered Sleeping Beauty mediates therapeutic Factor VIII expression in liver sinusoidal endothelial cells of hemophilia A mice. *The Journal of clinical investigation* **119**, 2086–99 (2009).
 187. Montini, E. *et al.* In vivo correction of murine tyrosinemia type I by DNA-mediated transposition. *Molecular therapy : the journal of the American Society of Gene Therapy* **6**, 759–69 (2002).
 188. Huang, X. *et al.* Sleeping Beauty transposon-mediated engineering of human primary T cells for therapy of CD19+ lymphoid malignancies. *Molecular therapy : the journal of the American Society of Gene Therapy* **16**, 580–9 (2008).
 189. Singh, H. *et al.* Redirecting specificity of T-cell populations for CD19 using the

- Sleeping Beauty system. *Cancer research* **68**, 2961–71 (2008).
190. Jena, B., Dotti, G. & Cooper, L. J. N. Redirecting T-cell specificity by introducing a tumor-specific chimeric antigen receptor. *Blood* **116**, 1035–44 (2010).
191. Belcher, J. D. *et al.* Heme oxygenase-1 gene delivery by Sleeping Beauty inhibits vascular stasis in a murine model of sickle cell disease. *Journal of molecular medicine (Berlin, Germany)* **88**, 665–75 (2010).
192. Ohlfest, J. R., Lobitz, P. D., Perkinson, S. G. & Largaespada, D. A. Integration and long-term expression in xenografted human glioblastoma cells using a plasmid-based transposon system. *Molecular therapy : the journal of the American Society of Gene Therapy* **10**, 260–8 (2004).
193. Ortiz-Urda, S. *et al.* Sustainable correction of junctional epidermolysis bullosa via transposon-mediated nonviral gene transfer. *Gene therapy* **10**, 1099–104 (2003).
194. Wang, X. *et al.* Long-term reduction of jaundice in Gunn rats by nonviral liver-targeted delivery of Sleeping Beauty transposon. *Hepatology (Baltimore, Md.)* **50**, 815–24 (2009).
195. Liu, L., Liu, H., Visner, G. & Fletcher, B. S. Sleeping Beauty-mediated eNOS gene therapy attenuates monocrotaline-induced pulmonary hypertension in rats. *FASEB journal : official publication of the Federation of American Societies for Experimental Biology* **20**, 2594–6 (2006).
196. Belur, L. R. *et al.* Gene insertion and long-term expression in lung mediated by the Sleeping Beauty transposon system. *Molecular therapy : the journal of the American Society of Gene Therapy* **8**, 501–7 (2003).
197. Liu, L. *et al.* Endothelial targeting of the Sleeping Beauty transposon within lung. *Molecular therapy : the journal of the American Society of Gene Therapy* **10**, 97–105 (2004).
198. Kreda, S. M. *et al.* Characterization of Wild-Type and F508 Cystic Fibrosis Transmembrane Regulator in Human Respiratory Epithelia. *Molecular Biology of the Cell* **16**, 2154–2167 (2005).
199. Dv, V. *et al.* 993. Non-Viral Integrating Vectors for the Lung: Sleeping Beauty Transposons. *Molecular Therapy* **5**, S323–S324 (2002).
200. Cooney, A. L., Singh, B. K. & Sinn, P. L. Hybrid Nonviral/Viral Vector Systems for Improved piggyBac DNA Transposon In Vivo Delivery. *Molecular Therapy* **23**, 667–674 (2015).
201. Galla, M. *et al.* Avoiding cytotoxicity of transposases by dose-controlled mRNA delivery. *Nucleic Acids Research* **39**, 7147–7160 (2011).
202. Wilber, A. *et al.* Messenger RNA as a Source of Transposase for Sleeping Beauty Transposon-mediated Correction of Hereditary Tyrosinemia Type I. *Molecular Therapy* **15**, 1280–1287 (2007).
203. Bello-Roufaï, M., Lambert, O. & Pitard, B. Relationships between the physicochemical properties of an amphiphilic triblock copolymers/DNA complexes and their intramuscular transfection efficiency. *Nucleic acids research* **35**, 728–39 (2007).
204. Roques, C., Bouchemal, K., Ponchel, G., Fromes, Y. & Fattal, E. Parameters affecting organization and transfection efficiency of amphiphilic copolymers/DNA carriers. *Journal of Controlled Release* **138**, 71–77 (2009).

8 PUBLICATION

Original articles

- Johler Sarah, Joanna Rejman, **Shan Guan** and Joseph Rosenecker. Nebulisation of IVT mRNA complexes for intrapulmonary administration. Plos One. 10 (2015) 10: e0137504.

Review

- **Shan Guan**, Sarah M. Johler, Carsten Rudolph and Joseph Rosenecker. Topical application of in vitro transcribed mRNA to the airways as novel gene therapy approach for the treatment of cystic fibrosis. Clinical Immunology, Endocrine& Metabolic Drugs. 3 (2016) 148-161.
- **Shan Guan**, Joseph Rosenecker. Nanotechnologies in delivery of mRNA therapeutics using nonviral vector-based delivery systems. Gene Ther. 24 (2017) 133-143.

9 ACKNOWLEDGEMENTS

Four years represent just a small piece of one's lifetime and are even negligible in the perspective of human history. But it is the very four years that I spent in LMU enabled me to have a wonderful journey of exploring the mystery scientific world. Such experience made me realize that this thesis is not an accomplishment of the trip, it is more like a ticket for boarding me onto the ship of science initiating the "Age of Discovery". Before commencing, I would like to express my sincere gratitude to all people who helped me during my study in Germany.

My deepest gratitude goes first to Prof. Dr. Joseph Rosenecker and PD. Dr. Carsten Rudolph, for offering me the opportunity to perform my doctoral training at LMU. I am very grateful for their professional guidance and enlightening discussions over the past four years. Their valuable advice and encouragement always help me to overcome various kinds of scientific difficulties.

I would particularly thank Antje Munder (Hannover Medical School, Hannover, Germany) and her colleagues in Hannover Medical School as well as Günther Hasenpusch (ethris GmbH, Planegg, Germany), who helped to perform the animal studies, this thesis could not be done without their help.

Special thanks to Georges Vassaux (University of Nice-Sophia Antipolis, Nice, France) and Bruno Pitard (University of Nantes, Nantes, France) for introducing and providing poloxamine⁷⁰⁴. I thank Johannes Geiger and Manish K Aneja (ethris GmbH, Planegg,

Germany) for providing SNIM mRNA, and thank Oliver Walisko and Zoltan Ivics (Paul-Ehrlich-Institute, Langen, Germany) for providing SB-plasmid.

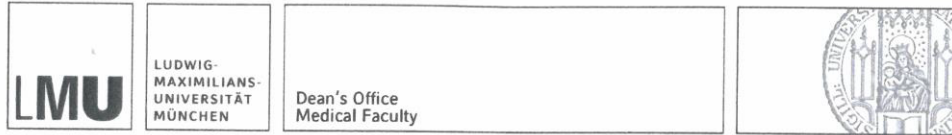
I would like to express my thanks to Christopher Hauser, Sarah M Johler and Petra Eckel for introducing me to this nice group. And many thanks to Anja Schultze and Longgui Zhang who came later to the group and helped me a lot.

Extraordinary gratitude to the China Scholarship Council for offering me the fellowship to study in LMU, and thanks for help from the international office of LMU for adapting my life in Munich.

Furthermore, I would like to thank my friend Hang Li (Technische Universität München, Garching, Germany) who helped me to go through the most difficult times when I had to move a lot in Munich.

Finally, I would like to acknowledge my family for their unconditional love and constant support. Their powerful support gives me courage and confidence to face whatever happened in the past and in the future.

AFFIDAVIT



Affidavit

Guan, Shan

Surname, first name

I hereby declare, that the submitted thesis entitled

**Peptide-based platform enabling amphiphilic
block copolymers to acquire *in vitro*
transfection ability and more potent *in vivo*
lung gene transfer for cystic fibrosis**

is my own work. I have only used the sources indicated and have not made unauthorised use of services of a third party. Where the work of others has been quoted or reproduced, the source is always given.

I further declare that the submitted thesis or parts thereof have not been presented as part of an examination degree to any other university.

München, 16. 08. 2017

Place, date

Shan Guan

Signature doctoral candidate